INFORMATION TO USERS

74-19,253

KAYS, Marvin Dale, 1931-
OPTIMAL SAMPLING OF A STRATOSPHERIC
SUDDEN WARMING.

The University of Oklahoma, Ph.D., 1974
Physics, meteorology

University Microfilms, A XEROX Company, Ann Arbor, Michigan

THE UNIVERSITY OF OKLAHOMA

GRADUATE COLLEGE

OPTIMAL SAMPLING OF A STRATOSPHERIC SUDDEN WARMING

A DISSERTATION

SUBMITTED TO THE GRADUATE FACULTY

in partial fulfillment of the requirements for the

degree of

DOCTOR OF PHILOSOPHY

BY

MARVIN DALE KAYS

Norman, Oklahoma

1974

OPTIMAL SAMPLING OF A STRATOSPHERIC SUDDEN WARMING

APPROVED BY

Amos Eddy

Claude E. Duchon

John C. Bripe

Eugene M. Wilkins

DISSERTATION COMMITTEE

ACKNOWLEDGEMENTS

My relationship with Dr. Amos Eddy as a co-worker and teacher-student has always been rewarding. He has provided the inspiration necessary for me to inquire, learn, and discuss concepts that not only apply to the design of meteorological experiments, but to philosophy on all sciences and life in general. His practical approach for attacking and solving problems is an enviable attribute.

I have had the interest and cooperation of Drs. Claude Duchon, Eugene Wilkins, John Brixey and Raymond Lutz while doing this research. Their suggestions and constructive criticism were always welcome. Many discussions with Marty Yerg ended with mixed emotions, but I appreciate his interest and his assistance was invaluable.

I also recognize the help of many of my co-workers from the Atmospheric Sciences Laboratory, White Sands Missile Range, New Mexico. Discussions with Pat Avara have always been intellectually stimulating as he never reaches an end of how to apply mathematical techniques to a variety of problems. Dr. Willis Webb gave encouragement and freedom to work on this research. I am grateful to Gene Morris for his interest and assistance.

I have to acknowledge the understanding of my family. I regret their deprivation of a father and husband when it was most needed.

Computations for this work were done on the UNIVAC 1108 and the CDC 7600.

TABLE OF CONTENTS

LIST OF TABLES

TABLE		Page

LIST OF ILLUSTRATIONS

FIGURE | Page

FIGURE Page

OPTIMAL SAMPLING OF A STRATOSPHERIC SUDDEN WARMING

CHAPTER I

INTRODUCTION

It is convenient to consider the atmosphere in terms of regions according to certain characteristic features, i.e., temperature, turbulence, composition, ionization, chemical reactions, magnetic fields, or circulation indices. The most common feature is based on thermal stratification and that is the characteristic that will be used here. To avoid confusion, as the same word used by different people sometimes different meanings, a brief definition of each region and boundaries of the atmosphere will be given and depicted in Fig. 1.

The troposphere is that layer of the atmosphere extending from the surface of the earth to the tropopause. Most of the meteorological phenomena such as clouds, thunderstorms, and tornadoes occur in this region. The troposphere has, on the average, a temperature lapse rate of 6.5C per km until the tropopause boundary is reached.

The tropopause is defined as the lowest level at which the temperature lapse rate decreases to 2C or less per km. The tropopause is higher and colder over the equatorial regions (approximately 18 km),

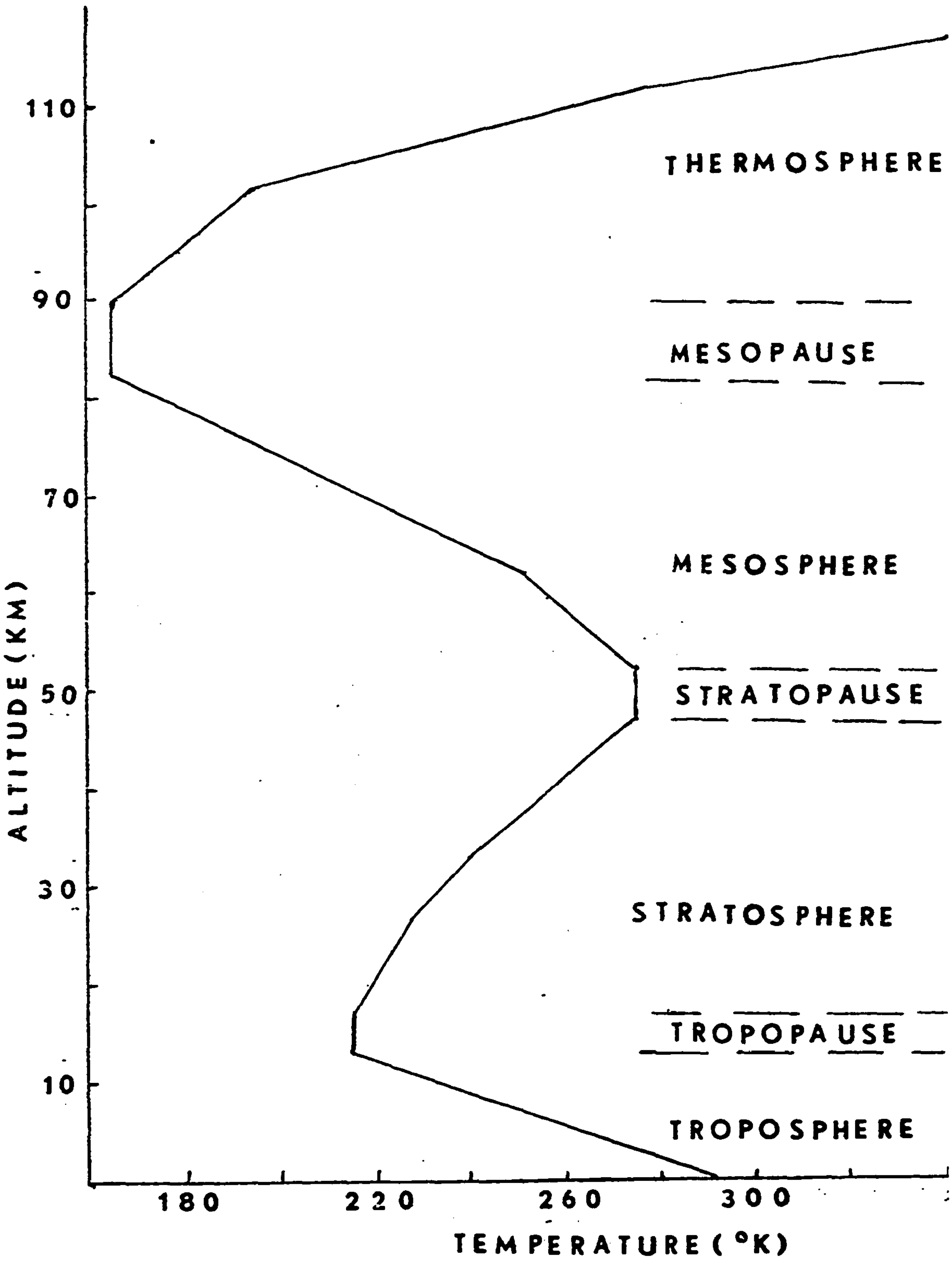

Fig. 1. 1966 U. S. Standard Atmosphere for the month of July at 45N latitude.

and lowers over the polar regions to 8 km. A value of 13 km is given in Fig. 1 based on the temperature profile given in the U.S. Standard Atmosphere, 1966, for July at 45°N.

Above the tropopause the temperature increases with height until the stratopause is reached. The stratosphere is the region between the tropopause and stratopause, and is the area of primary interest here as many intriguing and important phenomena occur in this region.

The temperature decreases with height above the stratopause until the mesopause is reached (approximately 80 km). The region between the stratopause and mesopause is the mesosphere. The mesosphere is an interesting area and no doubt influences the activities that occur in the stratosphere, and reciprocally, some of the circulation systems found in the stratosphere extend into the mesosphere.

The temperature increases with height above the mesopause in a region known as the thermosphere. Temperatures in the thermosphere have been calculated from the electron (or ion) density profiles and from observations of satellite drag (Glasstone, 1965).

CHAPTER II

LITERATURE SURVEY

As mentioned earlier our main concern is of the stratosphere and, in particular, warmings that suddenly occur in that region. The first sudden warming that was noticed was documented by Scherhag (1952) and occurred over Berlin, Germany during the 1951-52 winter. After more than 20 years of research and numerous reports, no one can definitely offer a complete explanation of the origin and maintenance of a sudden warming.

For a better understanding of some of the characteristics that define a stratospheric sudden warming, we should be familiar with the circulation of the stratosphere. Much knowledge has been gained about the stratospheric circulation due to the use of meteorological rockets (Webb, et al., 1961) and satellites (Shenk and Salomonson, 1970). As of January 1973, over 17,000 temperature and/or wind observations had been made by meteorological rocket payloads at 44 different locations over the world. The data are now published under the title of "World Data Center A -- High Altitude Meteorological Data" by the National Oceanic and Atmospheric Administration, National Climatic Center, Asheville, North Carolina.

The 10 mb constant pressure chart (approximately 30 km) is an excellent chart to portray the stratospheric circulation features as data used in the analyses have been obtained from balloon and rocket soundings. Fig. 2 illustrates a typical winter situation of a circumpolar low pressure cell that dominates the circulation. This means west winds (winds blowing from the west) are found over the middle and high latitudes. Wind speeds usually reach a maximum of 40 to 50 mps during December. A belt of high pressure can usually be found over the sub-tropical latitudes, and a trough of low pressure is present most of the time over the southwestern United States.

During the summer, high pressure is centered over the North Pole with easterly winds over most of the Northern Hemisphere as shown in Fig. 3. Speeds of 10 to 20 mps are common with the average maximum reaching 40 mps during July. Webb (1966) has plotted the average wind components of a 10 km layer between 45-55 km for different locations as shown in Fig. 4a and 4b. The mean zonal flow has more variability between winter and summer than the meridional. Note in Fig. 4a that the reversal of the winds from west to east occurs between April 15 and May 15 starting with the northern-most stations. The same sequence occurs in the fall with the winds reversing first at the northern-most stations, but the wind reversal at the mid-latitude stations occur within a few days of each other. These transition periods between the winter and summer circulations have been discussed by Miers (1963) and Webb (1966), and Webb has suggested that a variety of solar influences are prevalent in the stratospheric circulation.

Now that the main circulation features of the stratosphere have been presented, perhaps a definition of a warming that occurs in this medium is in order. An explicit definition of the stratospheric

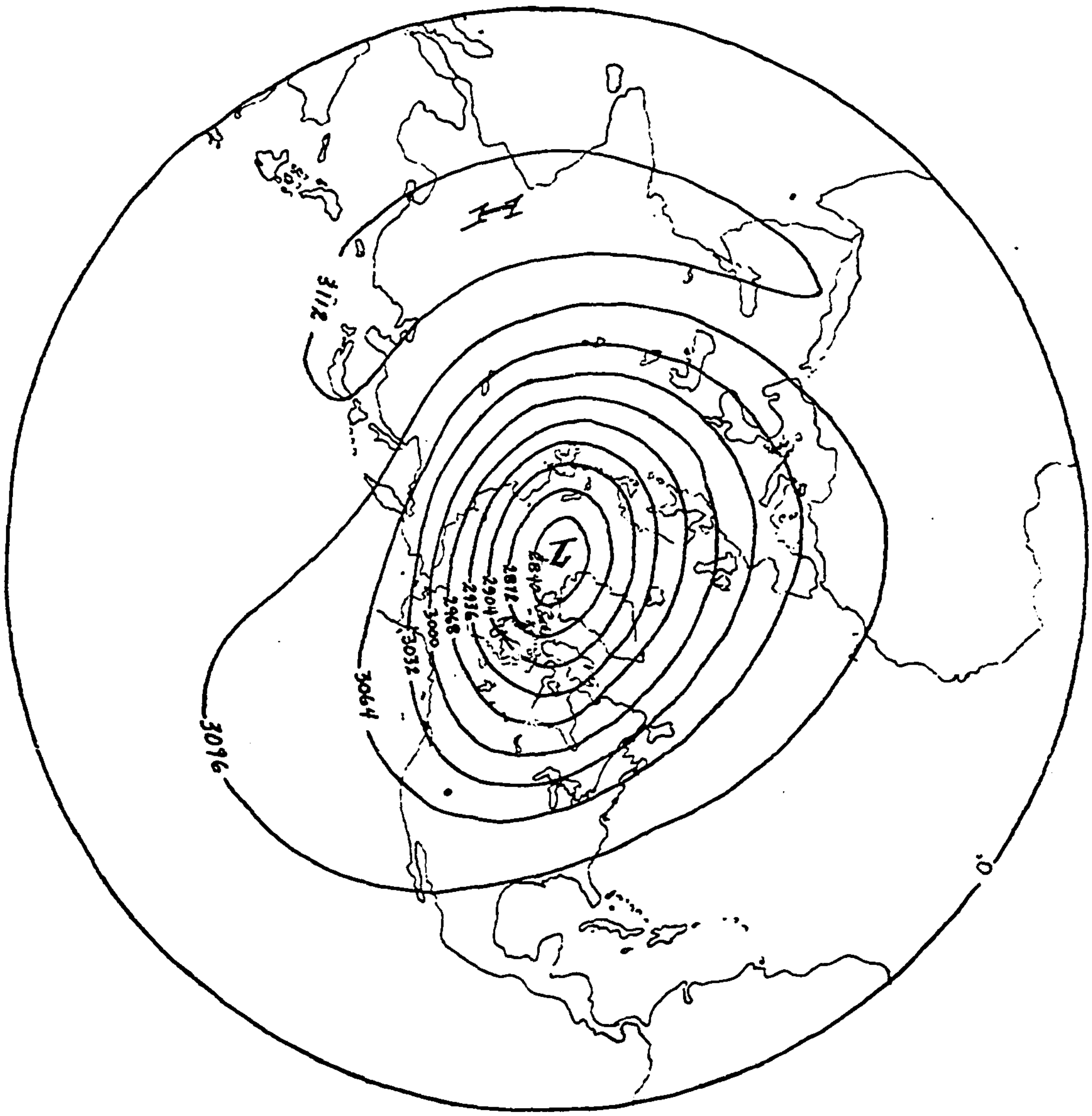

Fig. 2. Mean contour map of 10-mb surface during winter (after Kriester, et al., 1963–1965). Contour heights are in tens of geopotential meters.

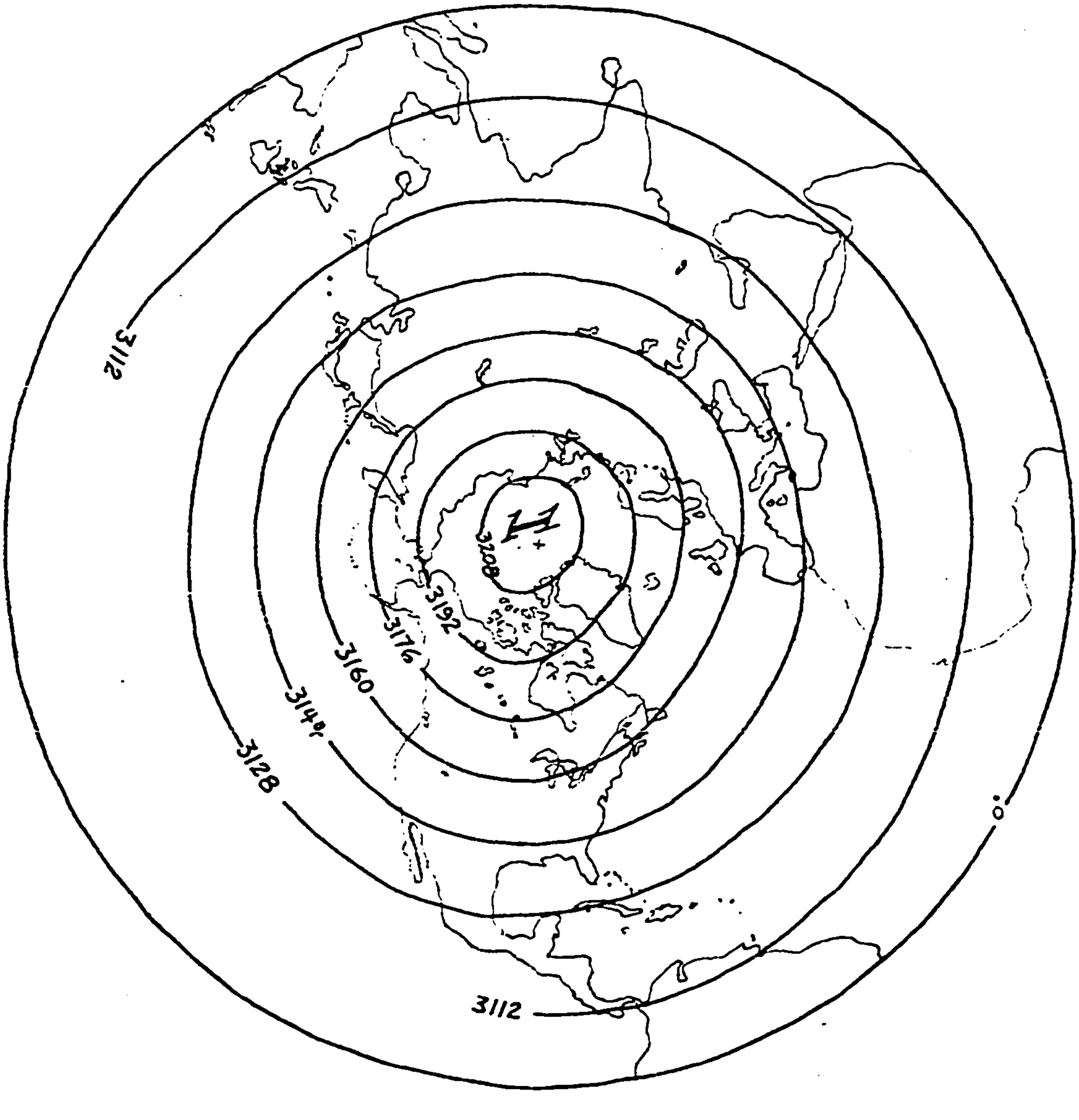

Fig. 3. Mean contour map of 10-mb surface during summer (after Kriester, et al., 1963–1965). Contour heights are in tens of geopotential meters.

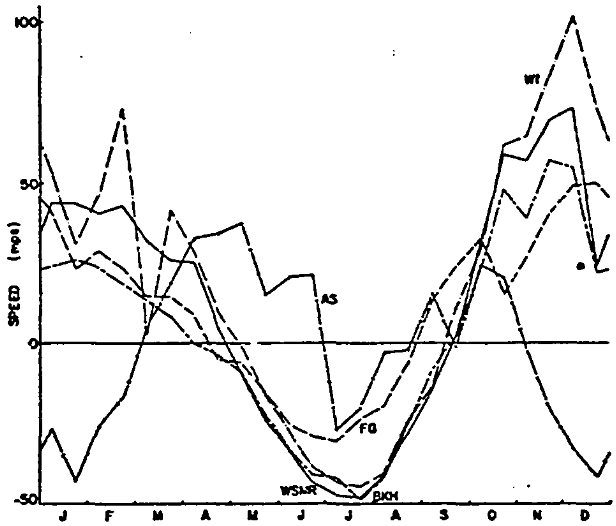

Fig. 4a. Mean zonal SCI data for selected stations plotted to illustrate the meridional structure of the stratospheric circulation. AS-Ascension Island, WI-Wallops Island, FG-Fort Greely, BKH-Barking Sands, WSMR-White Sands Missile Range. (after Webb, Structure of the Stratosphere and Mesosphere, Fig. 4.7)

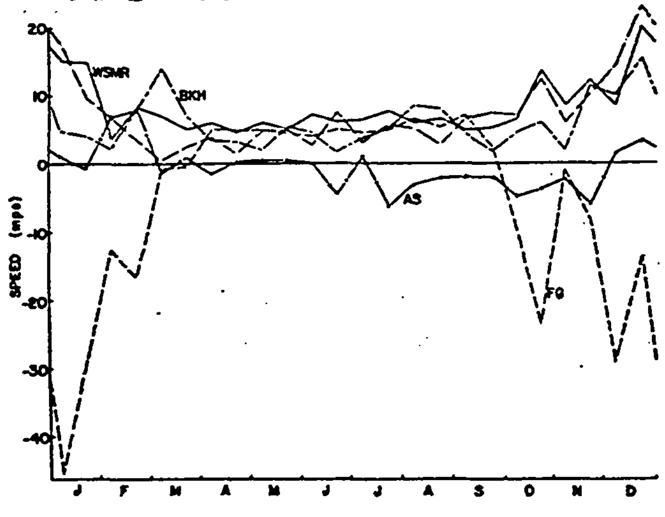

Fig. 4b. Mean meridional SCI data for the stations in Fig. 4a. (after Webb, Structure of the Stratosphere and Mesosphere, Fig. 4.8).

sudden warming has been made by Julian (1967) in which a distinction should be made between major, minor, and the warming that occurs just before the spring transition period. Webb (1966) offers this definition of a sudden warming - "a dynamic event in the stratospheric circulation which is principally characterized by a temperature increase in polar regions immediately above the stratonull level greater than 50C over a period of ten days or less, accompanied by a disruption of the usual westerly zonal circumpolar flow of the stratospheric winter circulation". The stratonull is a transition layer between the tropospheric and stratospheric circulation and is usually found in the 25 to 30 km region. Minimum values of wind components are usually found in this region.

Kellogg and Schilling (1951) were the first to utilize all available data sources (rockets, high level balloons, acoustic soundings, noctilucent clouds, meteor observations, and radio wave propogation) to propose a simple circulation model from the surface to 120 km. Their model included the winter westerlies, summer easterlies, prevailing westerlies above 80 km, sinking air over the winter polar region, and rising air over the summer pole. They concluded that the complex radiational heating that occurs in the stratosphere is sufficient to provide the driving force necessary for the stratospheric circulation.

After Scherhag's report of the sudden warming over Berlin in the 1951-52 winter, researchers began to think twice before discarding a suspiciously warm temperature value. The early research done on stratospheric sudden warmings and stratospheric circulation consisted of plotting temperature profiles on time-height cross sections and also analyzing the 100, 50, 25, and 10 mb constant pressure charts. [See the work of Scarse (1953), Teweles and Finger (1958), Teweles (1958), Craig and Hering (1959), Palmer (1959), Boville (1960), Hare (1960), Scherhag (1960), Teweles, Rothenberg and Finger (1960)]. All but Scrase discuss the January 1958 warming that occurred over Churchill, Canada. A warming of some 30C over North America is all that could be detected using the constant pressure charts, but by making use of rocket data (Teweles, 1961), grenade data (Stroud et al., 1960) and the falling sphere technique (Jones et al., 1959) it was found that a four day temperature increase of nearly 70C occurred over Ft. Churchill in the layer between 38 and 41 km. Teweles believed that subsidence as well as advection had to account for such a tremendous temperature increase.

Craig and Lateef (1962) computed vertical motions over North America, Canada, and North Atlantic area during the 1958 warming. Their vertical motion fields indicated that upward motion occurred east of troughs and downward motion west of troughs before a sudden warming started. After the commencement of a sudden warming a very large area of uniform downward motion existed. Extreme values were 8 cm per sec at 25 mb to 4 cm per sec at 100 mb. It had been hypothesized earlier by trace transport investigators that downward motion occurs over the winter time polar regions (Brewer, 1949; Dobson, 1956; Goldie, 1950; Palmer, 1959; Lilly and Palmer; 1960). However, Mahlman (1969) computed a stratospheric mean circulation for periods before, during, and after the 1958 warming by using a heat balance method. His calculations indicated rising motions over the polar cap during a sudden warming and that vertical motion cannot be explained by considering thermodynamic processes.

The need for synoptic analysis higher than the 10 mb level was apparent since time-height cross sections indicated that the largest temperature increase in the 1958 warming was near 40 km. Keegan (1962) used rocket data to illustrate that the entire region from 30 to 70 km is a region of considerable activity during the winter. Finger et al., (1963) discussed the procedures that could be used to do a synoptic analysis based on meteorological rocketsonde data at the 2 mb (near 42 km) and .4 mb (near 55 km) by building up from the 10 mb level. They illustrated that an explosive warming could be detected at higher altitudes. These charts were analyzed on a weekly bases by the Upper Air Branch, Numerical Methods Center (NMC), National Oceanic and Atmospheric Administration (NOAA), from 1964-1967 and are analysed for selective periods now.

The next major warming occurred during January 1963. Morris and Miers (1964) illustrated that the sudden warming developed over the Atlantic when a ridge of high pressure formed in symmetry with a Pacific ridge. On the 23rd of January, the polar vortex split and moved southward over Northwest Canada and Northeast Europe. The warm center appeared south and east of the cyclonic vortex over the Hudson Bay area and migrated poleward. By 30 January, the polar night westerlies had collapsed and disappeared. It was not until the middle of February that the winter circulation began to reappear as a cyclonic vortex was established over Siberia. They also noted that some of the circulation features observed near 30 km retained their identity above

50 km. Warnecke and Nordberg (1965) also noted that the Aleutian anticyclone extended up to 70 km. Finger and Teweles (1964) in their study of the 1963 midwinter warming stated that the 25 to 55 km region belongs to the same regime. The used 10, 2, and .4 mb constant pressure charts and time-height cross sections for their investigation. They concluded that major warmings are associated with regression of middle stratospheric systems and that the favored location of an initial warming is on the eastern side of a bipolar trough that extends into mid-latitude. All of the studies have noted that the warming starts at high altitudes and progresses downward. The slope of the warming seems to be in the direction of movement. The 1963 warming extended down to the 500 mb level and even caused a wind reversal there (Julian and Labitzke, 1965) Julian and Labitzke (1965) in their study of tropospheric events and relationship to stratospheric warmings found that warmings began during strong meridional circulations and that blocking conditons are typically upstream from the region of initial stratospheric warmings. However, blocking conditions do not guarantee that a warming will occur.

Fig. 5 illustrates the dramatic warming of 1963 by plots of mean temperature values at the 10 mb level for various latitudes at 0°. 90°W, 180°, 90°E longitudes. The curve that extends to -8C on 18 January is daily temperatures observed at 60°N, 90°W.

Labitzke (1965) surmised that there is a connection between the 26-month cycle in the lower stratospheric winds in the tropics and the cycle in stratospheric warmings. She used minor warmings to substaniate her theory that during alternate years the warmings originated

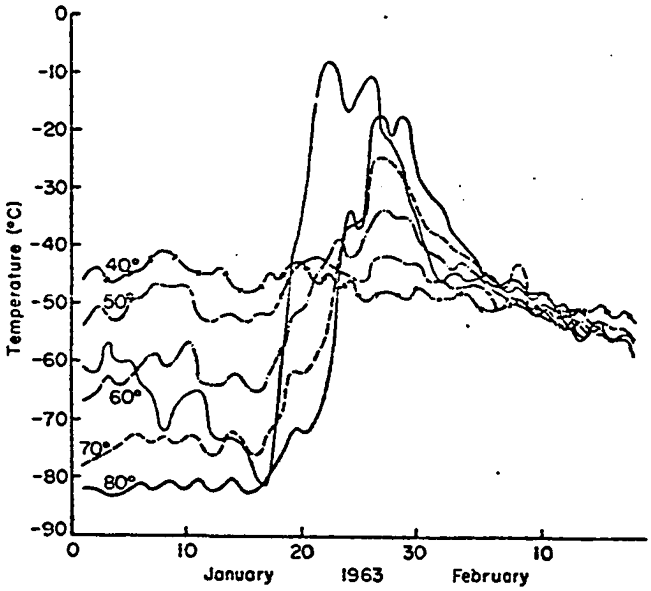

Fig. 5. Average temperature of various latitude circles on the 10-mb pressure surface of the upper stratosphere during the sudden warming event of January 1963. (after Webb, Structure of the Stratosphere and Mesosphere, Fig. 4.25).

over the Eastern United States and Canada or over Central and Eastern Europe. The relationship between the 26-month cycle of the stratospheric winds over the tropics and sudden warmings lacks in conclusive proof.

Williams (1968) analyzed 1 mb charts (near 47 km) at 3 day intervals to study a warming that occurred at the 30 to 55 km region in February 1966. The polar low did not split at 10 mb but did at the 1 mb level. He concluded that the circulation intensifies with height with higher wind speeds at the base of the mesosphere. High wind speeds were also noted by Quiroz (1969) in his work of the February 1966 warming. Quiroz utilized rocket data from Heiss Island, U.S.S.R. (80°37'N, 58°03'E) that portrayed a temperature increase of 85C at the 32 km level preceded by a record wind of nearly 400 kts at 39 km. Mesospheric data suggested that prior to a warming event the upper polar mesosphere is characteristically cold. This would substantiate Leovy's (1964) calculation of a -75C temperature at 75 km. Quiroz noted that the high winds were related to the pressure gradient intensification several days before the peak temperature.

Johnson (1969) compared the December 1967-January 1968 warming with previous warmings by using time-sections, spatial cross-sections, and the 2 and .4 mb charts. Williams and Miers (1969) discussed the same warming by using 40 and 50 km constant height charts, and constructing mean temperature charts between 40 and 50 km. They found that the largest temperature changes occurred near 30 km and amounted to 70C. They could not find a conclusive relationship between tropospheric and stratospheric events. This was also the conclusion of Miller and Johnson (1970) considering the 500 mb data.

Stratospheric warmings are not confined to the middle and upper northern latitudes. Mukherjee and Ramanamurty (1972) detected an increase of 26C at the 45 km level over Thunba India (8°N, 77°E) on 23 December 1970. Data from meteorological rockets fired from McMurdo Station, Antarctica as reported by Briggs (1965) were used by Quiroz (1966) to discuss a warming that occurred from mid-July to mid-August 1963. Quiroz states that arctic and antarctic warmings are similiar in that the circumpolar vortex is elongated and displaced. Finger and Wolf (1967) discuss the Southern Hemisphere circulation during March and April 1965 from data obtained by firing rockets from a ship that moved along the west coast of South America. They suspect that the Southern Hemispheric cyclone is more intense than the Northern Hemispheric cyclone.

Southern Hemispheric warmings have been the subject of many authors that have had access to satellite data (Kennedy et al., 1967; Julian, 1967; Shen et al., 1968; Belmont et al., 1968; Fritz and McInturff, 1972). Satellite data only gives information on an average temperature related value over a thick layer. However, sometimes it is sufficient to detect a sudden warming.

Nordberg et al., (1965), Zak and Panofsky (1968), Belmont et al., (1968), Fritz (1970), Fritz and Soules (1970), and Quiroz (1971) discuss the limitations of using satellite measured radiance data for deriving temperatures. Briefly, radiance in the CO_2 band centered at 15 microns is measured by an infrared spectrometer aboard the satellite. The radiances are a measure of a weighted mean temperature of approximately the upper 100 mb of the atmosphere. Belmont et al., (1968a) compared radiance values with temperatures at 100, 70, 50, 20, and 10 mb at 97 stations for 24 days and found a 0.7 correlation at both the 30 and 20 mb levels. Quiroz states that vertical temperature profiles inferred from infrared measurements do not appear to be ideally suited for monitoring sudden warmings above the 10 mb level. However, he uses the ratio of radiance change between two channels to determine the central altitude and amplitude of a warming. He derived warming amplitudes of about 20C in the lower stratosphere (20 km) and 30-35C in the upper stratosphere (40 km).

Relationships between the mesosphere and stratosphere have been investigated by several workers. Kellogg (1960 and 1961) studied the dynamics of the polar mesosphere and concluded that the polar mesosphere in winter should cool about 10C per day due to the loss of solar heat, but in fact the mesosphere is warmer in winter than in summer. Kellogg speculated that the loss of heat is compensated by the release of energy of recombination of atomic oxygen. Shapley and Beyson (1965) established by using 10 mb temperatures and daily values of ionospheric absorption that high values of absorption accompany stratospheric warmings. Hunten and Godson (1967) found a significant correlation between the sodium abundance at 90 km and 30 mb temperature values during a warming. Hook (1972) used wind patterns derived from meteor trails (75-105 km) over College, Alaska and found that winds reversed direction at those altitudes during the 1967-68 warming. Labitzke (1972) has inferred that the mesospheric and stratospheric areas interact because when there are temperature changes in the stratosphere there are opposite changes in the mesosphere.

The latest major warming occurred during the winter of 1969-70 and has been discussed only by Quiroz (1971) using satellite radiance data. Rocketsonde data from West Geirinish, Scotland indicates winds in excess of 150 mps and a temperature of +38C at 43 km on 27 December. It appears that the warm air moved over Northern Siberia and never moved over Alaska or the Northwest Territories.

The importance of learning more about the sudden warming can not be over emphasized. It does not take much imagination to visualize the change that occurs in the atmosphere during a sudden warming and some of the consequences. For example, communications could be disrupted in certain localities due to changes in or the temporary creation of an artificial ionosphere. Forecast trajectories of polar routed ballistic missiles could be in error due to the change in density and winds, but more important, the ability of radar detection and identification of such missiles would be impaired. Aircraft could take advantage of the reduced density and change in winds for a least cost flight path. The sudden warming is not only meteorologically intriguing but more knowledge of the phenomenon could be beneficial in several fields.

CHAPTER III

CASE STUDY OF THE DECEMBER 1967 - JANUARY 1968 WARMING

The stratospheric evolution that occurred during December 1967 - January 1968 was chosen for a case study for two reasons: this warming is an excellent example of a stratospheric sudden warming, and, data are available from the constant pressure charts that were prepared by the University of Free Berlin (Kriester, et al., 1967-1968).

Warm air (of -25C) was first detected over Southeastern Europe at the 5 mb pressure level on 17 December 1967 (Fig. 6). A belt of high pressure, located approximately near the 20 to 40 degree latitude circle, extends almost around the northern hemisphere. A trough of low pressure extends from the polar low, that is over Iceland, to Hudson Bay and southward to Northern Baja California, Mexico. The cold air is centered over Northern Greenland with a tongue of cold air extending to the north of the pressure trough. By 26 December (Fig. 7) the warmest air had increased in temperature to +10C and had moved over Southeastern Greenland. A circumpolar circulation still existed on 26 December, as evidenced by the low centered north of Victoria Island, Northwest Territories, but had weaken and filled 320 meters since 17 December. A high pressure cell over Central Siberia had intensified

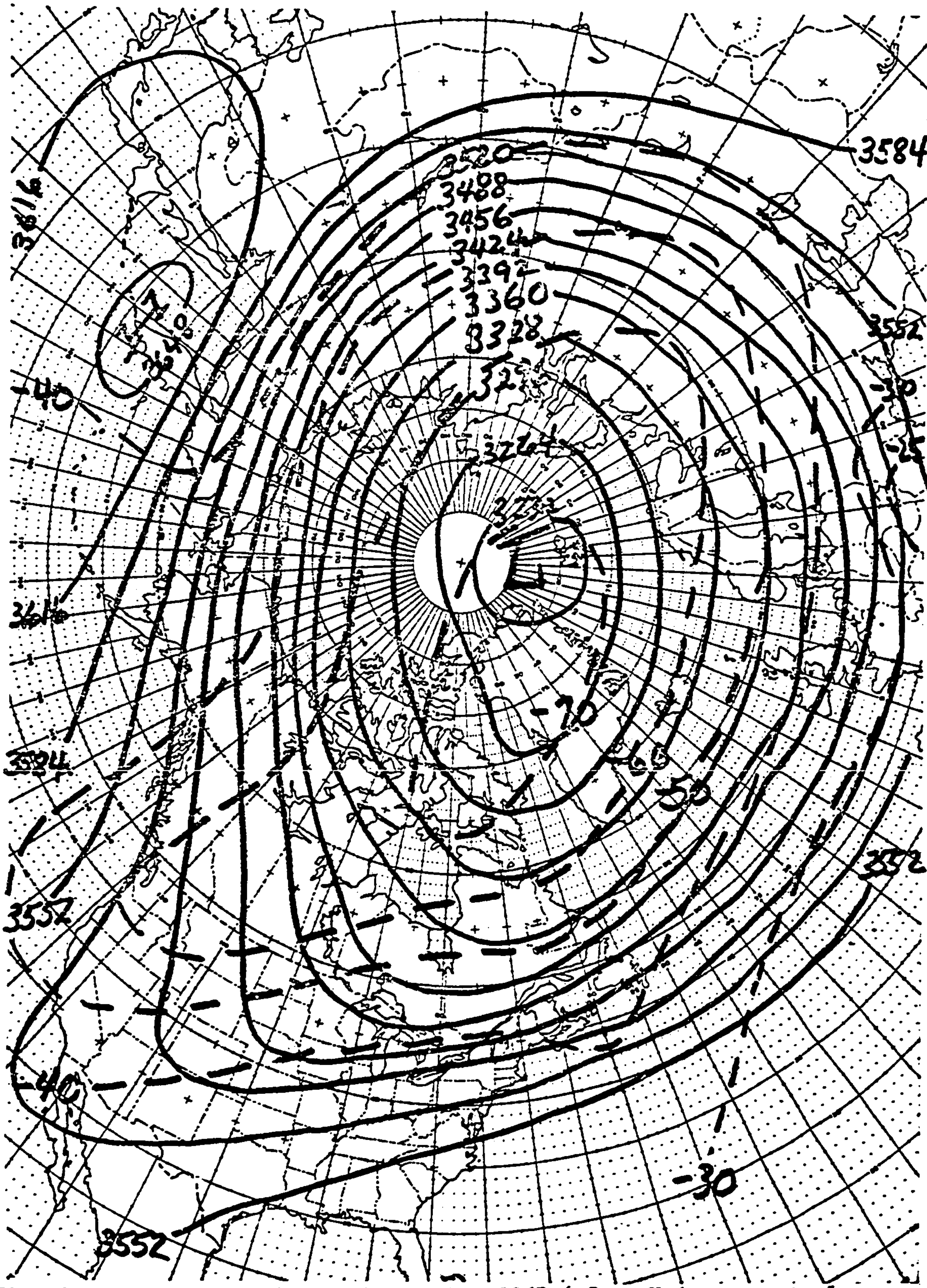

Fig. 6. 5 mb map at 00 GMT 17 December 1967 (after Kriester, et al., 1967). Contour heights are in tens of geopotential meters.

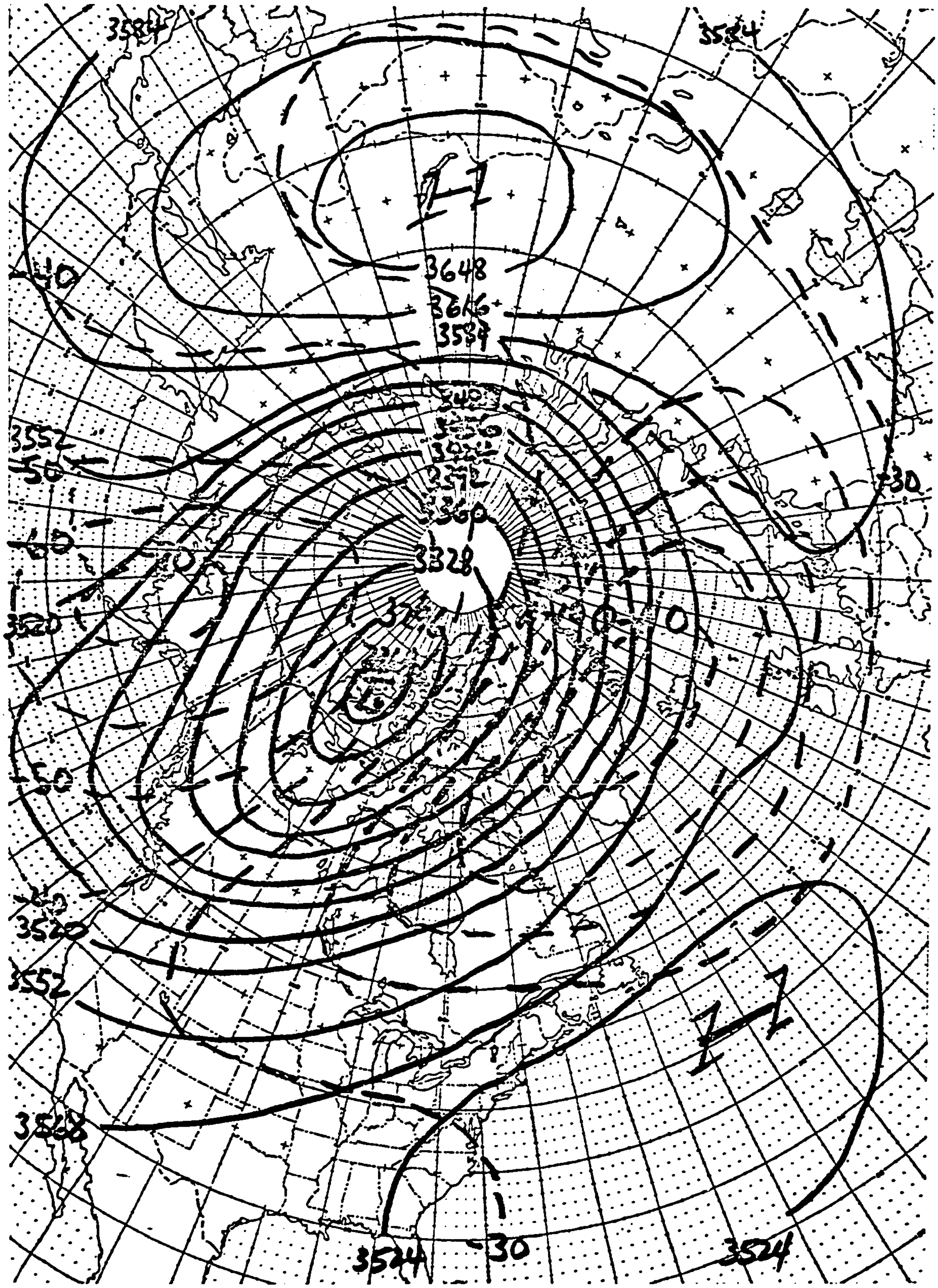

Fig. 7. 5 mb map at 00 GMT 26 December 1967 (after Kriester, et al., 1967). Contour heights are in tens of geopotential meters.

from 36480 to 36560 meters in the same nine day period. On 31 December (Fig. 8) the low pressure cell was located just southwest of Banks Island, Northwest Territories, and had become elongated in a north-south direction. The high pressure cell that was over Siberia moved eastward over Finland and intensified to a central value of 37040 meters. The warm air moved from Southeastern Greenland to Northern Hudson Bay and the temperature remained a +5C in the center.

On January 1, 1968 (Fig. 9) a low pressure center developed over Central Siberia; however, the main low pressure center moved southward from the previous day's location to Southern Yukon. This event marked the beginning of the cyclonic circulation associated with the sudden warming. The warm air center moved little from 31 December to 1 January, but maintained a +5C temperature although strong cold air advection was occurring.

By 5 January (Fig. 10) the low pressure cell was elongated by a southward push from a high pressure cell located just east of the southern tip of Greenland. The warm air broke into several centers with the main center remaining over Central Canada. The cooling of the warm air can be seen on 8 January (Fig. 11) as can the well defined double cyclonic circulation over Canada and Russia, and the high pressure ridge over the polar area near Greenland. The warm air moved over the Gulf of Alaska by the 12th (Fig. 12), although circum-polar cyclonic circulation did not return until 21 January.

The movement of the warm and cold air center for the period of 17 December 1967 to 12 January 1968 is shown in Fig. 13. The warm air was located to the west of Northern Africa on the 17th, moved

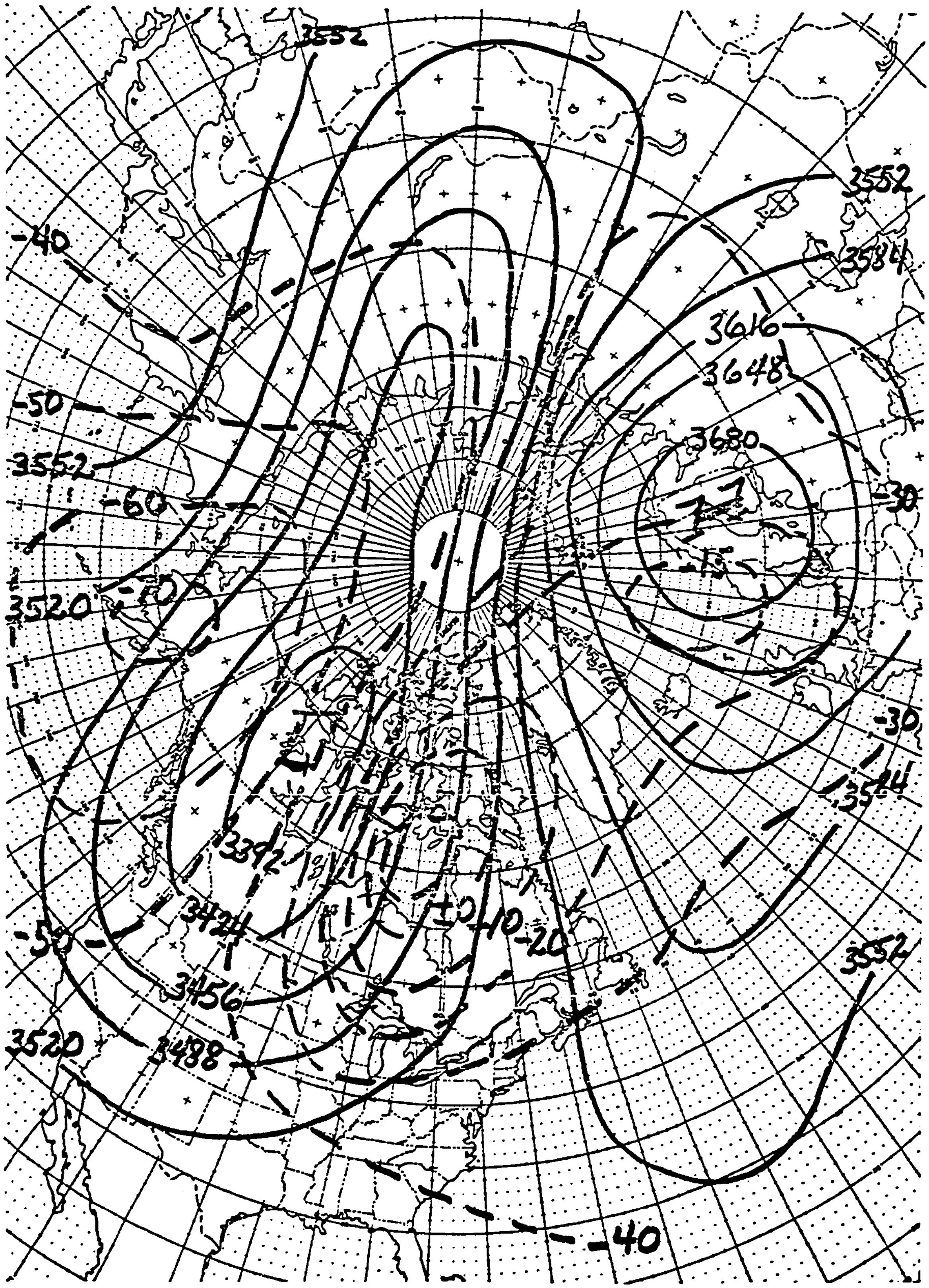

Fig. 8. 5 mb map at 00 GMT 31 December 1967 (after Kriester, _et al._, 1967). Contour heights are in tens of geopotential meters.

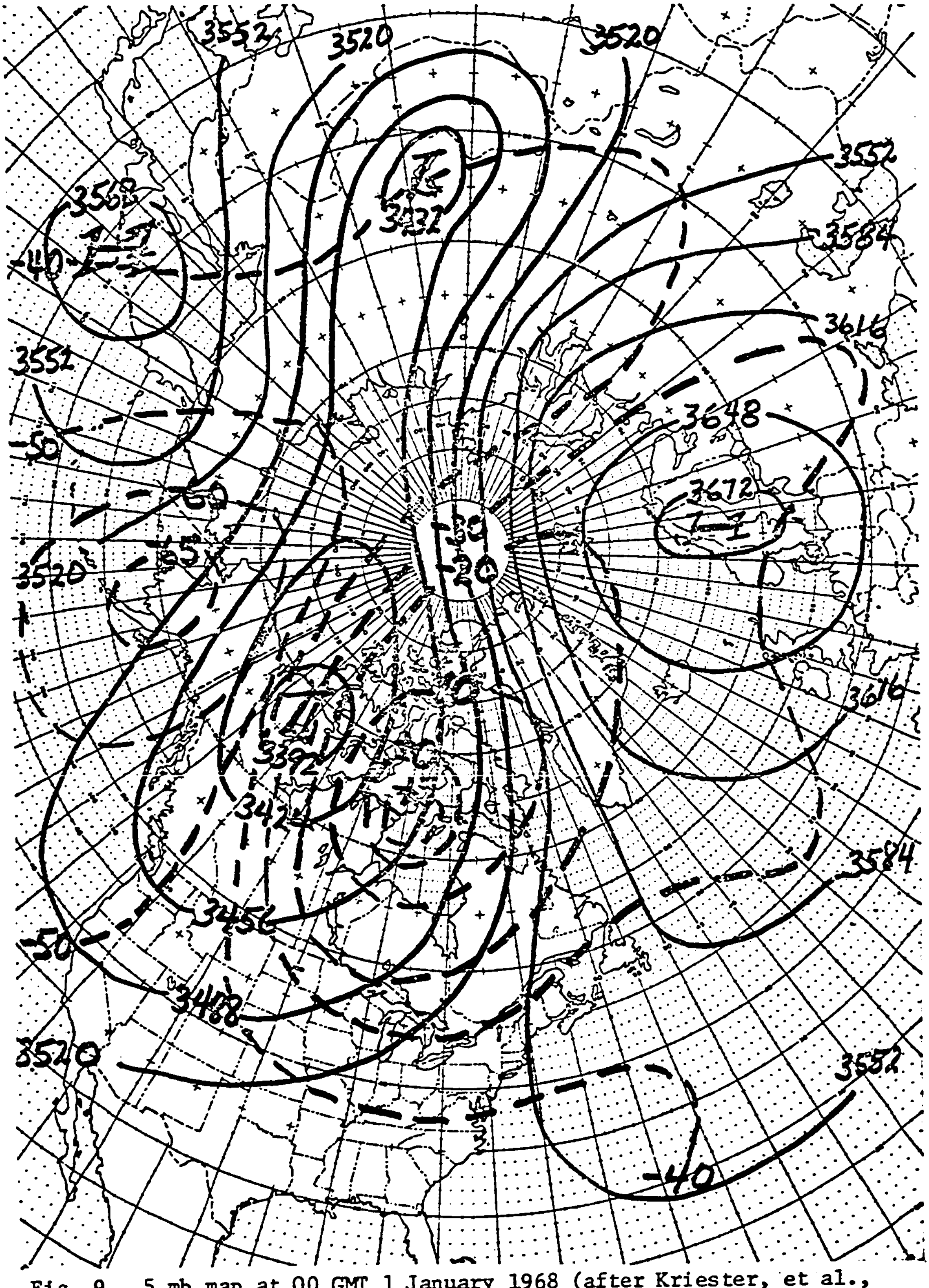

Fig. 9. 5 mb map at 00 GMT 1 January 1968 (after Kriester, et al., 1967). Contour heights are in tens of geopotential meters.

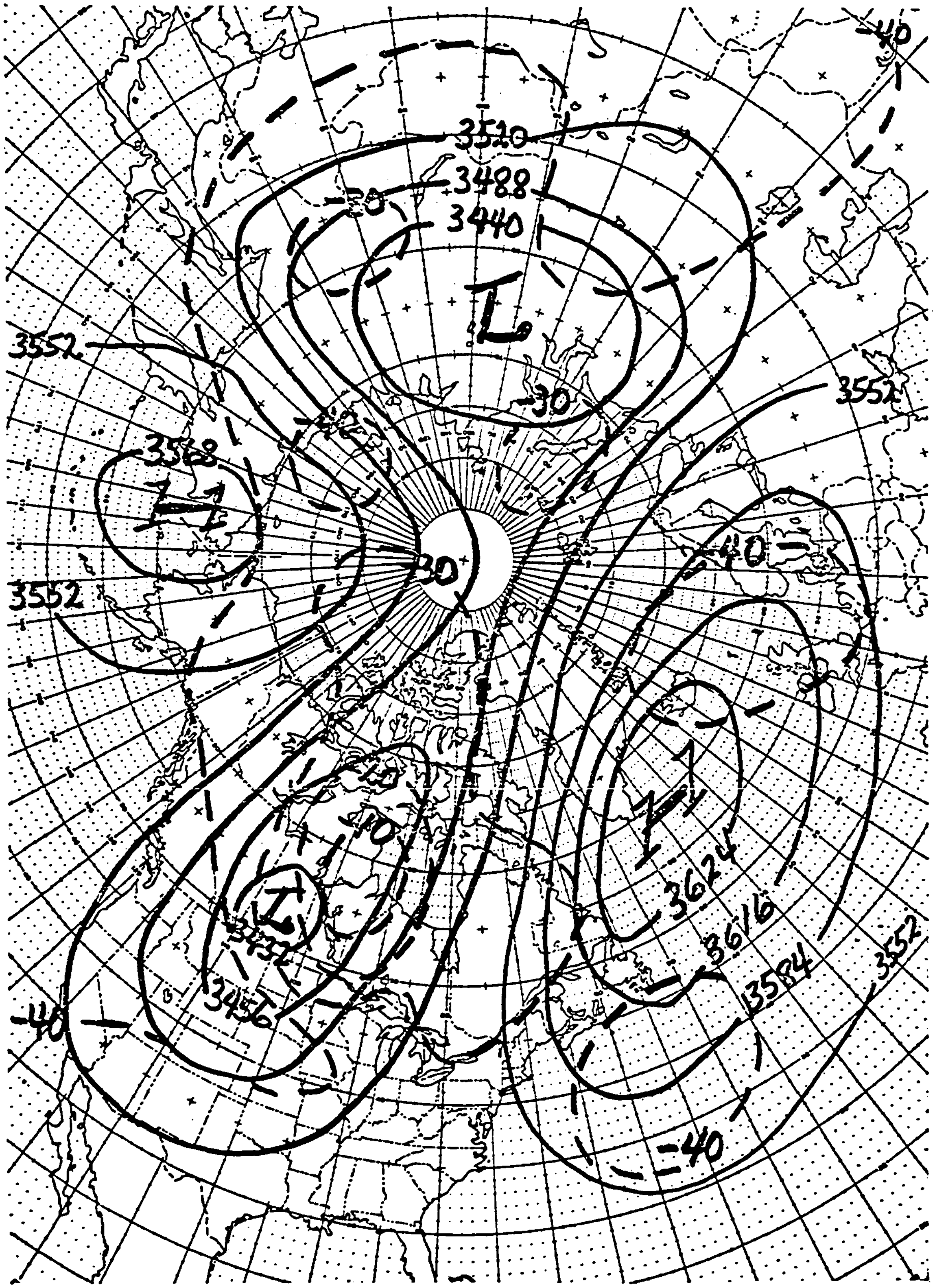

Fig. 10. 5 mb map at 00 GMT 5 January 1968 (after Kriester, et al., 1967). Contour heights are in tens of geopotential meters.

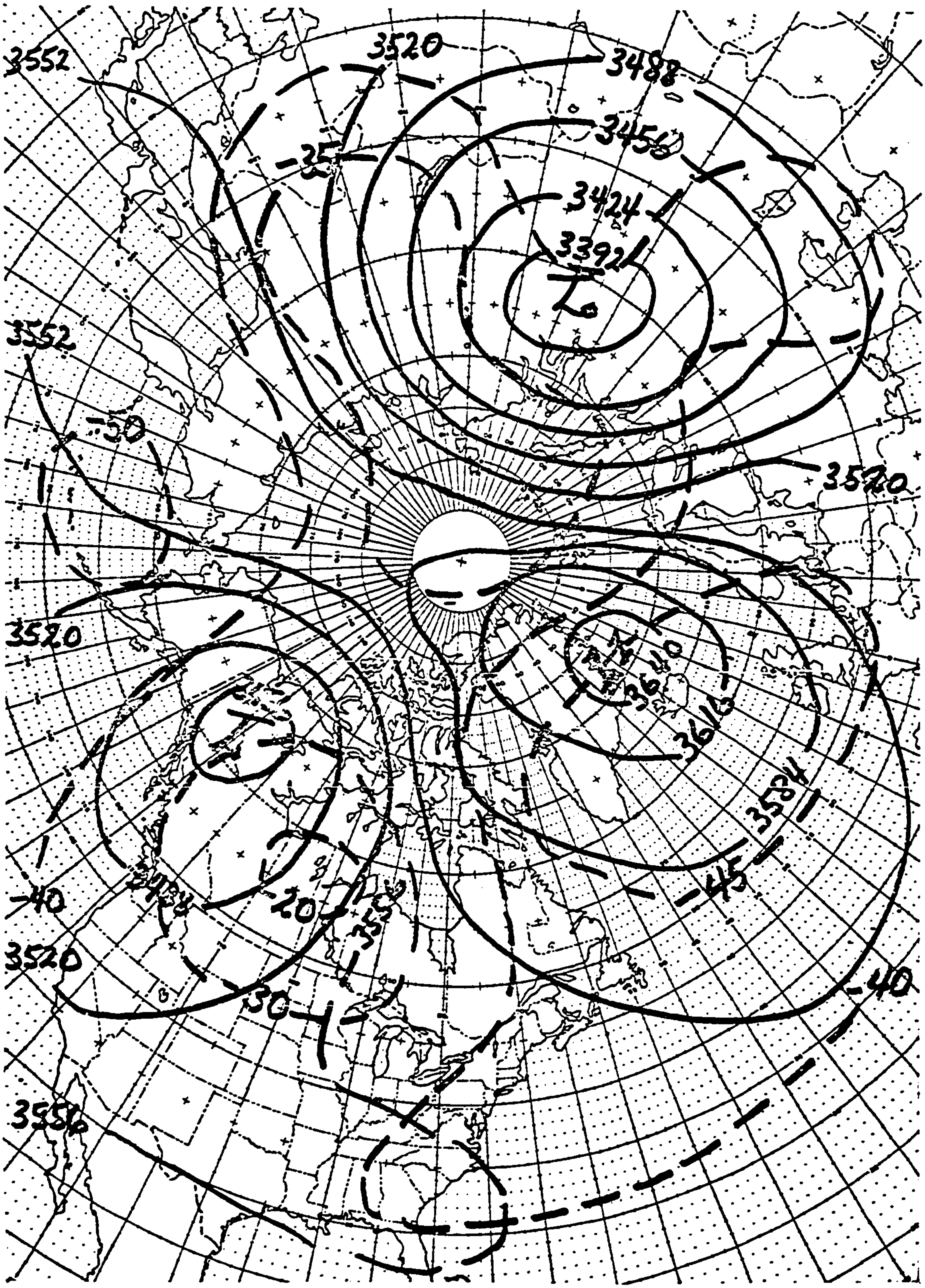

Fig. 11. 5 mb map at 00 GMT 8 January 1968 (after Kriester, et al., 1967). Contour heights are in tens of geopotential meters.

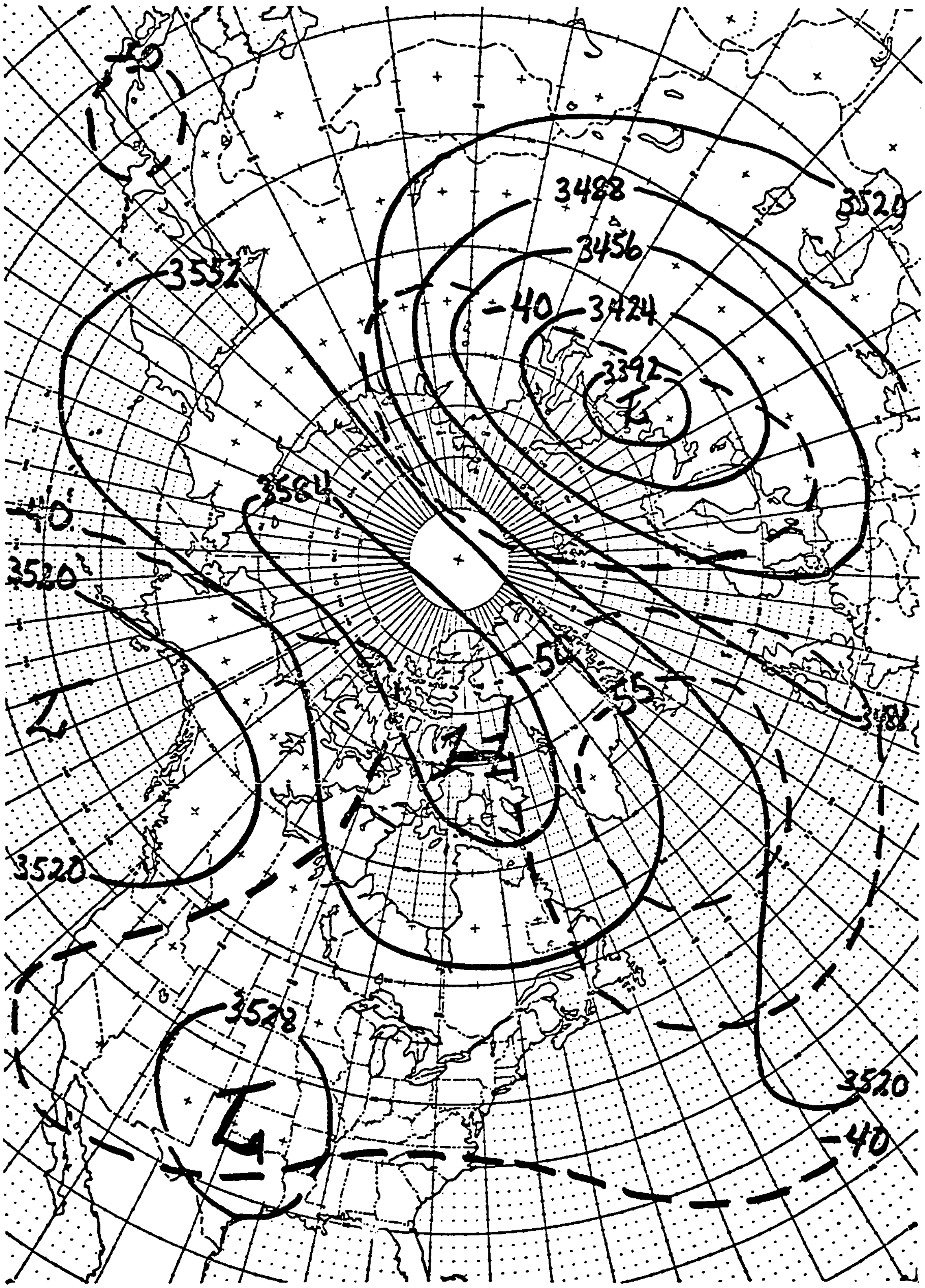

Fig. 12. 5 mb map at 00 GMT 12 January 1968 (after Kriester, et al., 1967). Contour heights are in tens of geopotential meters.

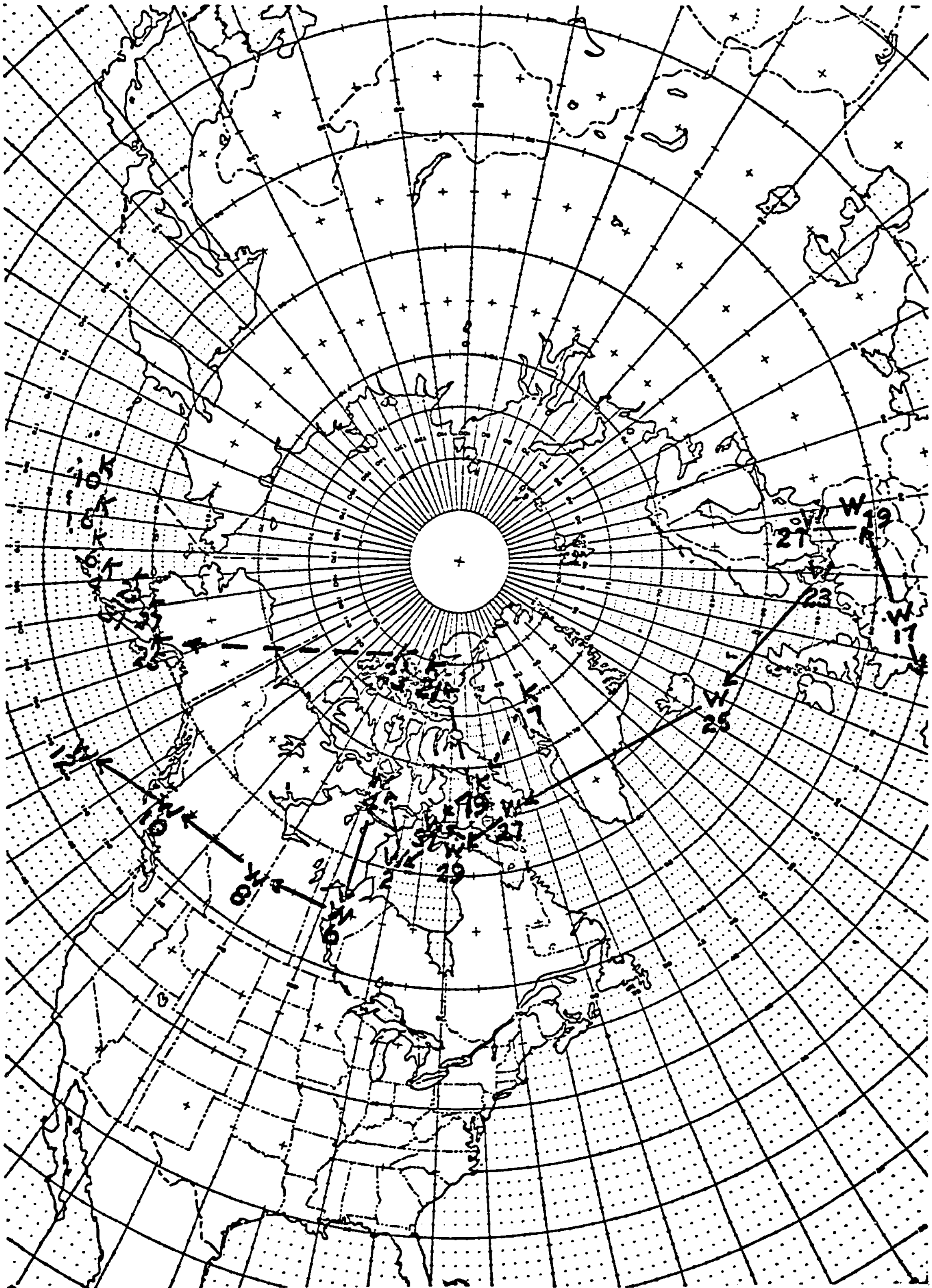

Fig. 13. Movement of the warm (W) and cold (K) air centers in two day increments from 17 December 1967 to 12 January 1968.

northeastward to Poland on the 19th and then began moving to the west; passing over Southern Greenland, southern tip of Baffin Island, Hudson Bay, and Southwestern Canada.

The maximum intensity of the warming that occurred at the 5 mb level was reached on 27 December (Fig. 14). Figs. 14, 15, and 16 are daily temperature plots from 20 December 1967 to 12 January 1968 for the 5, 10, 30, 50, and 100 mb levels for different latitude and longitude locations. Note the spectacular temperature increase of 80C in Fig. 14 as the temperature rose from a -67C on the 20th to a +13C on the 27th at the 5 mb level. The temperature increase associated with the warming was not as dramatic at the 10 and 30 mb levels and was not noticeable at the 50 and 100 mb levels.

The temperature did increase at the 50 and 100 mb levels, but it appeared as a gradual increase and not as a sudden warming. There was a two day lag in the maximum temperature increase between the 5 mb to the 30 mb level. This effect suggests that the maximum warming propagates downward in the atmosphere with time.

Figs. 17-21 show the distribution of pressure and temperature for 28 December 1967 for the 5, 10, 30, 50, and 100 mb levels. The warm air sloped to the southeast from the 5 mb down to the 30 mb level. The warm air is centered over Southhampton Island on the 5 mb chart, over Northern Quebec on the 10 mb chart, and over Goose Bay, Labrador on the 30 mb chart. The cold air slopes to the east from Southern Alaska at the 5 mb level to Yukon at the 10 mb level, and then northward to the Beaufort Sea at the 30 mb level. There was no indication of a warming effect over the Western Atlantic at the 50 and 100 mb levels.

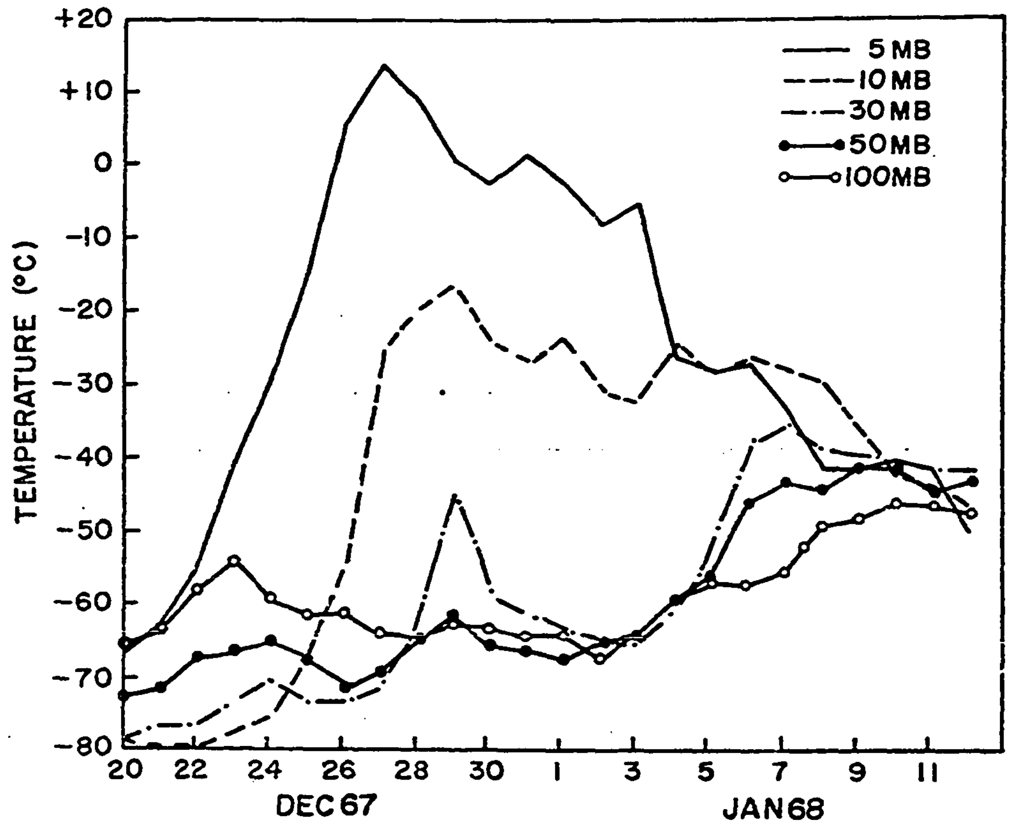

Fig. 14. Daily temperature values for the 5, 10, 30, 50, and 100 mb levels at 65N, 70W during 20 December 1967 to 12 January 1968.

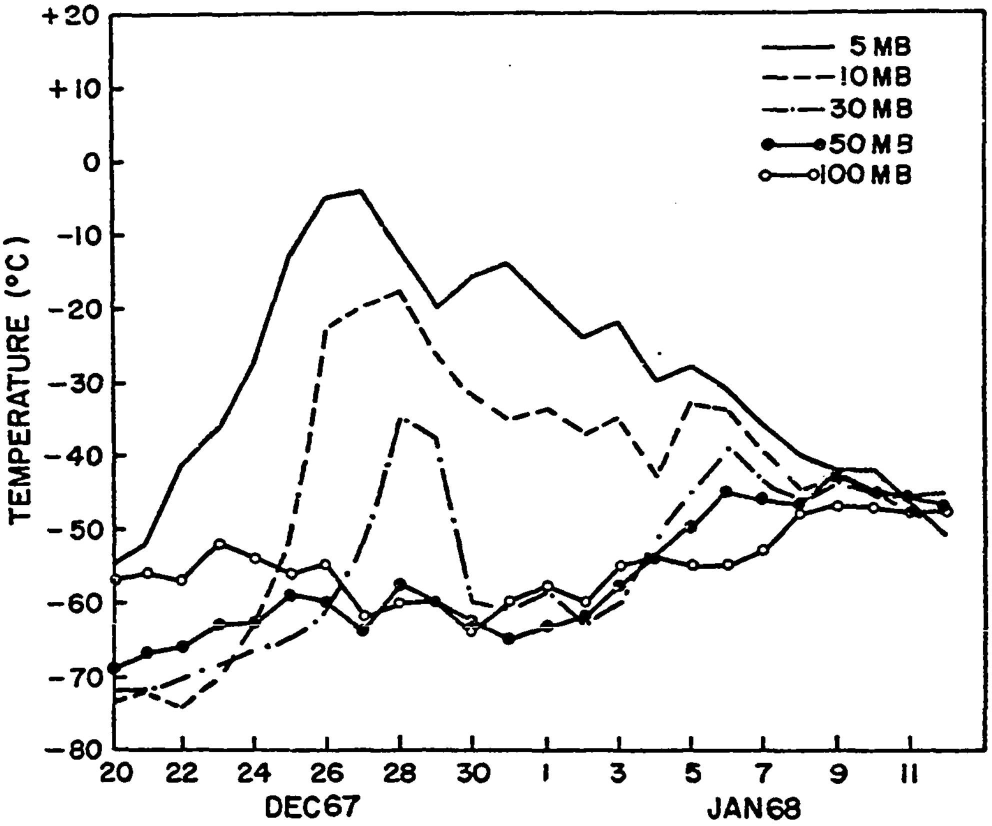

Fig. 15. Daily temperature values for the 5, 10, 30, 50, and 100 mb levels at 55N, 85W during 20 December 1967 to 12 January 1968.

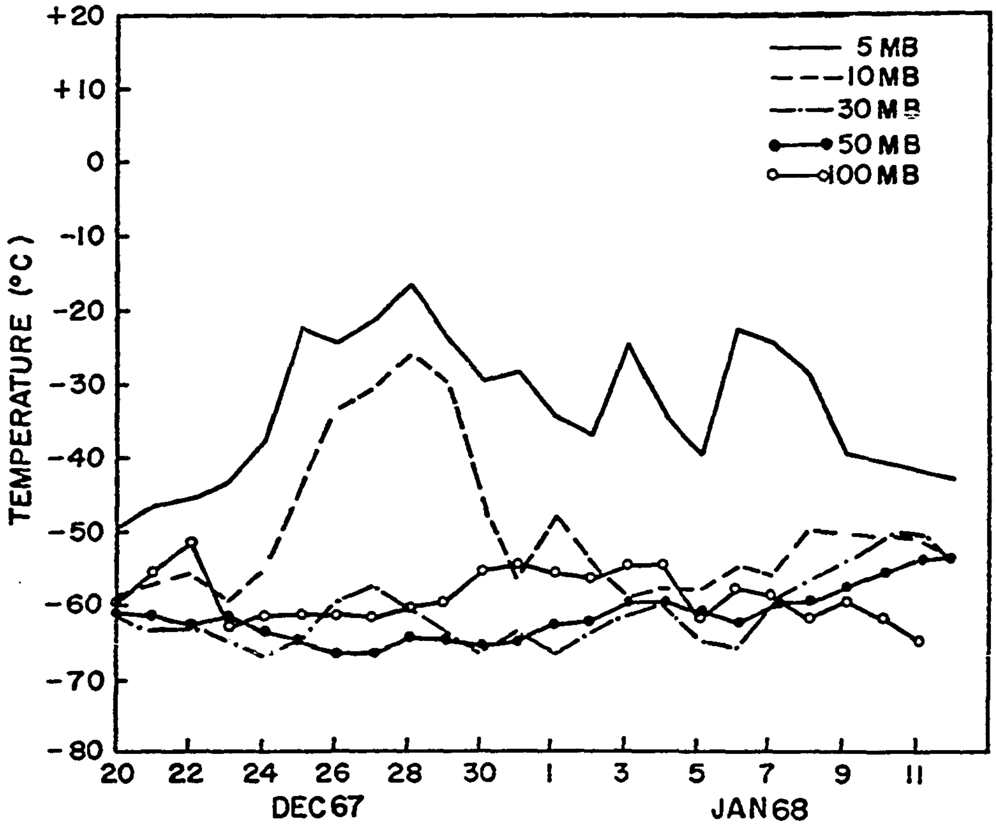

Fig. 16. Daily temperature values for the 5, 10, 30, 50, and 100 mb levels at 45N, 100W during 20 December 1967 to 12 January 1968.

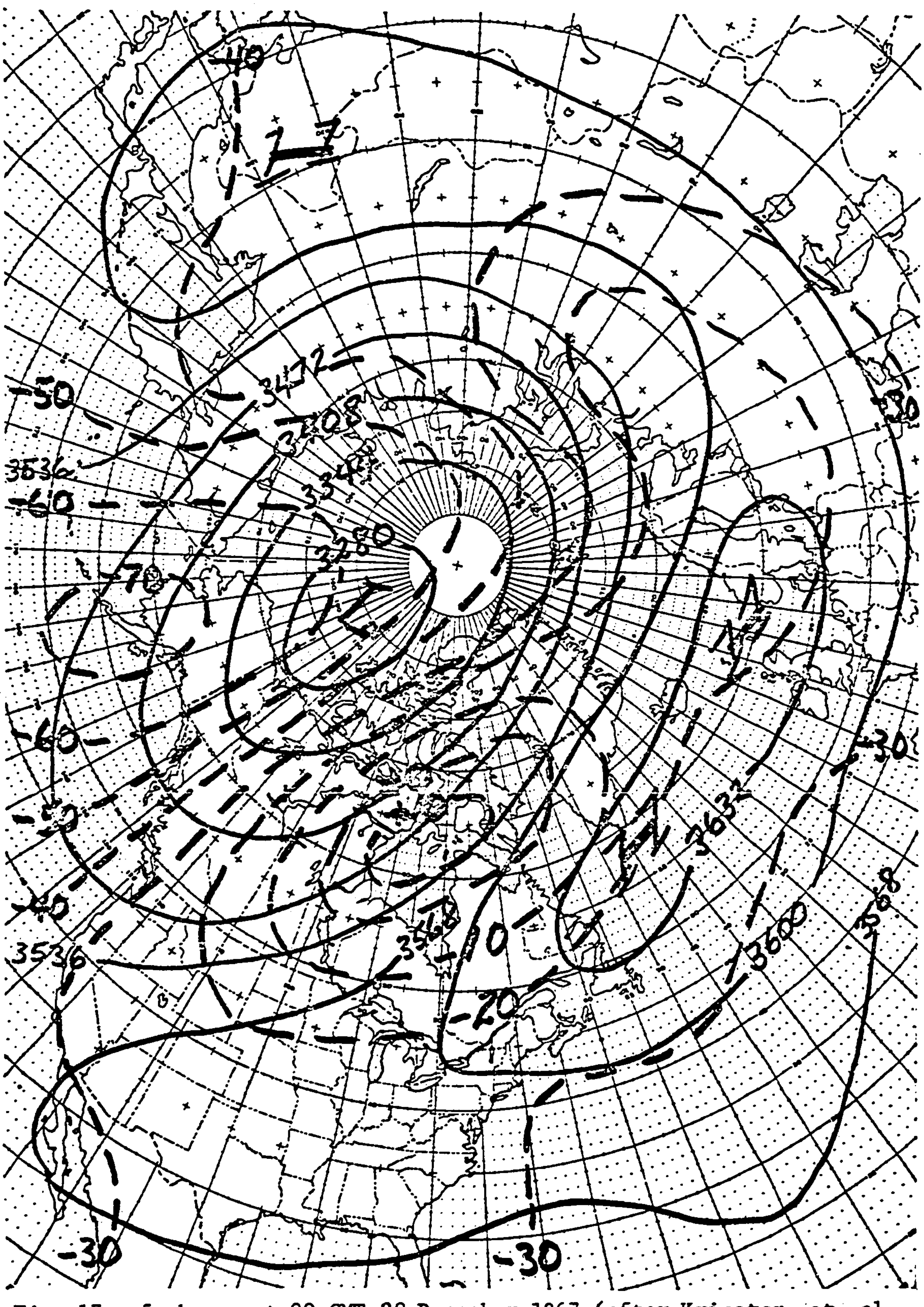

Fig. 17. 5 mb map at 00 GMT 28 December 1967 (after Kriester, et. al., 1967). Contour heights are in tens of geopotential meters.

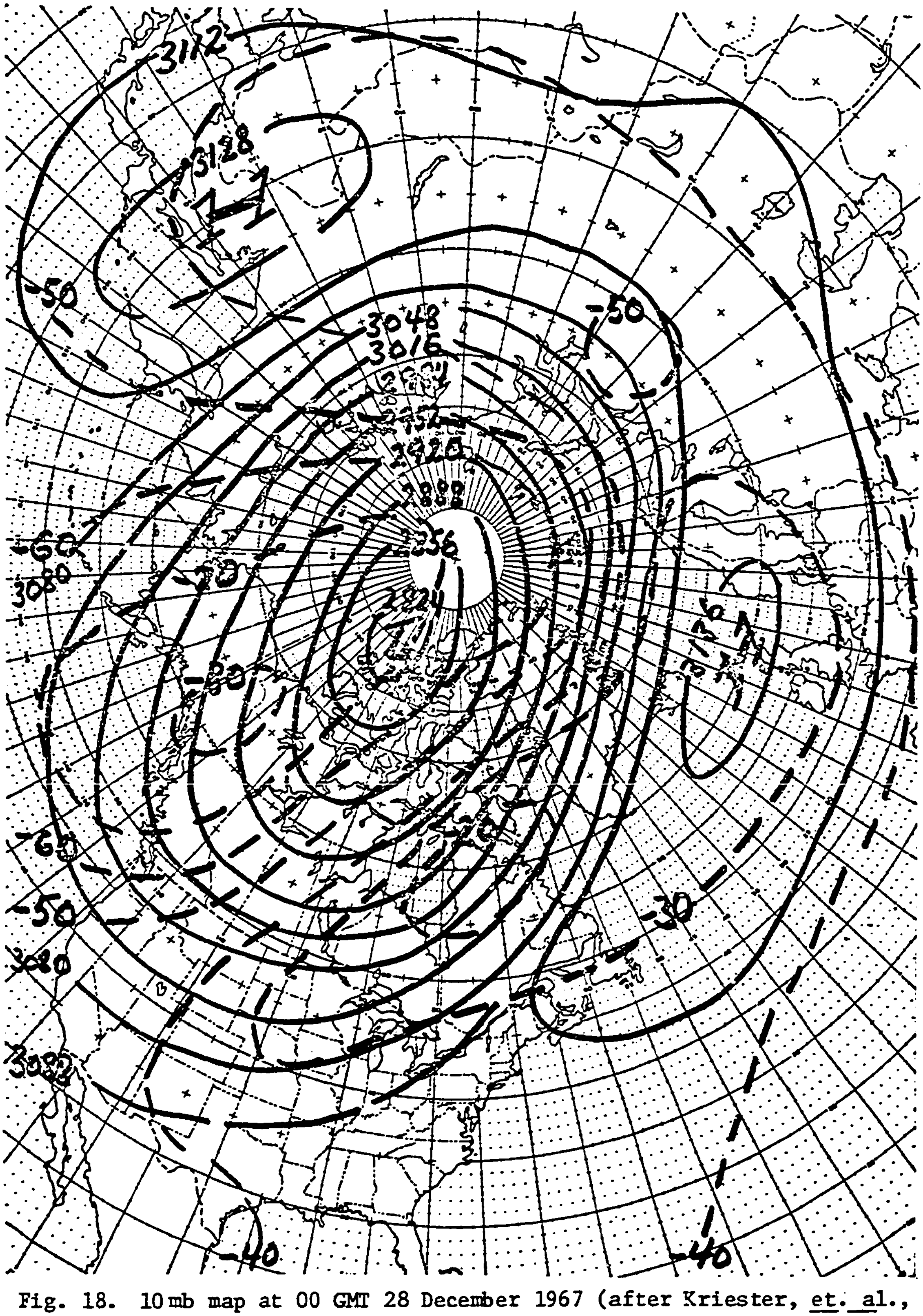

Fig. 18. 10 mb map at 00 GMT 28 December 1967 (after Kriester, et. al., 1967). Contour heights are in tens of geopotential meters.

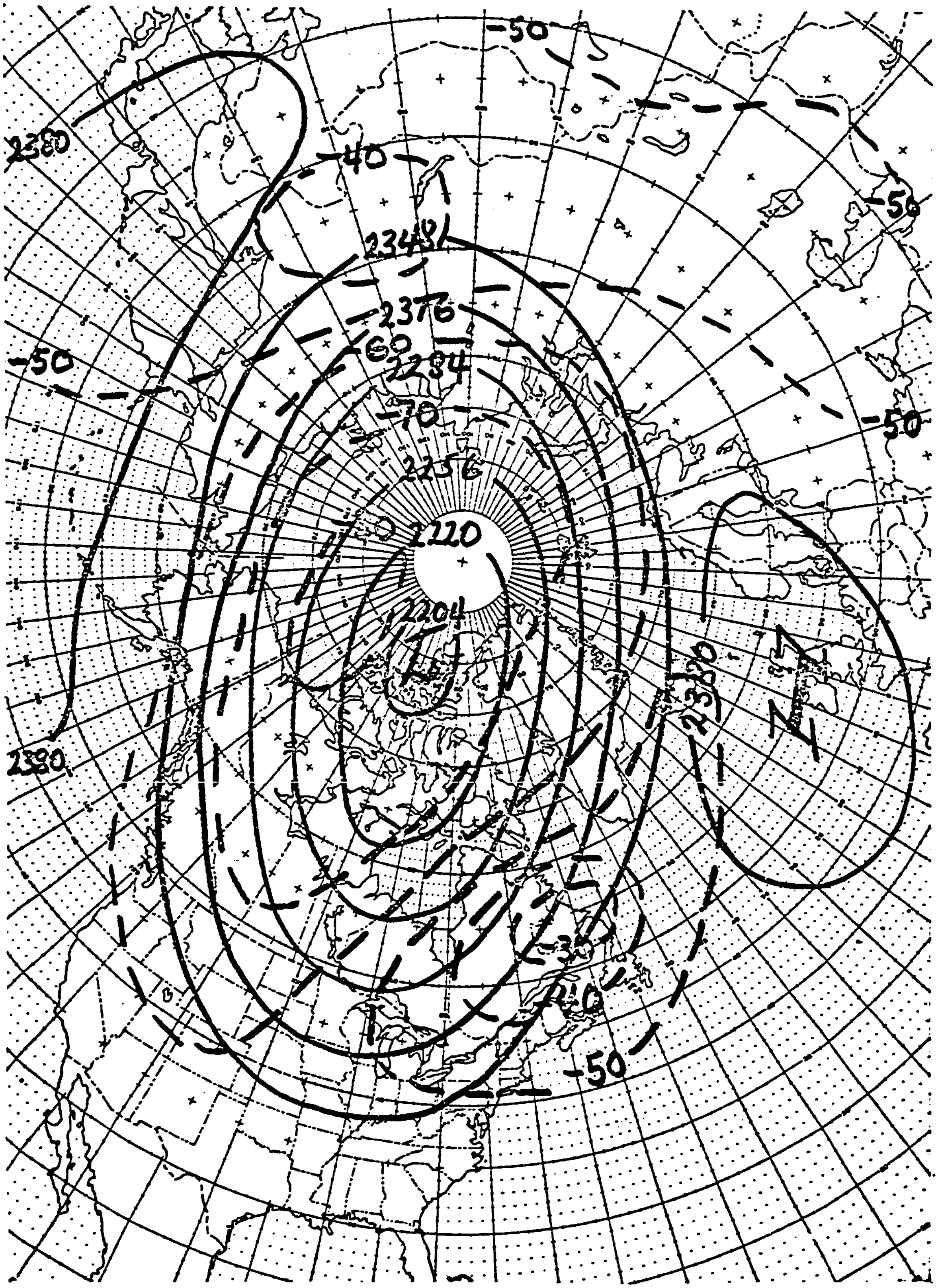

Fig. 19. 30 mb map at 00 GMT 28 December 1967 (after Kriester, et. al., 1967). Contour heights are in tens of geopotential meters.

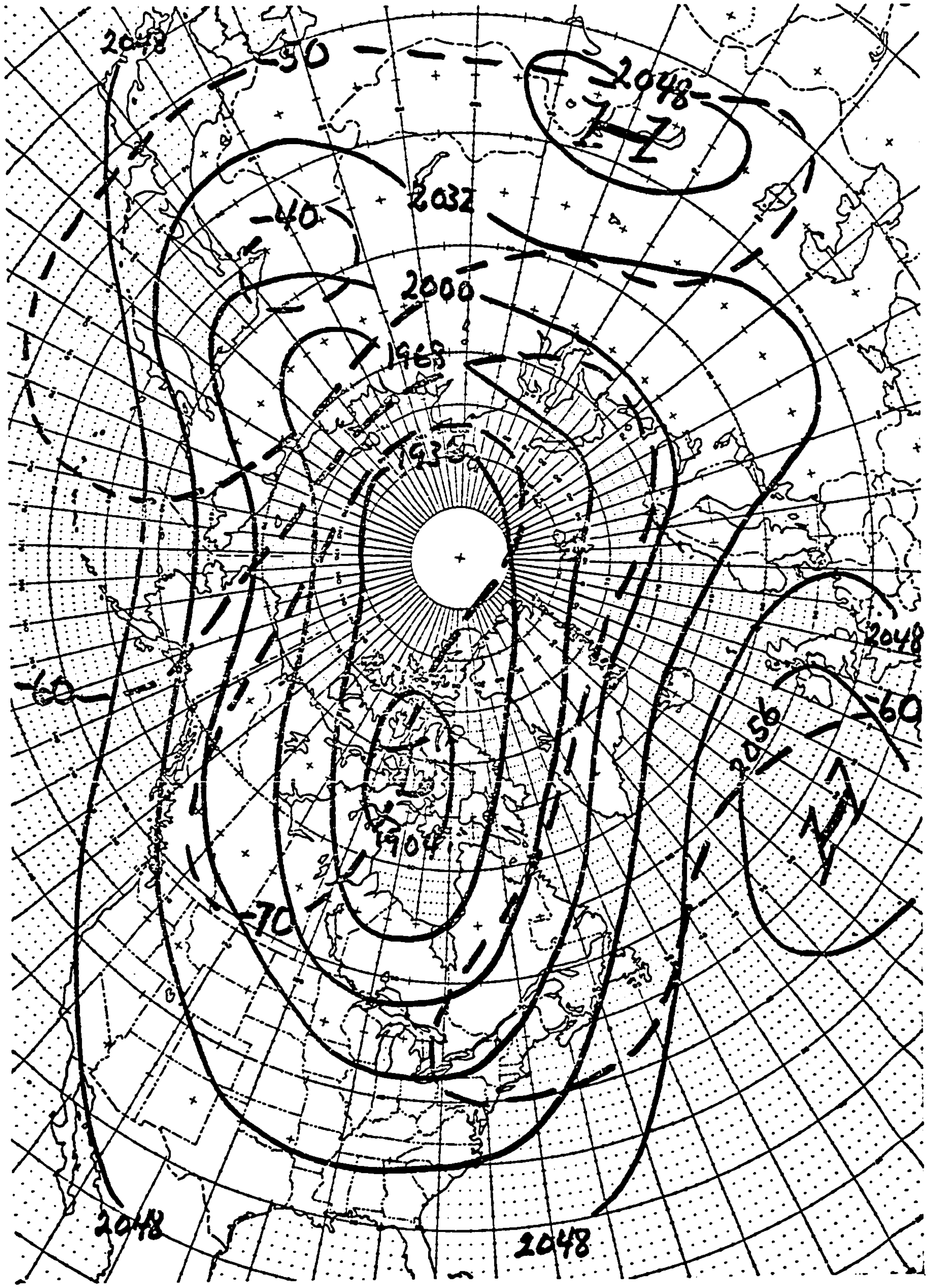

Fig. 20. 50 mb map at 00 GMT 28 December 1967 (after Kriester, et. al., 1967). Contour heights are in tens of geopotential meters.

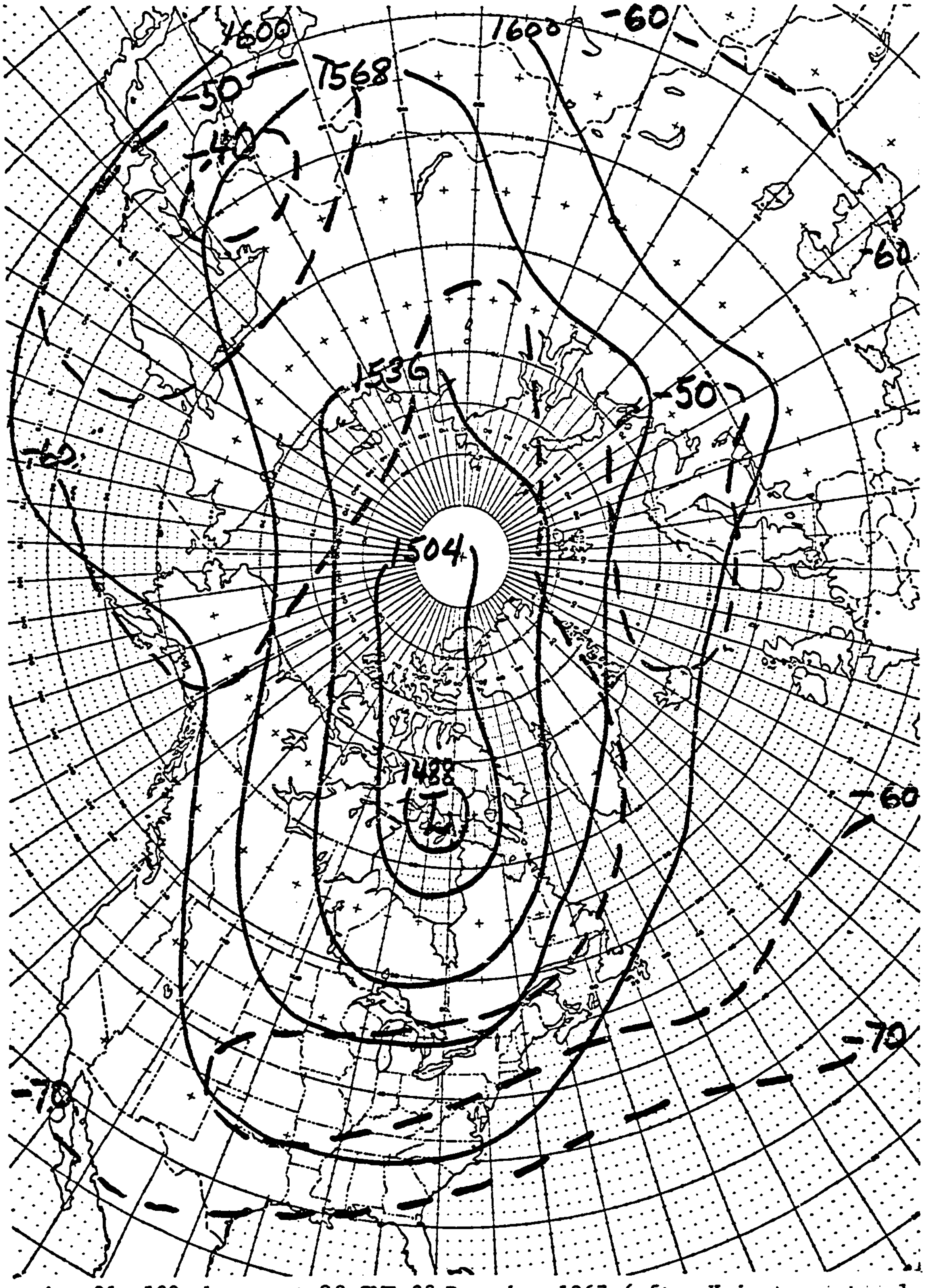

Fig. 21. 100 mb map at 00 GMT 28 December 1967 (after Kriester, et. al., 1967). Contour heights are in tens of geopotential meters.

The low pressure cell slopes to the east from the 5 mb level to the 30 mb level, and then southward to the 100 mb level.

An empirical stratospheric sudden warming model can be constructed from the described observational studies. The above data suggests that only three levels would be sufficient for constructing a model, and these are the 5, 10, and 30 mb levels. A higher level, such as the 2 or 1 mb level, might be desired but the 5 mb level definitely portrays the characteristics of a sudden warming.

An empirical model will be proposed and then transformed into a statistical-mathematical format which will permit studies in optimal sampling of a stratospheric sudden warming.

CHAPTER IV

EMPIRICAL MODEL

It has been noted in the literature survey that the effects of stratospheric warmings have been observed at meteor trail altitudes (approximately 100 km). The warmings are first observed at high altitudes and propagate downward with time, reaching maximum intensity in the 35 to 45 km altitude range. Very seldom does a warming penetrate lower than the 20 to 25 km altitude. One can only spectulate at the altitude the warming origiuates because the formation is above the balloon altitude of 30-35 km and not usually in the vicinity of a meteorological rocket site.

The life of a warming may last as long as four to five weeks and could cause the polar cyclonic circulation to be disrupted from six to eight weeks. The time span of the warming at its maximum intensity is in the one to two week range.

The movement of the warming is approximately 15 degrees of latitude per day during the early stages to only 5 degrees or less during the maximum intensity period. As the warming begins to weaken, the movement will usually increase to near 10 degrees per day. The movement is predominatly from east to west, usually from Europe, eastward to Greenland, then in a general southeast direction to over Southern Canada and Northern United States. The movement is usually perpendicular to the wind flow, although occasionally it is against the wind flow.

The warm air is elongated in a north-south direction and the air mass is on the order of 2500-5000 km long. The dimensions are quite arbitrary because one person might use the 0C isotherm as the boundary of warm air while another might use the -20C isotherm. At any rate, the east-west dimension is approximately one-half that of the north-south. The isotherms are packed tighter on the west side of the warm air indicating a steep surface on that side and a trailing off on the east side. The tight gradient on the west side is to be expected as the main cold air center is usually located on the west side of the warm air center. There appears to be no significant difference in the slopes of the north and south sides of the warm air dome.

The average amplitude of the warm air is 30 to 35C. The amplitude is centered about 40 km and extends some 15 km higher and lower (25 to 55 km).

The warm air maintains itself in spite of almost unbelievable cold air advection. For example, wind speeds of 65 mps were noted over Eastern United States on 27 December 1967 and were perpendicular to the isotherms. The temperature gradient was 30C/2050 km. The equation for computing horizontal temperature advection is $V|-\Delta_H T| * \text{Cos } \phi$ where ϕ is the angle between the wind speed V and the horizontal temperature gradient $-\Delta_H T$. Substituting our data into the above equation

$$65\text{m/sec}* 1\text{ km}/10^3\text{m}*3600\text{ sec/hr}*30\text{C}/2050\text{ km}* \text{Cos } 0°=3.4\text{C/hr}.$$

This is a little more than 80C per day! How the warm air maintains itself is one of the most fascinating events to occur in the atmosphere, and yet so many tropospheric minded meteorologists are not even aware of the phenomenon.

The sampling of a stratospheric sudden warming could lead to a very complex and expensive experiment. The purpose of this research is not to perform an actual field experiment, but to illustrate that optimal sampling techniques presented here have applications to the real world. The time, money, and energy savings, and/or the enhancement of the results of a successfully designed field experiment could be phenomenal. The determination of correct sensor placement, as well as when to sample and how much data to collect, could result in the saving of several expensive rockets or other types of sensors. The collection of only the data significant for an optimal variance explanation analysis is an important factor to consider in the design of an experiment. The determination of the above factors before the field experiment is actually done can be accomplished by the use of simulation. The closer the simulation model is to the phenomena being sampled, then the better the results will be from the field experiment.

An optimal sampling technique has been developed by an experimental design group at the University of Oklahoma (Eddy, Avara, Yerg, Kays, and others). An objective analysis technique that utilizes the time and space covariance relationships of the signal as well as the noise has been developed (Eddy, 1973; Best, 1973; Lacy, 1973). The objective analysis furnishes a relation between the sensors' locations and the confidence in the analyzed parameter values through the modeled covariance. The objective of the whole scheme is to determine the placement of sensors that will provide the optimum explanation of variance of the signal. The number of mobile sensors could be fixed;

or there could be an unlimited supply of sensors and the goal would be to determine when it is of no significant value to add an extra sensor.

If the sensor locations are fixed in space, then the problem becomes one of time — when would be the best time to fire a rocket, or rockets, in order to obtain an optimal analysis? The rocket firings could either be simultaneous or sequential.

Optimal sampling networks have been devised by several authors (Gandin, 1963; Kasahara, 1972; Alaka and Elvander, 1972; Huss, 1971; and Steinitz, et al., 1971). Most are a variation of Gandin's "optimal interpolation" scheme where linear interpolated values of the analyzed elements are found at grid points of a regular predetermined network. These values are found by using climatological data to determine the statistical structure (correlation surfaces) of the meteorological fields and weights (determined by a regression technique). Observational random errors are considered to be noncorrelated with the field variables. Sensor separation, signal and noise characteristics, sensor error, etc., are changed to yield the solution that provides the optimal explanation of variance between the "true" and "forecast" field. What makes Eddy's technique superior is that the noise and signal covariance function can be modeled to give the optimal analysis. Considerable work has been done by Best (1973) on the noise model and Lacy (1973) has performed extensive tests on the sensitivity of the technique to the modeling of the signal and noise covariance functions.

The covariance of the signal and noise can be evaluated by taking the expected values of parameters and their cross products located at pairs of points in x,y,h,t over the range of the varying parameters. An analytical description of an empirical model can be utilized to obtain an estimate of the modeled covariance; however, the analytical function must represent the desired system. The function should be as simple as possible yet contain adequate parameters to describe the system. An exponential function developed by Avara (1973) is used to represent a stratospheric sudden warming.

Let $S(x,y,t)=Z(x,y,h,t)+\varepsilon(x,y,h,t)$

where

$S(x,y,h,t)=$ the observation at point (x,y,h,t)

$Z(x,y,h,t)=$ the signal at point (x,y,h,t)

and

$\varepsilon(x,y,h,t)=$the noise at point (x,y,h,t).

Assume $E\{\varepsilon(x_1,y_1,h_1,t_1)\varepsilon(x_2,y_2,h_2,t_2)\}=\rho_n^{|t_2-t_1|} * \sigma_n(x_1,y_1,h_1,t_1)$
$* \sigma_n(x_2,y_2,h_2,t_2)$.

Define $Z(x,y,h,t)=A(t)[\exp[(-1/2)Q(x,y,t)]f(h)]$

where $A(t)$ is a time dependent random process

and

$$Q(x,y,t)=B_{xx}(t)[x-x_o(t)]^2+2B_{xy}(t)[x-x_o(t)][y-y_o(t)] + B_{yy}(t)[y-y_o(t)]^2.$$

$f(h)$ is the altitude function and its expected value is developed in Appendix B. $x_o(t)$ and $y_o(t)$ are time dependent random processes defining the center of the system at time t. The $E\{x_o(t)\}=\hat{x}_o(t)$ and $E\{y_o(t)\}=\hat{y}_o(t)$. Let $A(t)$ (amplitude) be a linear first order Markov process with expected value $A_o(t)$, standard deviation $\sigma_a(t)$, lag $-\tau$, and correlation coefficient ρ^{τ}_{a}. The coefficients B_{xx}, B_{xy}, and

B_{yy} change with time to form an ellipse in the x-y plane with one axis along the direction of movement and the other perpendicular to the direction of movement. As time increases the ellipse may change to a circle and then back into an ellipse. The system may follow any specified path such as a straight line, parabola, etc.

The altitude fuction may be expressed by Sin $(\omega h+\phi)$ where $\omega=2\pi/T$, T is the fixed period, ϕ is the angle between movement of the system and the x axis and is a normally distributed random variable with mean $\overline{\phi}$ and standard deviation σ_ϕ.

The expected value of S and the covariance between S at one point in space and time and S at a different point is found by taking the expected values over A(t), $x_o(t)$, $y_o(t)$ and ϕ. The development of the expected values are shown in Appendix A and B.

The expected value may be written as

$$E\{S(x,y,h,t)\}=(A_o/[(1+b_x\sigma_x^2)(1+b_y\sigma_y^2)]^{\frac{1}{2}})\exp\{-\tfrac{1}{2}[M_{xx}(x-\hat{x}_o)^2$$
$$+2M_{xy}(x-\hat{x}_o)(y-\hat{y}_o)+M_{yy}(y-\hat{y}_o)^2](-\ \sigma_\phi^2)\}[\mathrm{Sin}(\omega h+\mu_\phi)]$$

where

$$M_{xx}= dx\ \mathrm{Cos}^2\phi + dy\ \mathrm{Sin}^2\phi$$
$$M_{xy}= (dx-dy)\ \mathrm{Sin}\phi\ \mathrm{Cos}\phi$$
$$M_{yy}= dx\ \mathrm{Sin}^2\phi + dy\ \mathrm{Cos}^2\phi\ .$$

The covariance can be expressed as

$$E\{S(x_1,y_1,h_1,t_1)S(x_2,y_2,h_2,t_2)\}= \frac{\rho_a^{\tau}\sigma_a(t\ )\sigma_a(t_2)+A_o(t_1)A_o(t_2)}{[g_x(t_1,t_2)g_y(t_1,t_2)]^{\frac{1}{2}}}$$

$$[\exp(-\tfrac{1}{2}(\tilde{x}-\tilde{\bar{x}}_o)^t M(\tilde{x}-\tilde{\bar{x}}_o))][\tfrac{1}{2}\{\cos[\omega(h_1-h_2)]-\exp[-2\sigma_\phi^2][\cos(\omega(h_1+h_2)+2\mu_\phi)]$$

$$+\rho_n^{\tau}\sigma_n(x_1,y_1,h_1,t_1)\sigma_n(x_2,y_2,h_2,t_2)$$

The covariance is a result of varying the ever-changing ellipsoid shaped system back and forth over x_o, y_o, and h. The relation of the synoptically discovered parameters to the signal function is quite simple. It was noted that an amplitude of some 30 to 35 degrees occurred during a warming, therefore, an amplitude parameter (A) was included in the signal function. The horizontal shape of a warming was observed to vary with time, and the B_{xx}, B_{xy}, and B_{yy} variables relate this variation. The vertical or altitude function, Sin $(\omega h+\phi)$, characterizes the downward propagation and shape that a warming portrays. The parameters assume a less simple relation with other variables, as given by the expected value equations. The direction and curvature parameters, and the correlation of the signal with time are included in the expected value development.

The advantage of the exponential function is that it is extremely flexible in that the quadratic form may take on any reasonable shape and the direction of movement may be specified.

Simulation

The sudden warming was simulated by the exponential function moving across a 7 x 7 grid containing a network of sensors. The 7 x 7 grid is a compromise between finer resolution obtained from a larger grid number and less computer time for a smaller grid. The units in the mesh size were made compatible with the parameter units. The purpose for simulation was to determine the size and behavior of certain parameters under changing conditions, and to establish a climatological feel for the parameters.

The sudden warming enters and exits from the grid as determined by two preset parameters; the curvature and the lowest grid point that is reached as the warming moves across the grid. The lowest point was (3.0, 3.5). The warming enters the grid from the upper right corner, proceeds to the lower middle, and then to the upper left corner. The grid, its coverage of the earth's surface, and the location of sample sites are shown in Fig. 22.

The time of the analysis was specified as well as the altitude. The station locations for the optimal sampling are shown as squares in Figs. 23-37. Figs. 23-37 illustrate the horizontal shape of the system for three altitudes as it moves across the grid. Notice that the system does not appear at Z=0 and T=6, but does appear when T=8. The system propogates downward with time and weakens again when Z=0 and T=14. The system has the largest amplitude at the highest altitude. The altitudes of 0, 15, and 30 km were arbitrarily chosen to verify the computer program. The values of 25, 40, and 55 km would be realistic altitudes to use in a real warming situation.

The similarity between the horizontal shape of the system and the isotherm patterns in Figs. 7-11 are striking. The +10 degree isotherm contour in Fig. 7 is shaped like an ellipse as it approaches

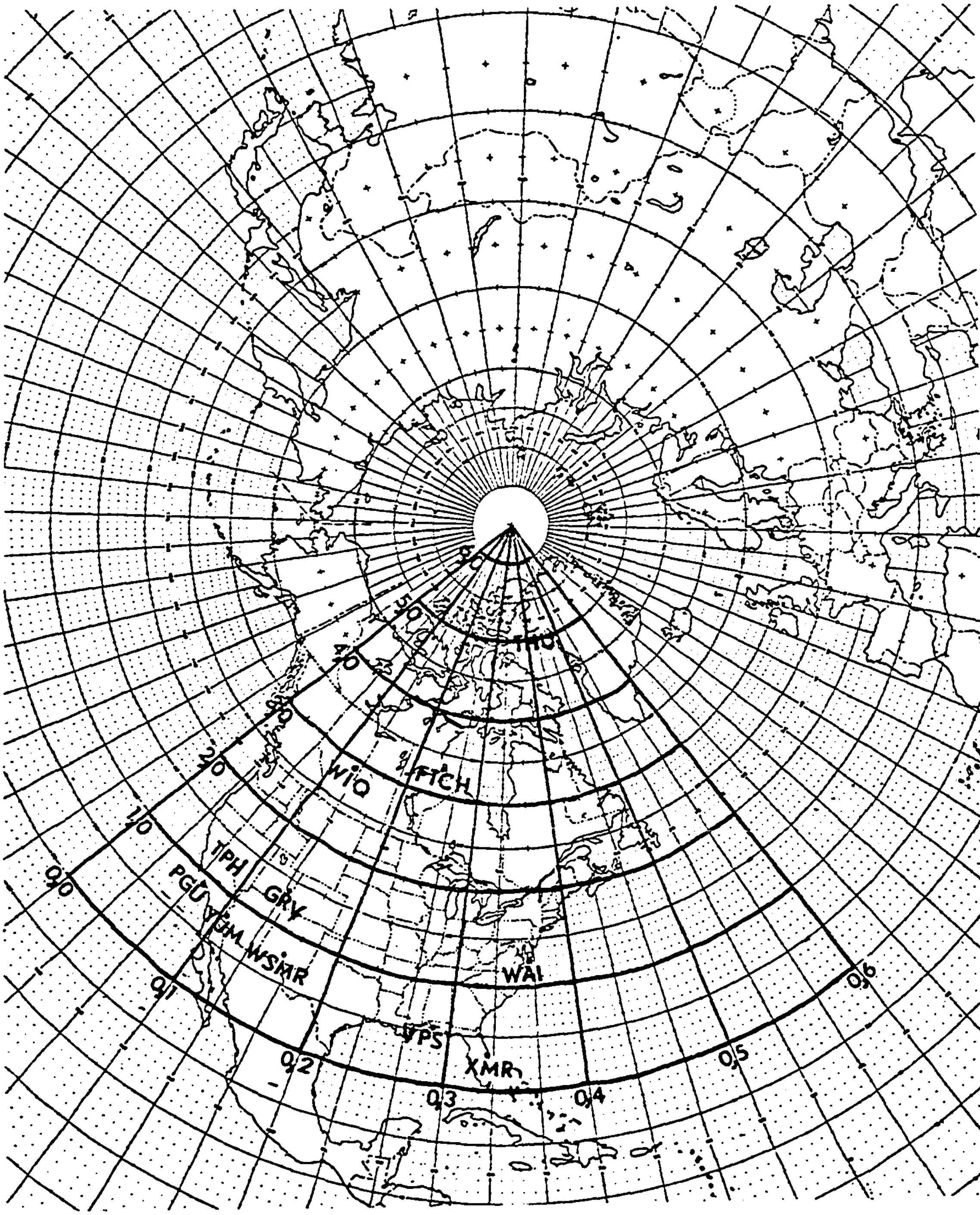

Fig. 22. Grid used for simulating a stratospheric sudden warming with locations of rocket sites. (WAI, Wallops Island, Va.; XMR, Cape Kennedy, Fla.; VPS, Eglin AFB, Fla., WSMR, White Sands Missile Range, N.M.; YUM, Yuma, Ariz.; PGU, Point Mugu, Ca.; GRV, Green River, Utah; TPH, Tonapah, Nev.; WIQ, Primrose Lake, Alberta, Canada: FTCH, Fort Churchill, Canada; THU, Thule, Greenland.)

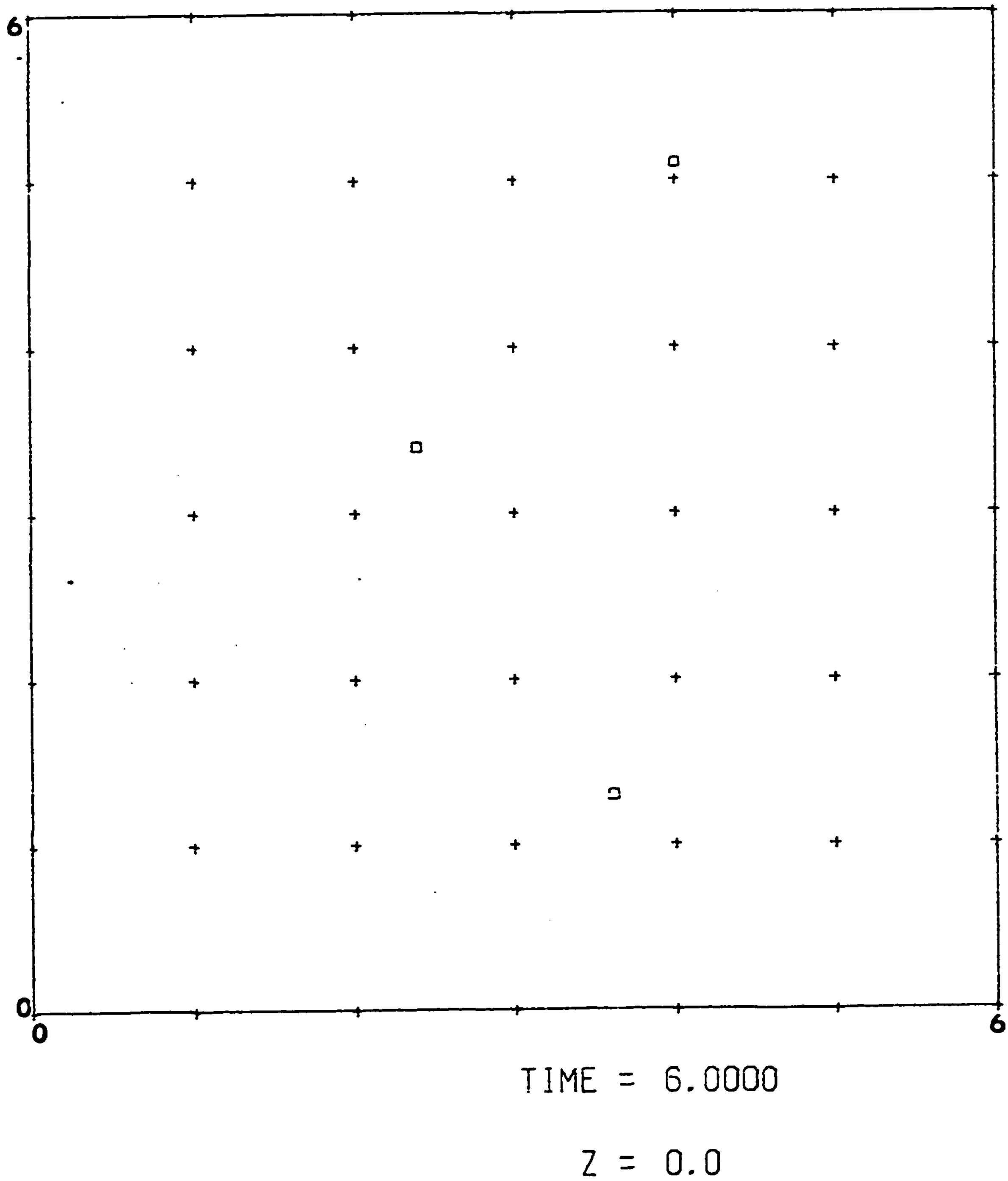

Fig. 23. A two-dimensional representation of a simulated meteorological phenomena for the indicated time and altitude. A square represents a sensor location (predictor) and a plus represents a grid point (predictand). Z is in tens of km and T in hours.

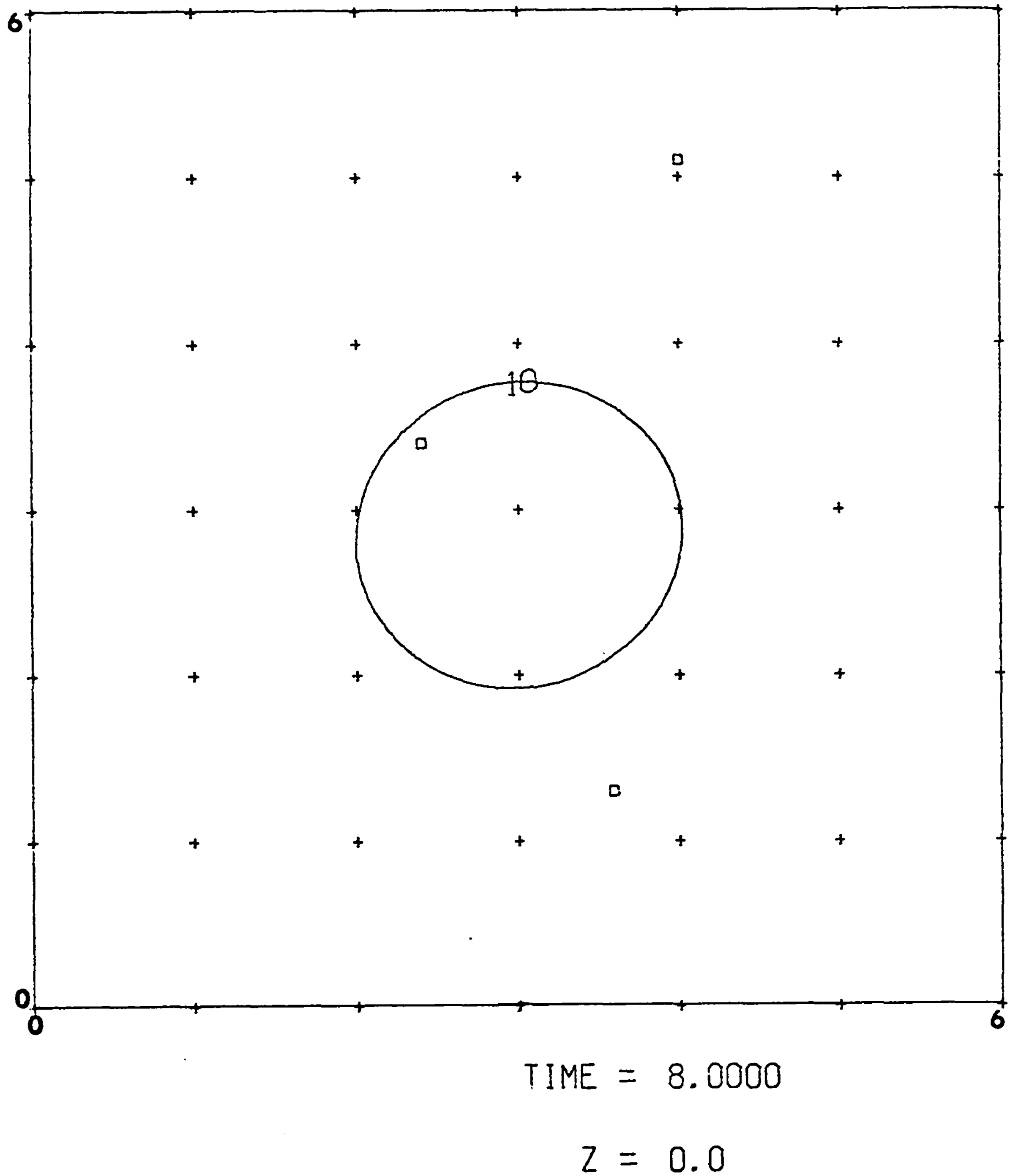

Fig. 24. A two-dimensional representation of a simulated meteorological phenomena for the indicated time and altitude. A square represents a sensor location (predictor) and a plus represents a grid point (predictand). Z is in tens of km and T in hours.

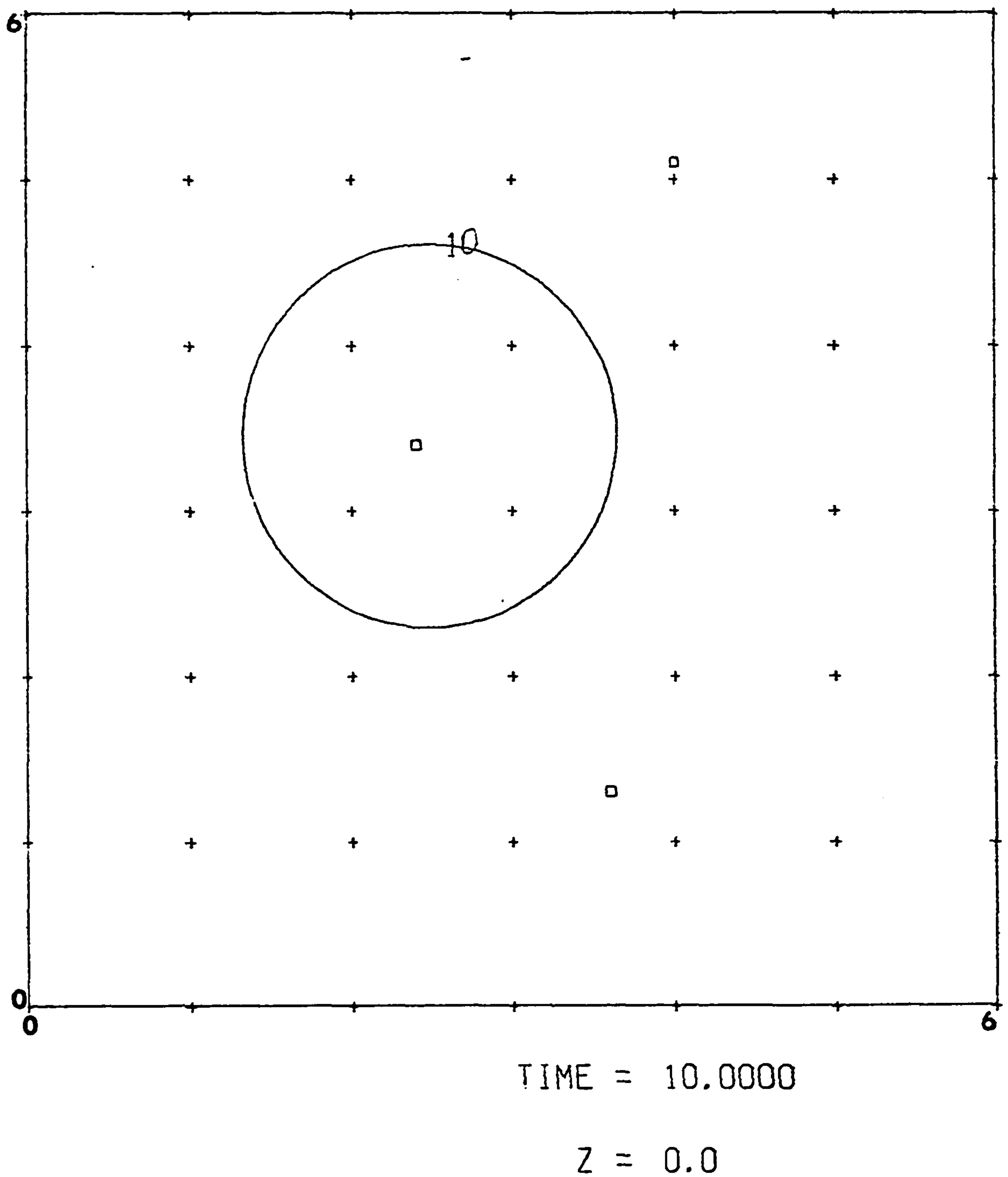

Fig. 25. A two-dimensional representation of a simulated meteorological phenomena for the indicated time and altitude. A square represents a sensor location (predictor) and a plus represents a grid point (predictand). Z is in tens of km and T in hours.

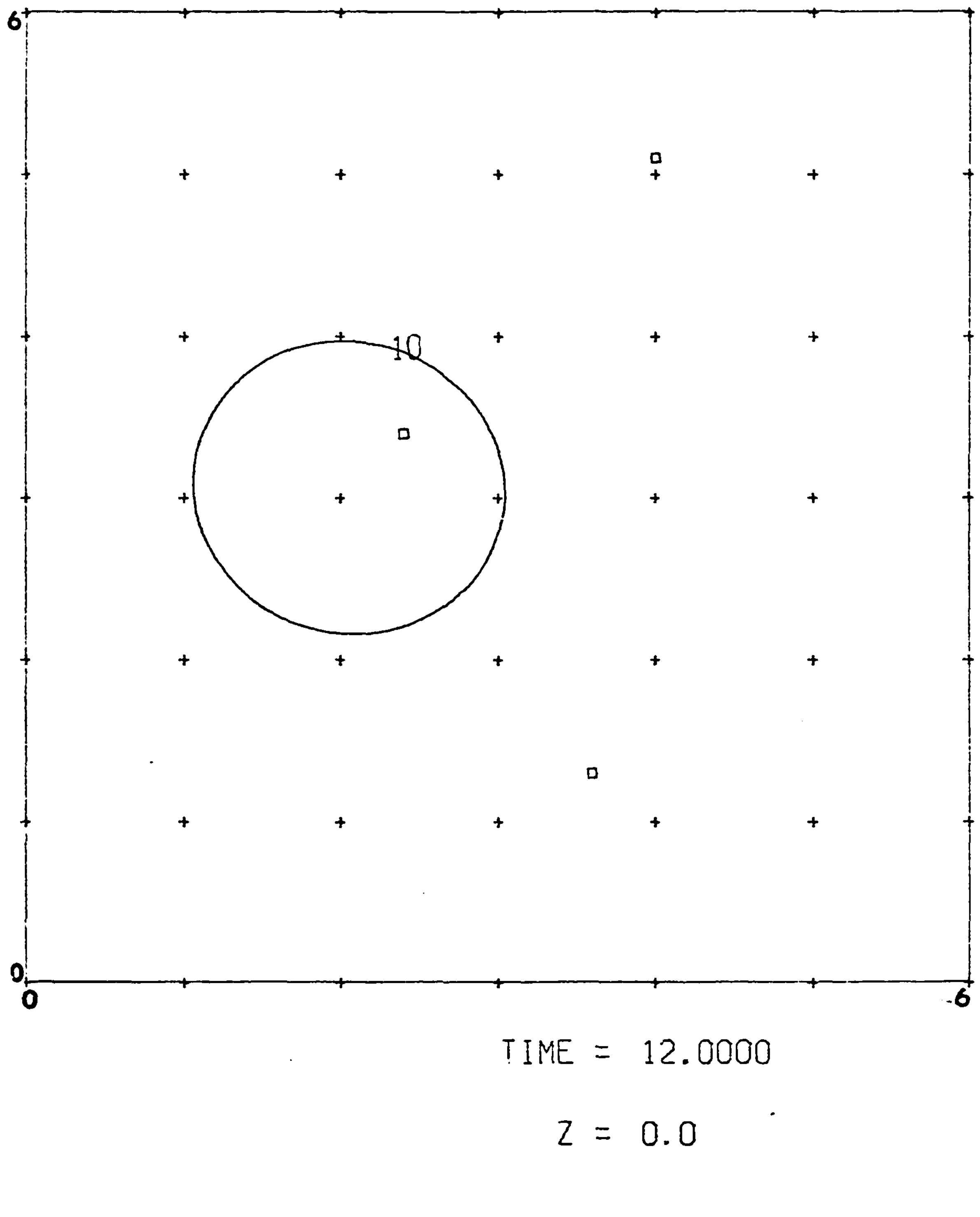

Fig. 26. A two-dimensional representation of a simulated meteorological phenomena for the indicated time and altitude. A square represents a sensor location (predictor) and a plus represents a grid point (predictand). Z is in tens of km and T in hours.

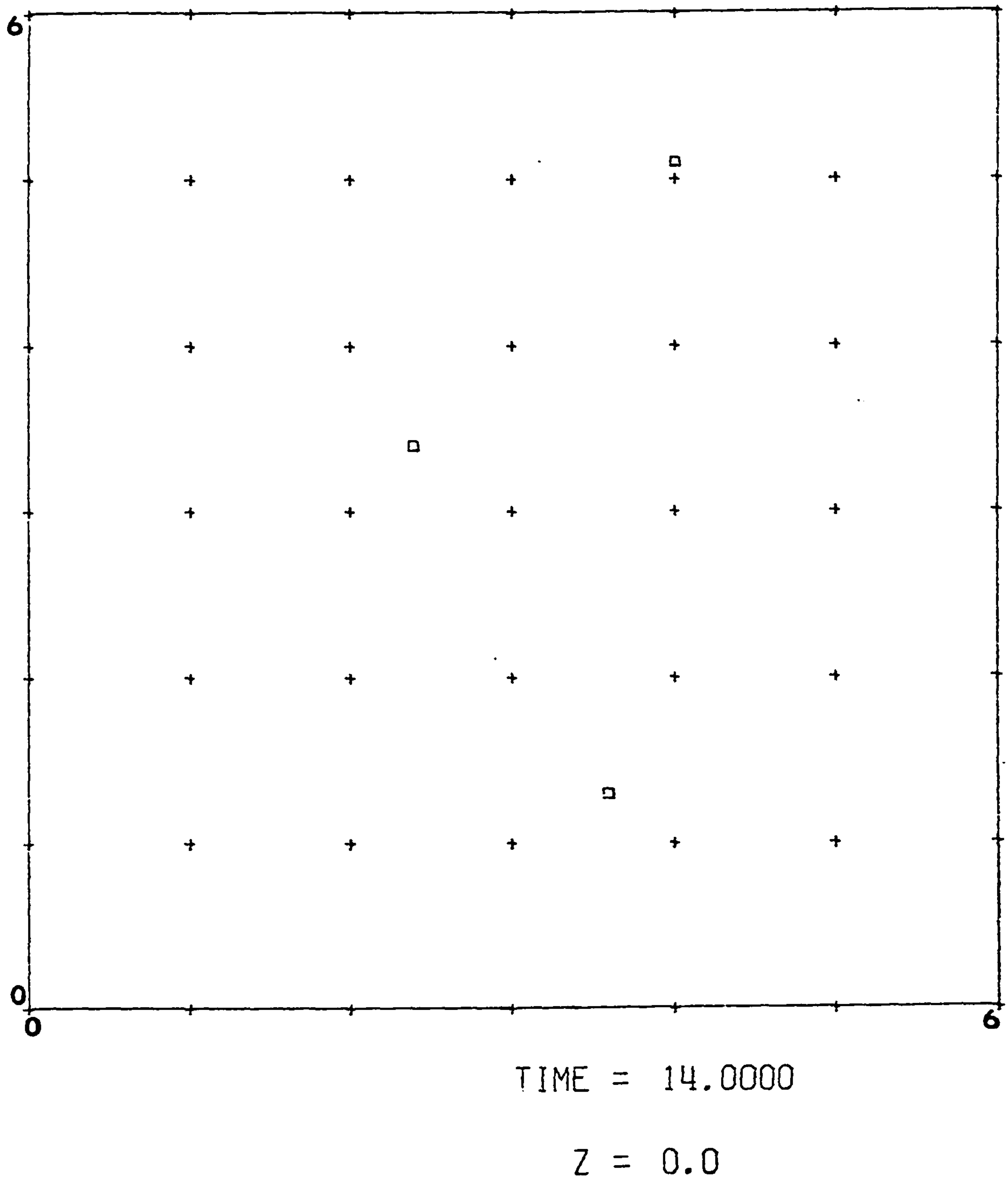

Fig. 27. A two-dimensional representation of a simulated meteorological phenomena for the indicated time and altitude. A square represents a sensor location (predictor) and a plus represents a grid point (predictand). Z is in tens of km and T in hours.

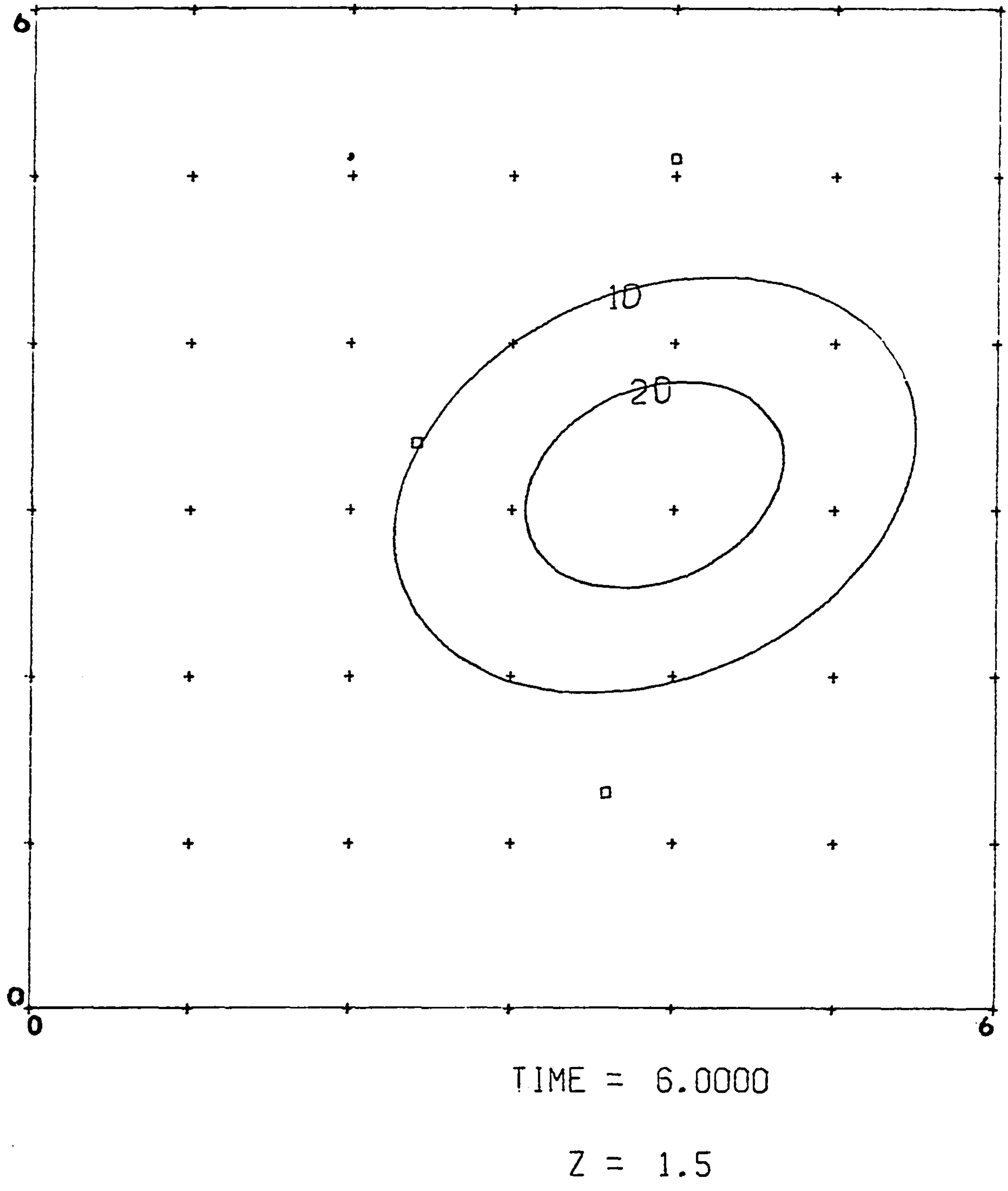

Fig. 28. A two-dimensional representation of a simulated meteorological phenomena for the indicated time and altitude. A square represents a sensor location (predictor) and a plus represents a grid point (predictand). Z is in tens of km and T in hours.

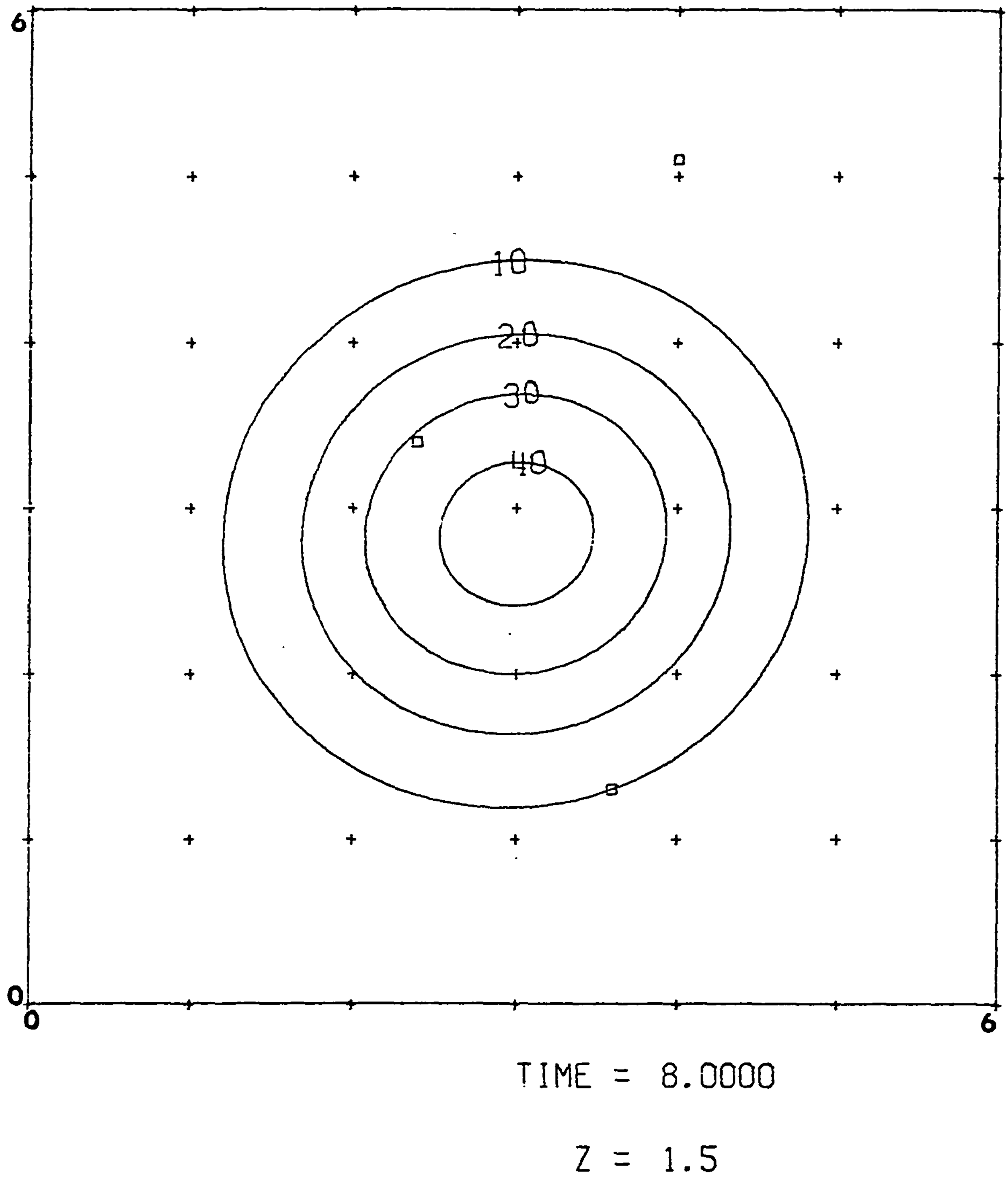

Fig. 29. A two-dimensional representation of a simulated meteorological phenomena for the indicated time and altitude. A square represents a sensor location (predictor) and a plus represents a grid point (predictand). Z is in tens of km and T in hours.

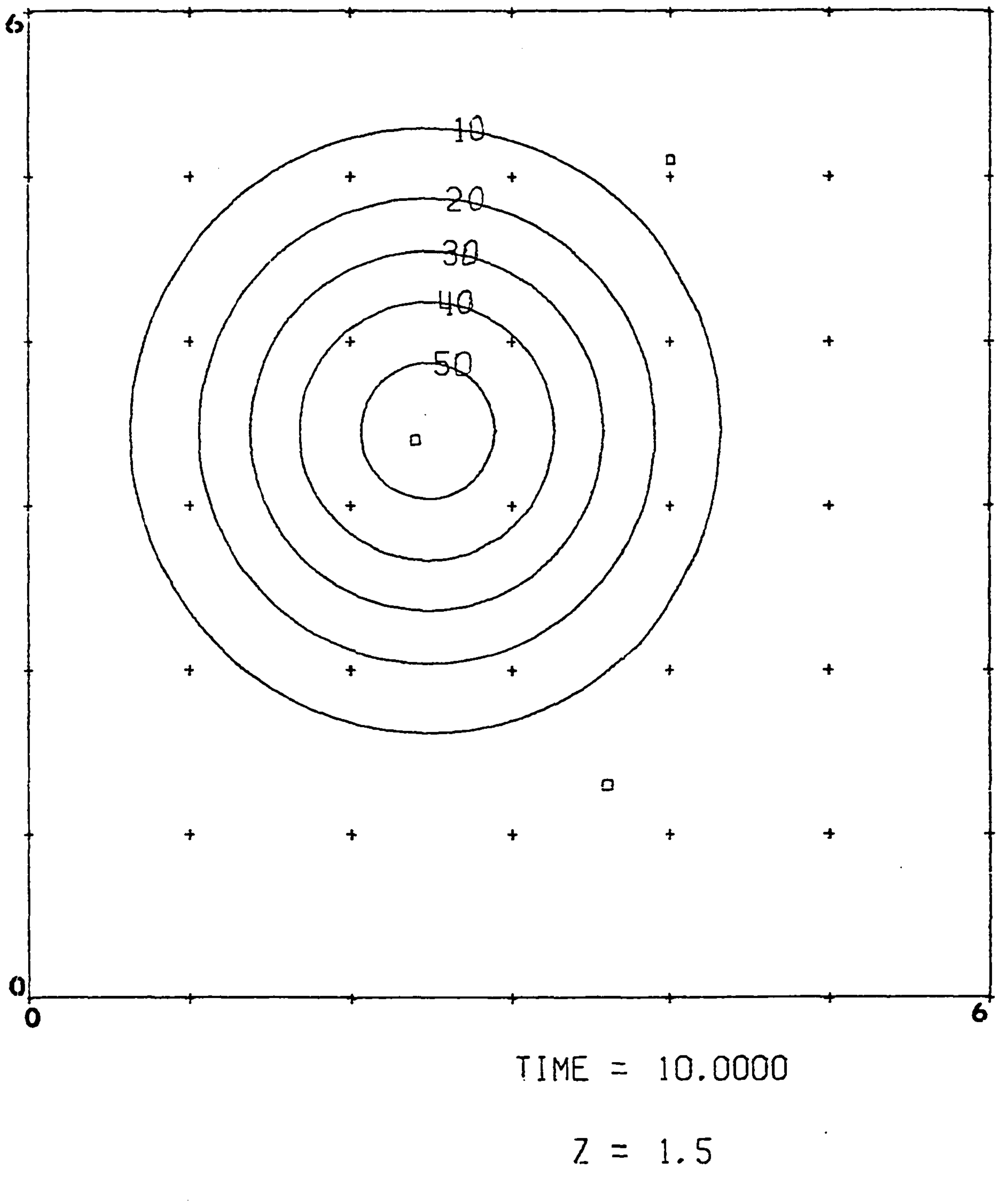

Fig. 30. A two-dimensional representation of a simulated meteorological phenomena for the indicated time and altitude. A square represents a sensor location (predictor) and a plus represents a grid point (predictand). Z is in tens of km and T in hours.

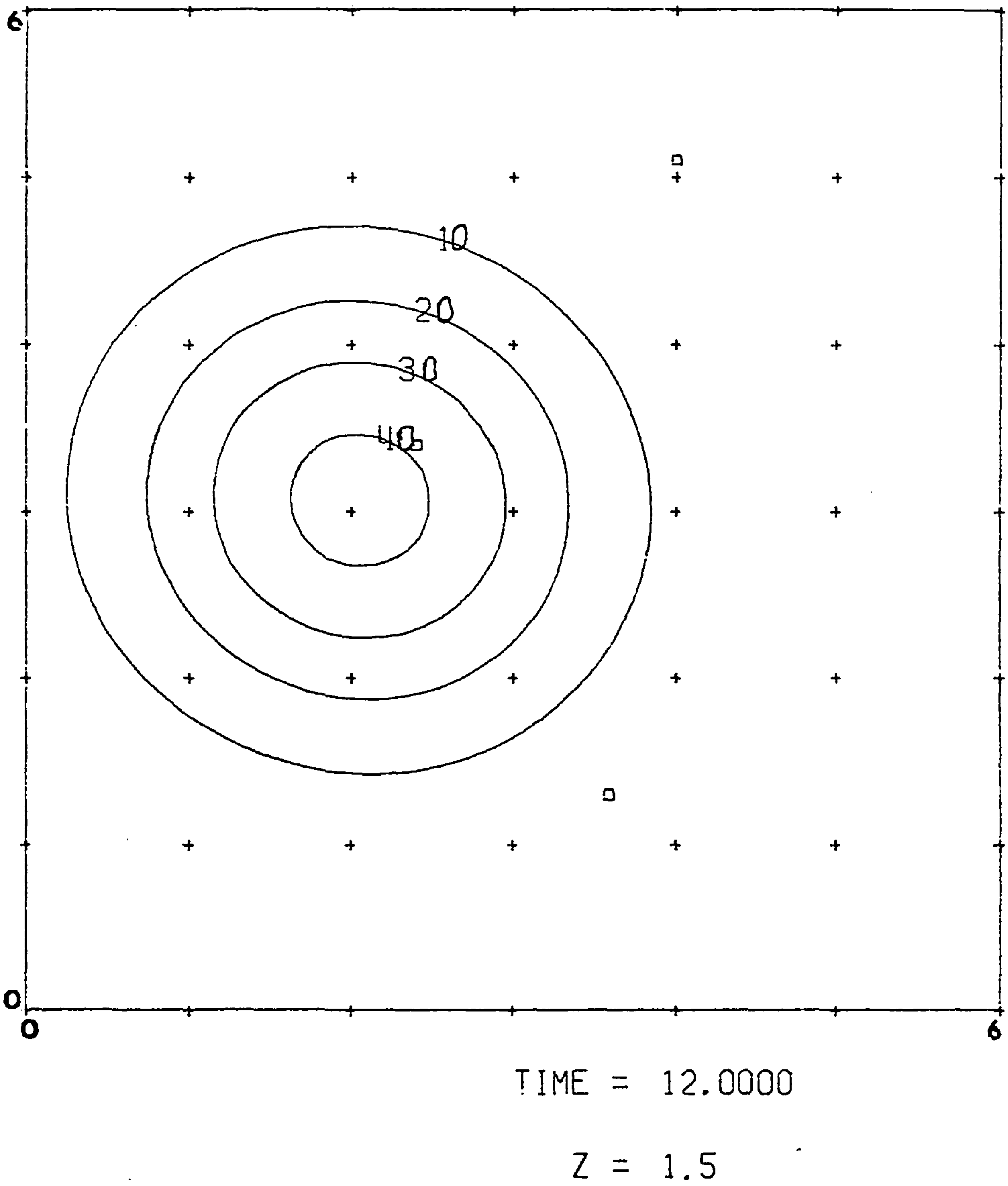

Fig. 31. A two-dimensional representation of a simulated meteorological phenomena for the indicated time and altitude. A square represents a sensor location (predictor) and a plus represents a grid point (predictand). Z is in tens of km and T in hours.

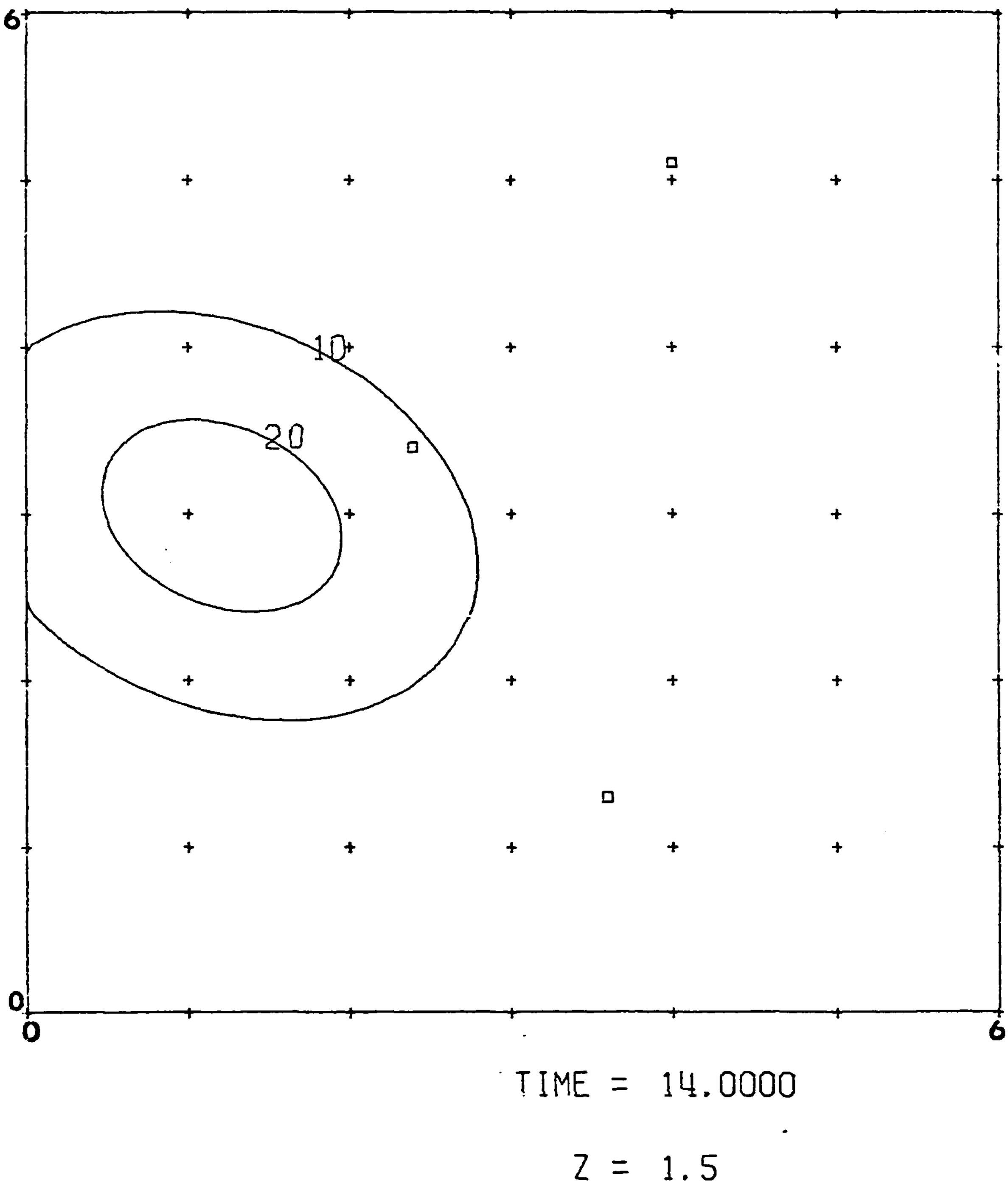

Fig. 32. A two-dimensional representation of a simulated meteorological phenomena for the indicated time and altitude. A square represents a sensor location (predictor) and a plus represents a grid point (predictand). Z is in tens of km and T in hours.

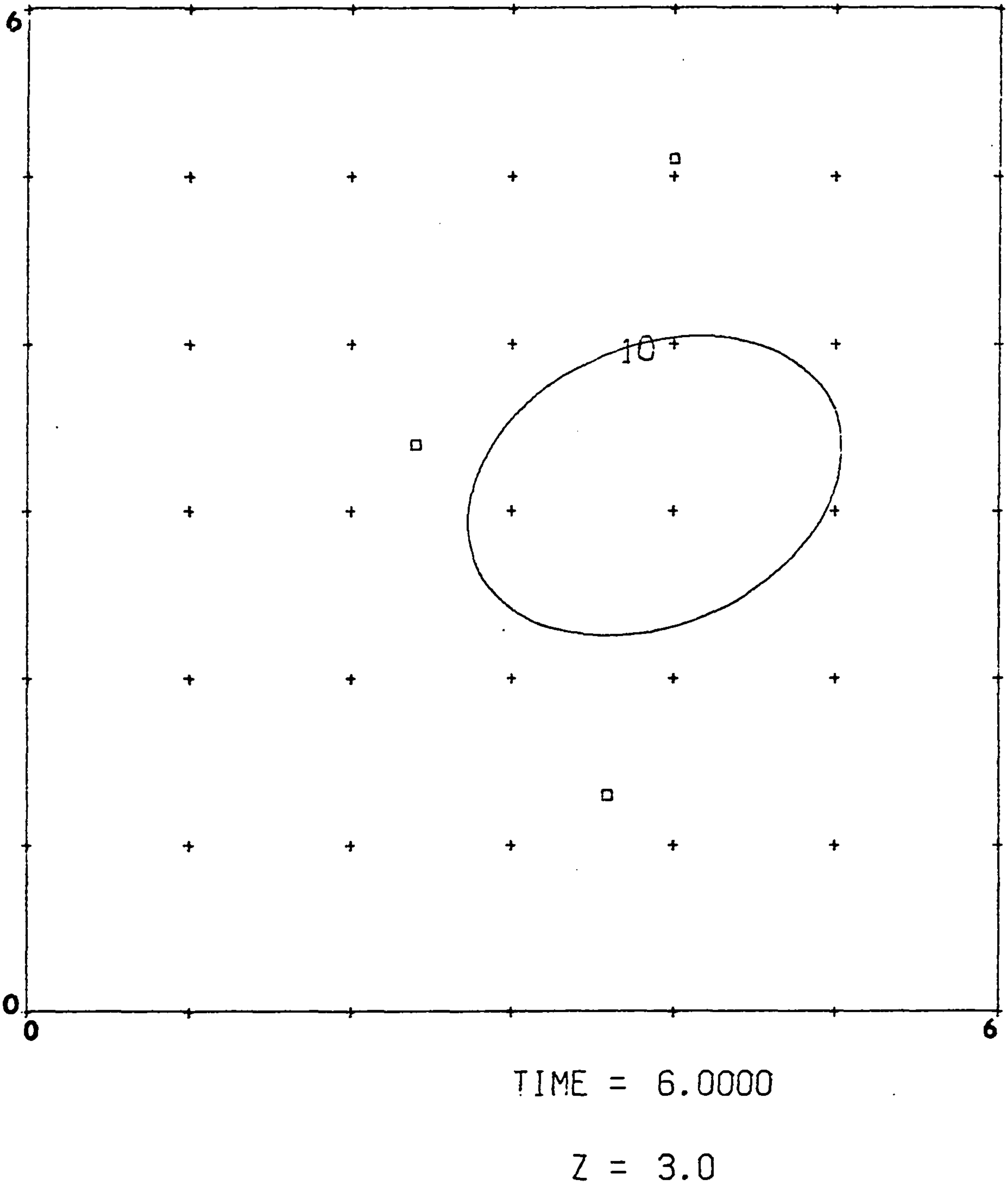

Fig. 33. A two-dimensional representation of a simulated meteorological phenomena for the indicated time and altitude. A square represents a sensor location (predictor) and a plus represents a grid point (predictand). Z is in tens of km and T in hours.

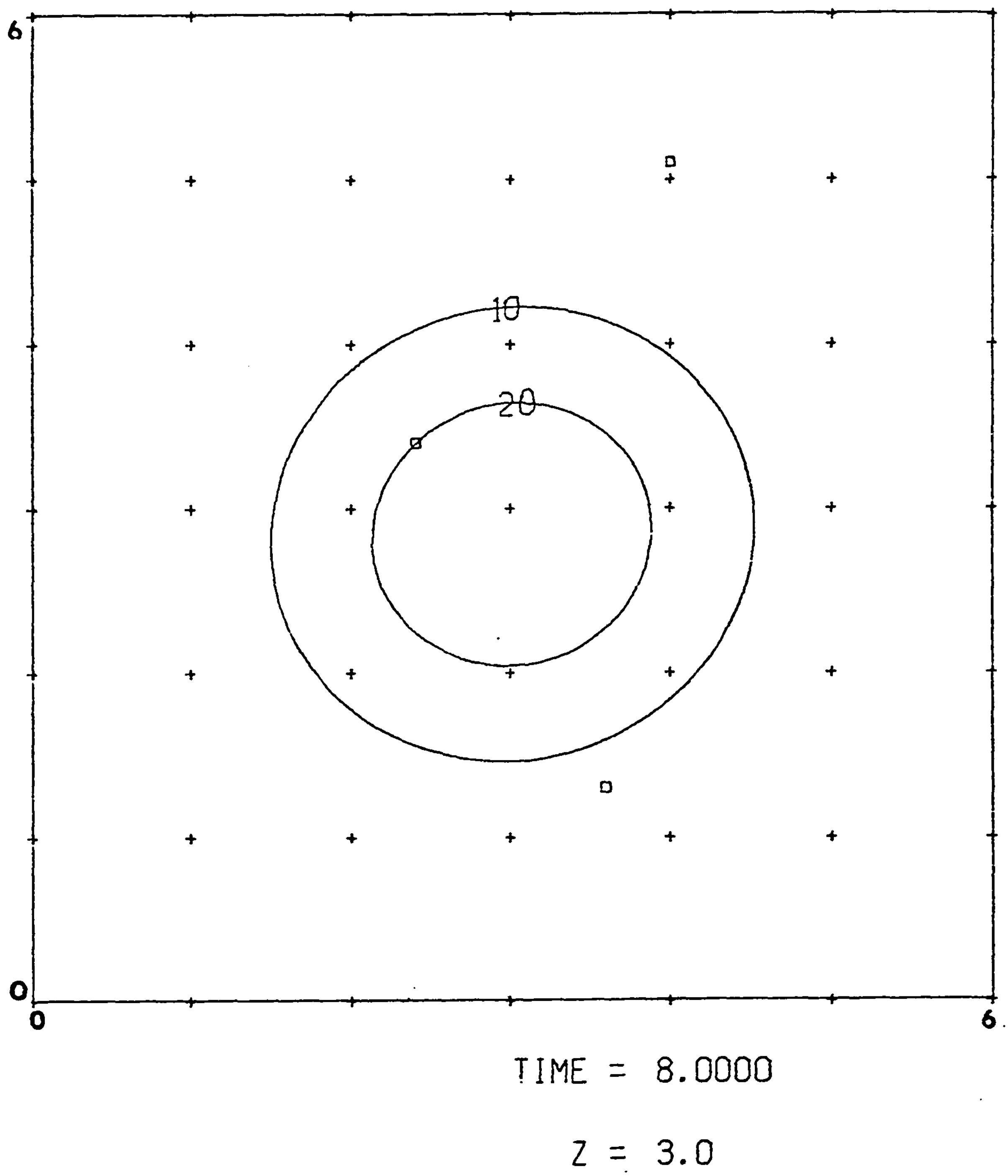

Fig. 34. A two-dimensional representation of a simulated meteorological phenomena for the indicated time and altitude. A square represents a sensor location (predictor) and a plus represents a grid point (predictand). Z is in tens of km and T in hours.

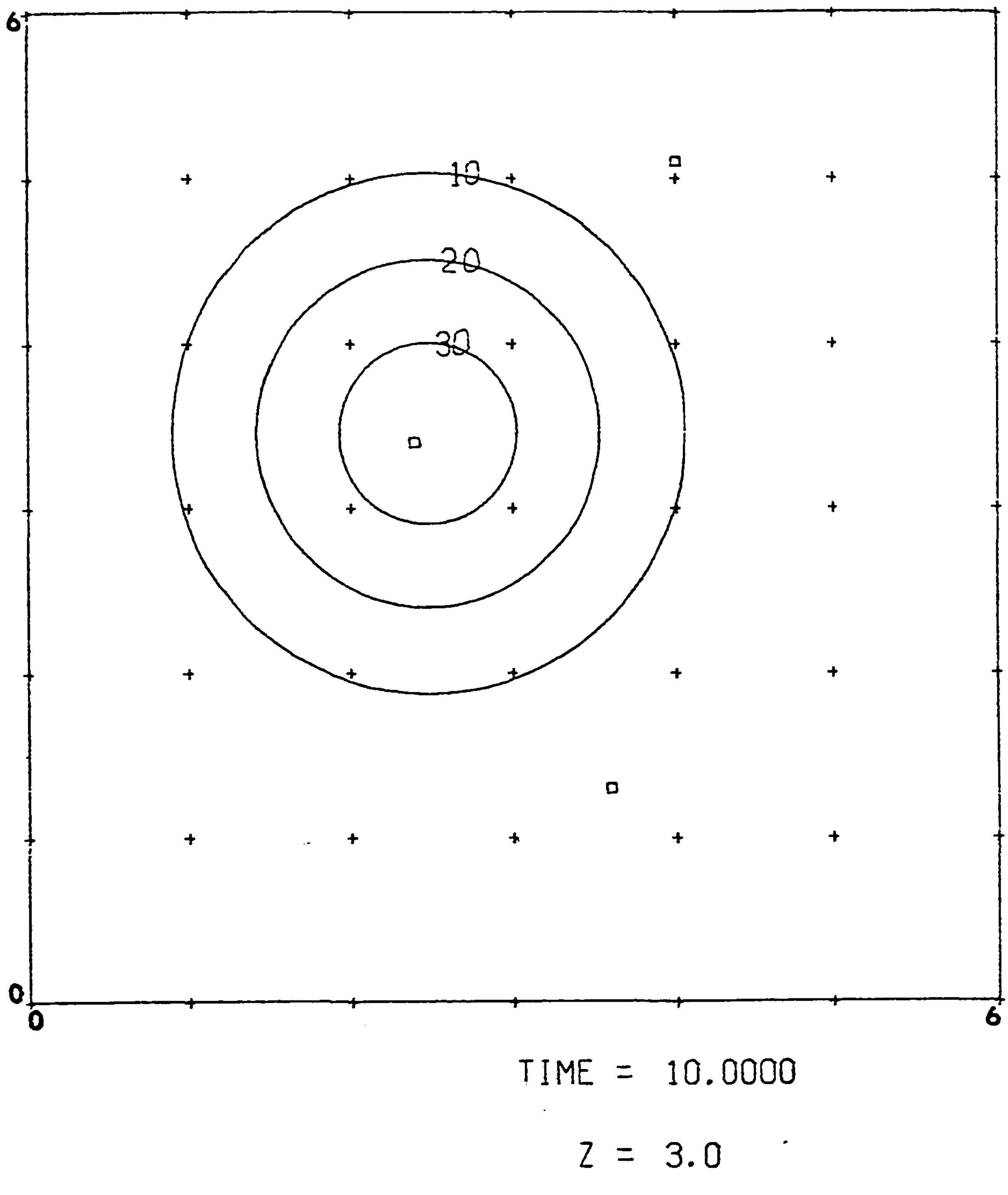

Fig. 35. A two-dimensional representation of a simulated meteorological phenomena for the indicated time and altitude. A square represents a sensor location (predictor) and a plus represents a grid point (predictand). Z is in tens of km and T in hours.

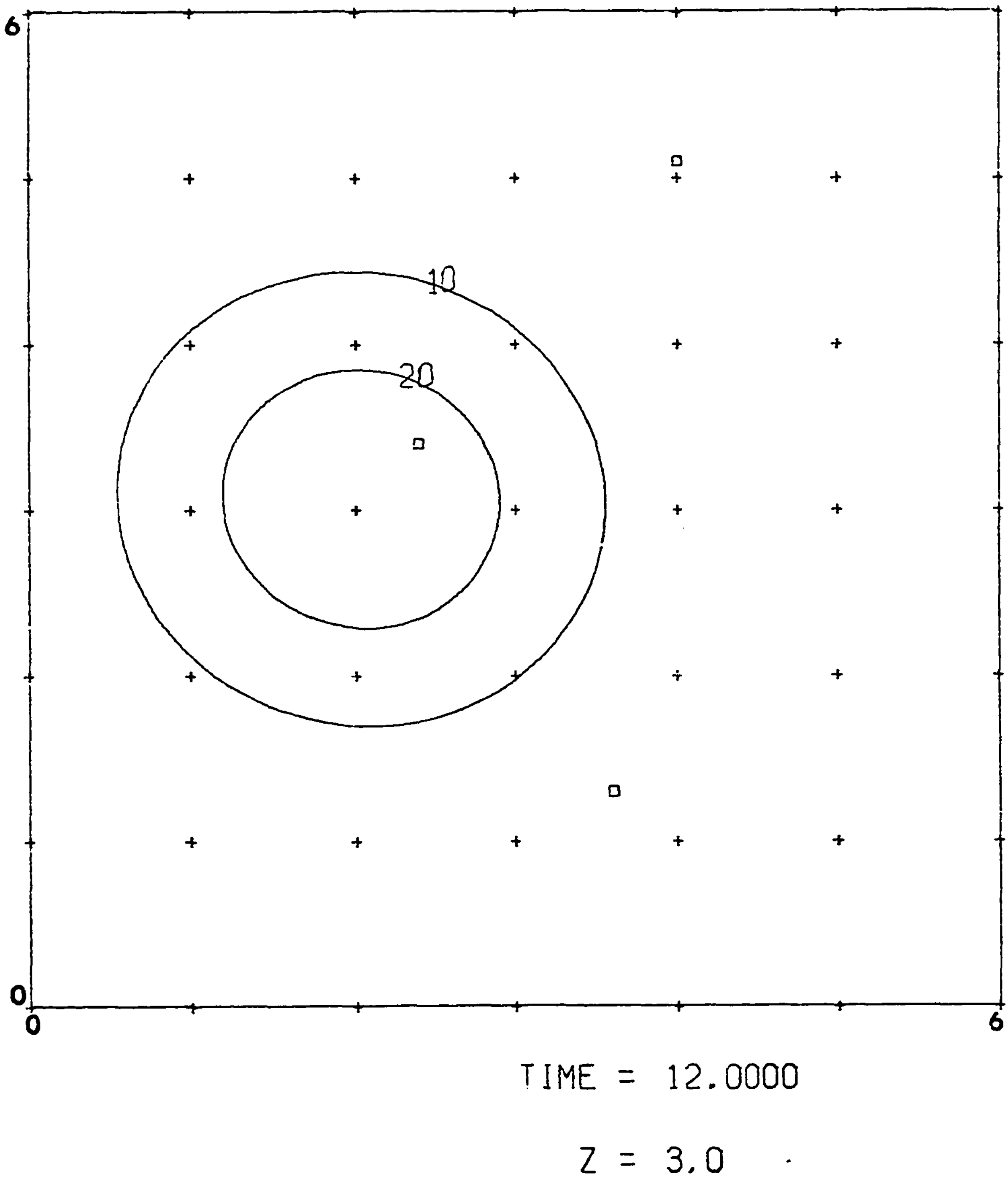

Fig. 36. A two-dimensional representation of a simulated meteorological phenomena for the indicated time and altitude. A square represents a sensor location (predictor) and a plus represents a grid point (predictand). Z is in tens of km and T in hours.

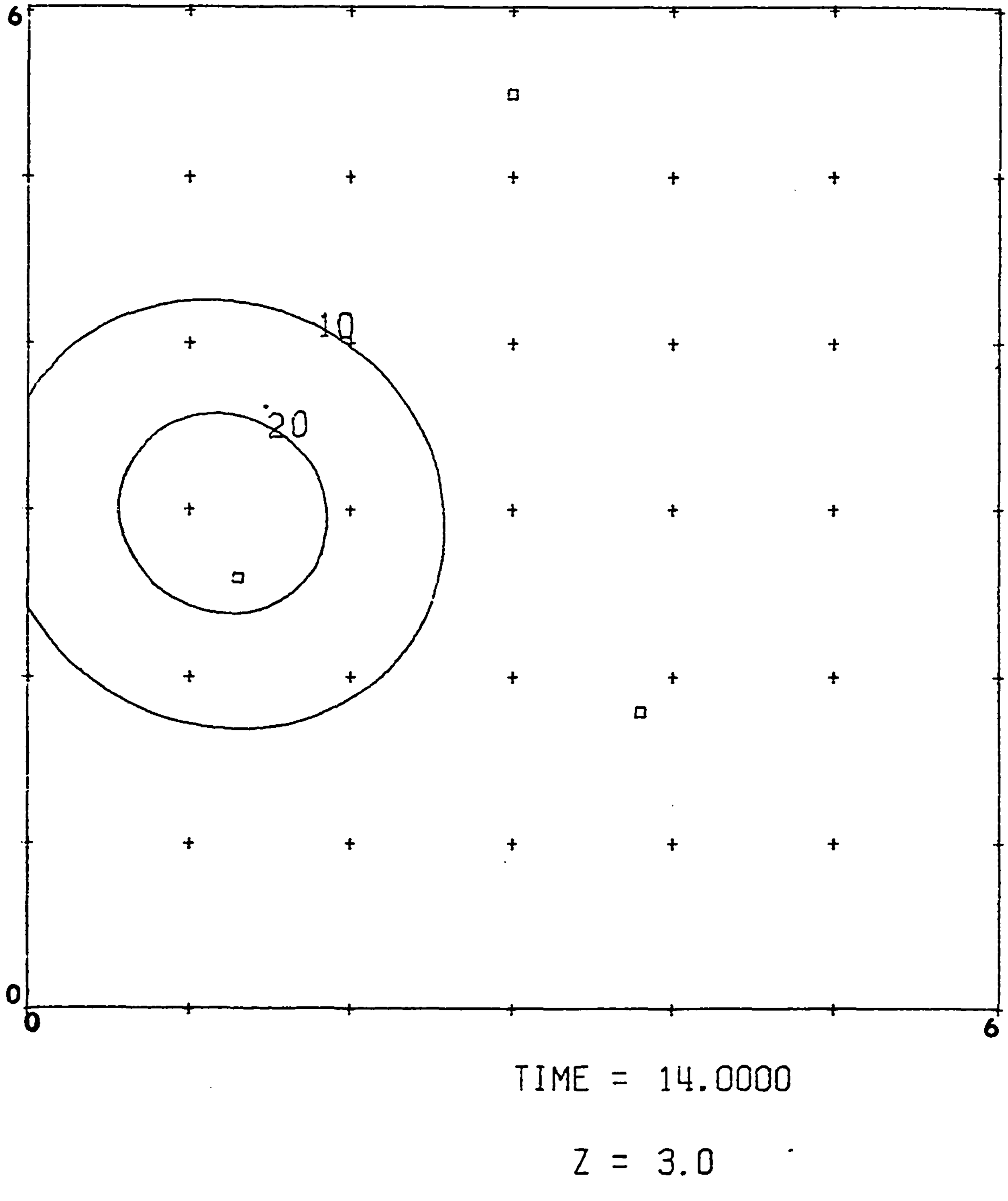

Fig. 37. A two-dimensional representation of a simulated meteorological phenomena for the indicated time and altitude. A square represents a sensor location (predictor) and a plus represents a grid point (predictand). Z is in tens of km and T in hours.

Baffin Island. Note the elliptic shape of the contours in Fig. 28. The isotherms become circular as time progresses as can be seen in Fig. 9 by noting the ±0 degree isotherm contour. The -30 degree isotherm in Fig. 11 is shaped somewhat like an ellipse as the warming weakens and moves westward.

A three dimensional representation of a sudden warming illustrated by the expected average signal is shown in Figs. 38-40 for T=10, 13, and 15.5. The amplitude decreases with time and the expected average signal exits from the upper left of the grid. The location of stations were fixed and it was determined which one of the available stations gave an OVEA using the 49 grid points. Then using the selected station and 49 grid points, a second station was selected and so on. The time that a station should sample was computed by associating the time when the minimum variance occurred.

The selection of stations and times are done sequentially instead of simultaneously. Sequential sampling seems to be a practical approach in planning an experiment to sample a sudden warming. The chances of success of simultaneously firing rockets at all stations, having all the payloads expel and function properly, or radar and the receiver to track and receive the payload would be marginal. The probability of obtaining usable data from one rocketsonde is 85 percent (personal communication with Tillman Powell, electronic technician at White Sands Missile Range). The probability of a simultaneous occurrence of a number of independent events is the product of the separate probabilities. The probability of obtaining usable data from only three stations would be 61.4 percent and 44.4 percent from five

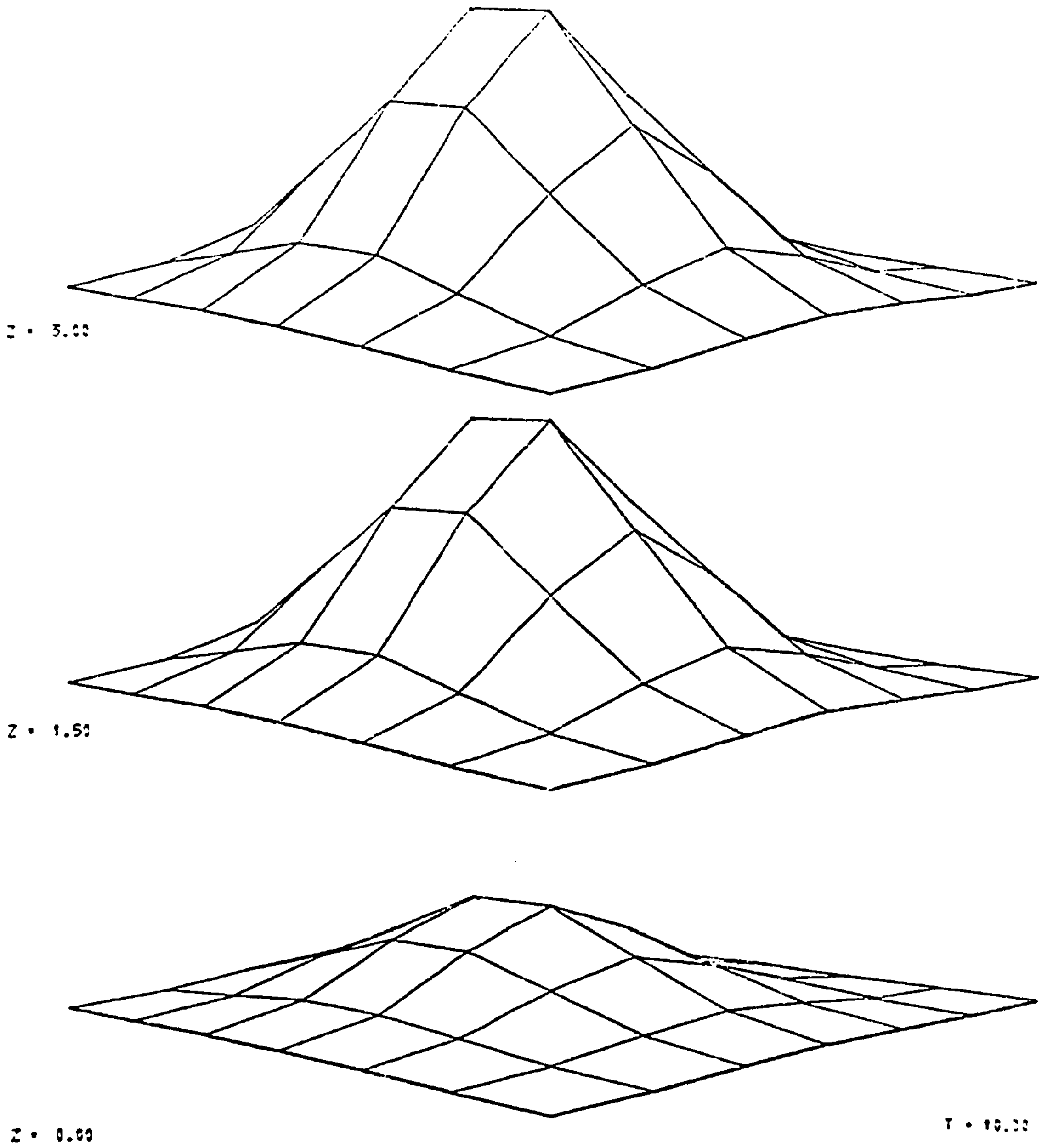

Fig. 38. A three-dimensional representation of a simulated meteorological phenomena for the indicated time and altitude.

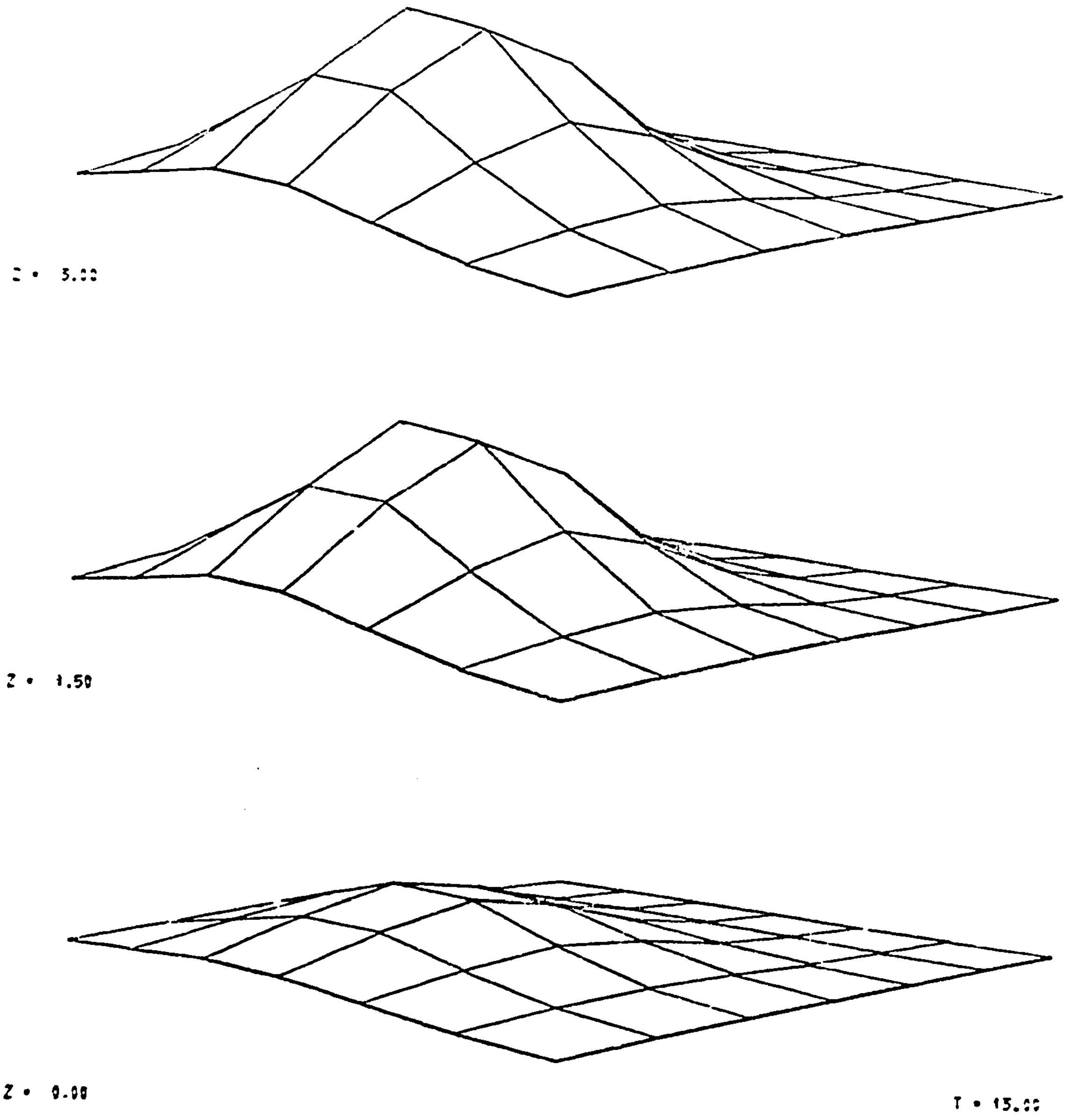

Fig. 39. A three-dimensional representation of a simulated meteorological phenomena for the indicated time and altitude.

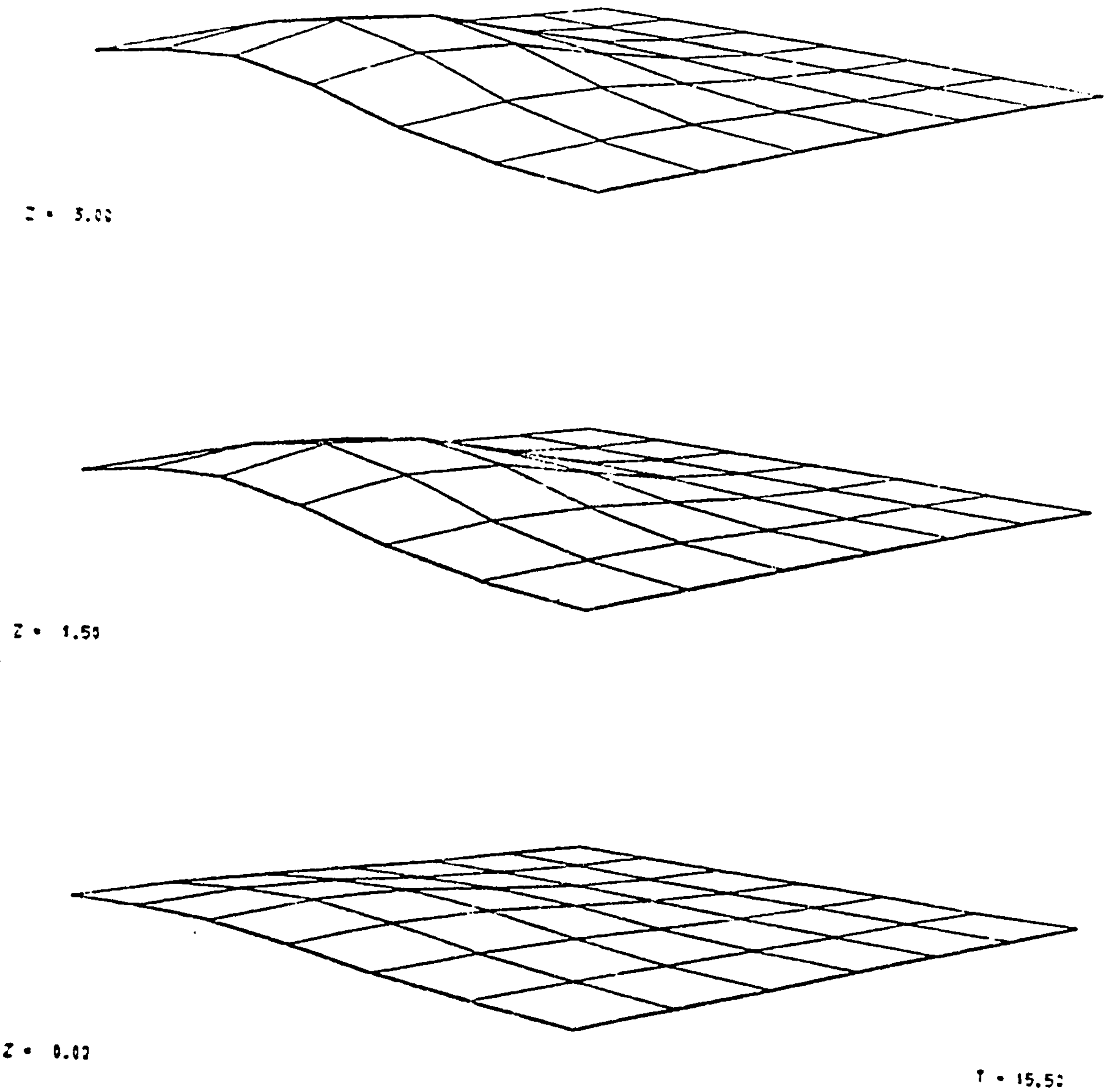

Fig. 40. A three-dimensional representation of a simulated meteorological phenomena for the indicated time and altitude.

stations.

An evaluation of parameters could be made after each sampling time if the sequential method was utilized. This would allow the researcher to conclude the experiment after receiving sufficient data to satisfy his needs.

Parameters

The parameters used in the exponential simulation model were the amplitude, horizontal and vertical shape, sampling time, speed and curvature.

The amplitude (A) is a Markov process with

$$E\{A\}= Ap \ \exp[-\sigma_a^2 \ (t-\bar{A})^2]$$

standard deviation of $\sigma_a A_o(t)$ and lag one correlation coefficient ρ_a. The A_p parameter was assigned a value of 60,ρ_a of 0.95, and σ_a of 0.1.

The horizontal shape was controlled by a factor "omega" in the computer program. A typical value for omega was 2 π/20. The vertical shape was controlled by three variables; omegaz (ω_z), philbar ($\bar{\phi}$) and sigmap (σ_p^2). Realistic values for these variables were ω_z=2π/12, $\bar{\phi}$=20 π/180, and σ_p^2=10 π/180.

The speed parameter (c) has a negative value to move the system from right to left across the grid. A value of -0.3 proved to give satisfactory results.

The curvature parameter (a) moved the system in an elliptic path through a preset point near the bottom of the grid. The preset point determined the place of maximum amplitude. A value of 0.16667 gave realistic results.

The sampling time could be any value between zero and an arbitrary value of 22. The most frequent used were either 8, 10, or 12 because the system was close to the center of the grid and at a near maximum intensity at those times. The time increment was given a value of two allowing only 12 available times.

Abar ($\bar{A}$) is the time of maximum amplitude of the system. The maximum amplitude occurs at a preset point of (3.0, 3.5) on the 7 x 7 grid.

CHAPTER V

MATHEMATICAL MODEL

The optimal design problem may be approached by;

a) deciding on an objective analysis technique

b) choosing the observational points in space-time

c) obtaining samples (signal plus noise) of the parameter field at the chosen points

d) using the objective analysis transform the observations into a forecast or resultant parameter field

e) given the objective analysis scheme, is the forecast field the best approximation in the least squares sense?

The objective is to determine which observational points (not necessarily unique) will produce a "yes" to e above.

The objective analysis model (Eddy, 1973) is linear

$$Y=X\beta+\varepsilon$$

where the β and ε are unknown population values to be estimated from the observations. β is, in reality, a set of unique weights determined by the observation or sample points and the position of Y. β is estimated by b where b is obtained under the desired condition of minimizing the error sum of squares, $\varepsilon^t\varepsilon$, or

$$b=[X^tV^{-1}X]^{-1}\ X^tV^{-1}Y$$

with V, a noise correlation matrix, given by $\sigma^2V=E[\varepsilon\varepsilon^t]$, and $\varepsilon\sim N(0,\sigma^2V)$.

The manner in which V is estimated has been described by Best (1973). The inverse of the noise correlation matrix is

$$V^{-1} = \frac{1}{1-\rho^2} \begin{bmatrix} 1 & -\rho & 0 & \cdots\cdots & & 0 \\ -\rho & 1+\rho^2 & -\rho & 0 \cdots\cdots & & 0 \\ 0 & -\rho & 1+\rho^2 & -\rho \cdots\cdots & & 0 \\ \cdot & 0 & \cdot & & & \cdot \\ \cdot & \cdot & & \cdot & & \cdot \\ \cdot & \cdot & & & \cdot & 0 \\ \cdot & \cdot & & & & -\rho \\ 0 & 0 & \cdots & 0 & -\rho & 1 \end{bmatrix}$$

Best used simulated data with known ρ, then estimated $\hat{\rho}$. σ^2 can be estimated as $\hat{\sigma}^2$ by $\{1/[N-(M+1)]\ \ e^t V^{-1} e$ where N is the number of observational sets and M is the number of sensors.

The objective analysis, $\hat{Y}$, are given by

$$\hat{Y}=Xb$$

and the discrepancies, e, by

$$e=Y-\hat{Y}.$$

The multiple correlation coefficient, R , can be defined as the proportion of variance of Y accounted for by $\hat{Y}$. If

$$Y^t V^{-1} Y=\sigma_y \sigma_{\hat{y}}\ \ R$$

$$R = Y^t V^{-1} \hat{Y}/(Y^t V^{-1} Y)^{\frac{1}{2}}\ \ (\hat{Y}^t V^{-1} \hat{Y})^{\frac{1}{2}}$$

where

$$\sigma_y=(Y^t V^{-1} Y)^{\frac{1}{2}} \quad \text{and} \quad \sigma_{\hat{y}}=(\hat{Y}^t V^{-1} \hat{Y})^{\frac{1}{2}}$$

A similiar expression of R may be obtained by doing some manipulation.

Earlier b was expressed as

$$b=(X^tV^{-1}X)^{-1}X^tV^{-1}Y$$

now

$$\hat{Y}=Xb=X(X^tV^{-1}X)^{-1}X^tV^{-1}Y.$$

Multiplying both sides of the above equation by Y^tV^{-1} to obtain

$$Y^tV^{-1}\hat{Y}=Y^tV^{-1}X(X^tV^{-1}X)^{-1}X^tV^{-1}Y.$$

Evaluate $\hat{Y}^tV^{-1}\hat{Y}$

$$\hat{Y}^tV^{-1}\hat{Y}=Y^tV^{-1}X(X^tV^{-1}X)^{-1}X^tV^{-1}X(X^tV^{-1}X)^{-1}X^tV^{-1}Y$$

$$=Y^tV^{-1}X(X^tV^{-1}X)^{-1}X^tV^{-1}Y$$

therefore

$$\hat{Y}^tV^{-1}\hat{Y}=Y^tV^{-1}\hat{Y}.$$

Now

$$R^2=Y^tV^{-1}\hat{Y}/Y^tV^{-1}Y \qquad \text{............(1)}$$

and the $(1-R^2)$ is the amount of variance unaccounted for by regression. R^2, X, and Y relationship can be expressed by a covariance matrix W. Arrange all observations into a matrix A as follows

$$A = \begin{bmatrix} Y_1 & X_{11} & \cdots\cdots & X_{1M} \\ Y_2 & X_{21} & & X_{2M} \\ \cdot & \cdot & & \cdot \\ \cdot & \cdot & & \cdot \\ \cdot & \cdot & & \cdot \\ Y_N & X_{N1} & \cdots\cdots & X_{NM} \end{bmatrix}$$

The system is rotated by premultiplying by $V^{-\frac{1}{2}}$ to obtain $V^{-\frac{1}{2}}A$.

Define W as the covariance matrix from the rotated data,

$$W=[V^{-\frac{1}{2}}A]^t\ [V^{-\frac{1}{2}}A]$$

or

$$W=A^tV^{-1}A.$$

W can be partitioned as follows

$$W = \left[\begin{array}{c|c} Y^tV^{-1}Y & Y^tV^{-1}X \\ \hline X^tV^{-1}Y & X^tV^{-1}X \end{array}\right] = \left[\begin{array}{c|c} W_{11} & W_{12} \\ \hline W_{21} & W_{22} \end{array}\right] \quad \ldots.(2)$$

Equation 1 can be written using equation 2 as

$$R^2= W_{12}\ W_{22}^{-1}\ W_{21}/W_{11}$$

Note that R^2 is a function of the covariance between various points in the parameter field (predictor and predictand locations).

The determinant of W, $|W|$, is given by

$$|W|=|W_{11}-W_{12}W_{22}^{-1}\ W_{22}|\ \ |W_{22}|$$

so now

$$W_{11}(1-R^2)=|W|/|W_{22}|.$$

Obtaining the best objective analysis involves maximizing the correlation between Y and $\hat{Y}$, which means minimizing $1-R^2$. $1-R^2$ is the inability of the objective analysis to explain the "true" field at the desired grid points for a given set of sensors. The expected values found in Chapter IV are related to the terms in the W matrix. The noise covariance may be equal to $\sigma^2 I$ as the characteristics of the noise are unknown. This will enable us to delete V^{-1} term for the present and $X^tV^{-1}X$ becomes X^tX. Let i and j represent different locations and a g subscript represent grid point values, then

$$(X^tX)_{ij}=E\{S(x_i,y_i,h_i,t_i)S(x_j,y_j,h_j,t_j)\}$$
$$-E\{S(x_i,y_i,h_i,t_i)\}E\{S(x_j,y_j,h_j,t_j)\}.$$

$$(X^tY)_i= E\{S(x_i,y_i,h_i,t_i)S(x_g,y_g,h_g,t_g)\}-E\{S(x_i,y_i,h_i,t_i)\} -$$
$$E\{S(x_g,y_g,h_g,t_g)\}.$$

$$(Y^tY)_i= E\{S(x_g,y_g,h_g,t_g)^2\}-E\{S(x_g,y_g,h_g,t_g)\}^2.$$

The changes in $(1-R^2)W_{11}$ occurs as the positions of the sensors change with respect to changes in the signal. If the sensor is located some distance from the system, then the variance would be small. If the sensor is shifted (in x,y,h,t) and becomes closer to the system, then the variance should be larger. Several maxima and minima variance values will occur, however, we are interested in the global minimum.

CHAPTER VI

APPLICATION TO SUDDEN WARMING

Bayesian Approach

One objective in developing an empirical and mathematical model is to find the optimal time to sample a sudden warming that will give a minimum unexplained variance analysis from a fixed number of stations. Eddy's objective analysis combines the minimum unexplained variance concept along with the correlation over time-space distances and noise characteristics of the data. The objective analysis could also be used to determine which sensor location would yield an optimal variance explanation analysis (OVEA).

The exponential function contains parameters that can be varied to yield the desired model of a sudden warming. If complete knowledge were known about the parameters and their relation to corresponding atmospheric variables, there would be no need for variation. However, complete knowledge about any meteorological system is rarely the case in the real world. One approach that can be utilized in cases of uncertainty or incomplete knowledge is the Bayesian approach.

Excellent discussions on Bayesian statistics may be found in Chernoff and Moses (1959) and Winkler (1972). A Bayes strategy may be defined as the strategy that minimizes the expected variance of an objective analysis given to *a priori* probabilities for all possible outcomes. The approach of applying Bayesian statistics to an experimental design of a sudden warming is as follows:

(1) fix sensor location (ℓ)

(2) fix sample time (t)

(3) fix the curvature (a) and speed (c) of the system

(4) compute the average signal variance (σ^2_{ca}) for all grid points.

(5) Compute the signal variance for all combinations of c and a.

The Bayes risk for a location and time is defined as

$$BR_{\ell,t} = \sum_c \sum_a \rho_{ca} \, \sigma^2_{ca}$$

where ρ_{ca} is the probability factor found in Table 1. The probability factors were calculated from a bivariate normal distribution.

(6) cycle through time

(7) find the time when the risk is the smallest associated with that location, or

$$BR_{opt} = \min_{\ell,t} (BR_{\ell,t}).$$

TABLE 1

PROBABILITY MATRIX FOR CURVATURE (a) AND SPEED (c)

a \ c	-.40	-.30	-.20	TOTAL
.27	.102	.115	.102	.319
.16	.115	.131	.115	.362
.06	.102	.115	.102	.319
TOTAL	.319	.362	.319	1.000

The curvature and speed were not integrated out in the expected value process because they are realistic meteorological parameters. The speed and curvature may be assigned values based upon climatology or experience, but for the grid size that was used c= -.30 and a= 0.1667. Three different values were assigned c and a and the simulated sudden warming was projected across a network for each value. The grid points are used as predictands and the sensor sites (rocket stations) as predictors. The time to sample is also taken into consideration when determining which site to select. The expected average signal variance for each grid point for each combination of c and a was computed considering each sensor location, one at a time. The location that accounts for most of the expected average variance, using all 49 grid points, is chosen as the optimal station. The computations are repeated, holding the first optimal location fixed and finding a second location that, combined with the first, will give an OVEA. The process is repeated again for as many locations as desired. It was demonstrated in Chapter V that the quanity $1-R^2$ represents the fraction unexplained variance in the prediction by the regression; therefore R^2 is the fraction explained variance accounted for by the particular objective analysis technique being used. R^2 was computed for the first optimal station, first three optimal station, five optimal stations, and three sub-optimal statins for a simulated warming of sixty degrees amplitude moving through the 7x7 grid. These percentage values (multiplied by 100) for each combination of c and a are given in Table 2. The times and locations of the optimal stations are shown in Fig. 41.

It is rather obvious that as the number of optimal stations increase, the average variance accounted for by regression increases. The three sub-optimal staions are selected intuitively by choosing the stations closest to the phenomenon at the time and altitude of the analysis. If more than one time and altitude are specified, then

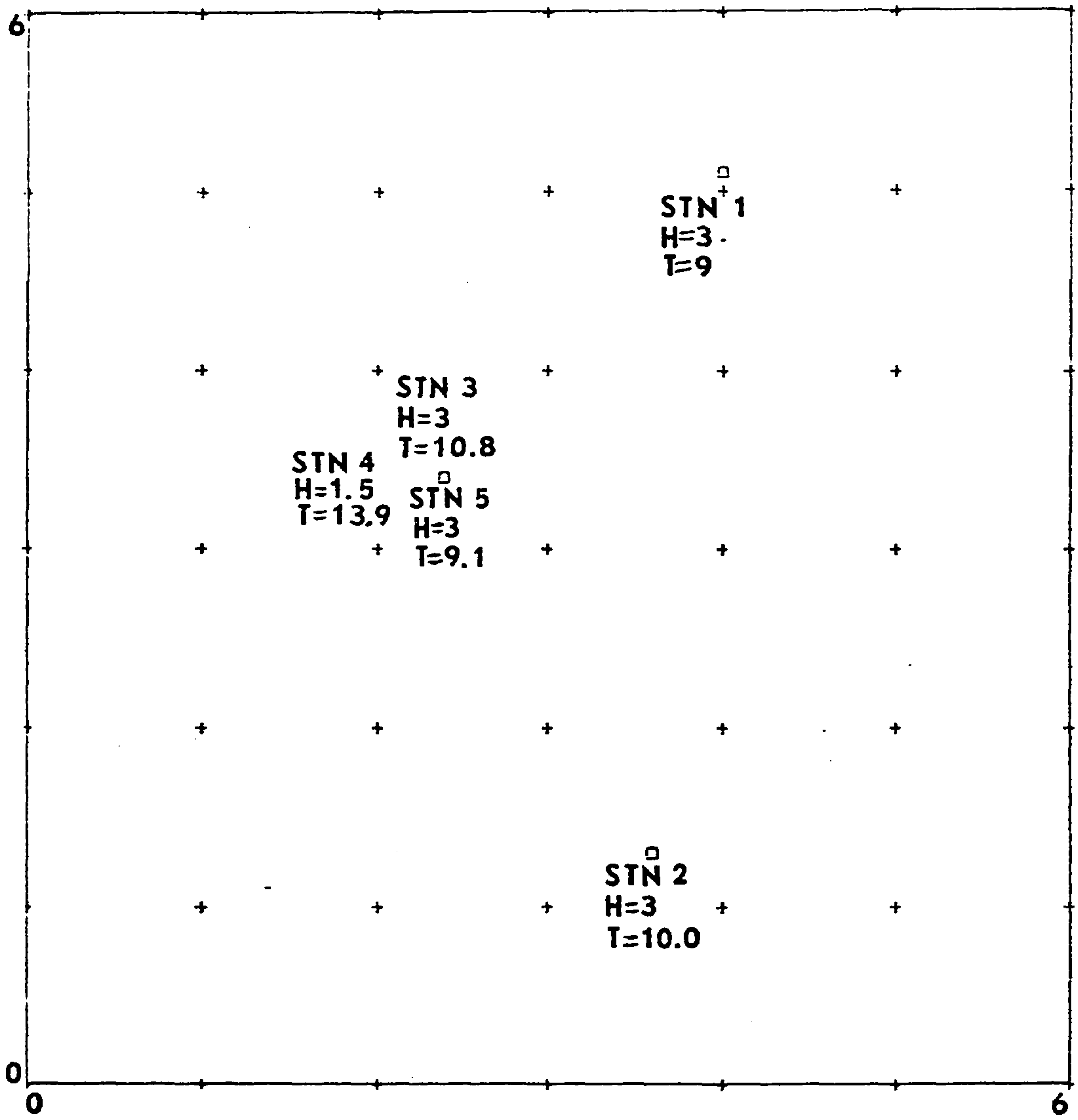

Fig. 41. Optimal station locations and their times and altitudes for a five optimal station variance explanation analysis when the T=10 hours and H=25 km. A square represents possible sensor locations and a dot is a grid point location.

the selected station would be the centroid of the space and time domain. In this particular case the three sub-optimal stations had just as good of an OVEA as the first three optimal stations. The sub-optimal station locations were probably identical with the first three optimal stations except for an altitude difference of one station.

The optimal station locations in Fig. 41 are about as expected due to the path of the warming. Stations 3, 4, and 5 are located in the same x-y location, but station 4 has a different altitude.

TABLE 2

PERCENTAGE AVERAGE VARIANCE EXPLAINED BY REGRESSION FOR DIFFERENT NUMBER OF SAMPLE STATIONS THAT GAVE AN OPTIMAL SOLUTION FOR DIFFERENT COMBINATIONS OF CURVATURE AND SPEED.

FIRST OPTIMAL STATION

a \ c	-.20	-.30	-.40
.05	33.43	33.00	32.42
.16	33.73	33.63	33.46
.27	33.88	33.94	33.94

FIRST THREE OPTIMAL STATIONS

a \ c	-.20	-.30	-.40
.05	54.51	55.09	55.48
.16	54.14	54.29	54.13
.27	53.77	53.53	52.99

FIVE OPTIMAL STATIONS

a \ c	-.20	-.30	-.40
.05	63.95	66.07	67.60
.16	63.64	65.06	65.69
.27	63.18	63.59	63.30

THREE SUB-OPTIMAL STATIONS

a \ c	-.20	-.30	-.40
.05	55.02	55.60	55.75
.16	54.62	54.65	54.19
.27	54.28	53.91	53.23

The researcher has the capability to refine or make better estimates of the Bayesian parameters as the experiment progresses. The sequence of events that might happen during an experiment are given in Table 3.

TABLE 3

SEQUENCE OF EVENTS USING *A PRIORI* AND *A POSTERIORI* INFORMATION

OBSERVATION	DECISION PARAMETERS	COMPUTE
None	Guess c_1^*, a_1^*	t_{11}, σ^2_{11}
		t_{12}, σ^2_{12}
		$\vdots \quad \vdots$
		t_{1m}, σ^2_{1m}
$t_1, \hat{\sigma}^2_1$	estimate c_2^*, a_2^*	t_{21}, σ^2_{21}
		t_{22}, σ^2_{22}
		$\vdots \quad \vdots$
		t_{2m}, σ^2_{2m}
$t_1, t_2, \hat{\sigma}^2_2$	estimate c_3^*, a_3^*	t_{31}, σ^2_{31}
		t_{32}, σ^2_{32}
		$\vdots \quad \vdots$
		t_{3m}, σ^2_{3m}

The researcher begins by making *a priori* estimates of the two Bayesian parameters (c* and a*) and then the sampling times (t_{1m}) and the unexplained variance (σ^2_{1m}) are calculated. The "observations" at times t_{ij} give a better estimate for c*, a* and new sampling times and variances are computed. The variance ($\hat{\sigma}_2^2$) and time (t_1) are now *a posteriori* estimates. $\hat{\sigma}_2^2$ can be compared with $\hat{\sigma}_1^2$ to determine if further sampling is needed. The sampling could continue until $|\hat{\sigma}_{M+1}^2 - \hat{\sigma}_M^2| < \varepsilon$, where the value of ε is based upon experience or some present criteria.

The importance of the Bayesian approach is that it allows variation in the speed and curvature parameters. Any parameter could have been a Bayesian parameter as there are no restrictions on the quantity. However, parameters should be chosen that will reveal some information about the phenomena being sampled.

Utility

The concept of an utility function can be utilized in the sudden warming experiment even though it is hard to put a value on a successful experiment. One would be hard pressed to put a monetary value on what a successful sampling of a sudden warming would mean to science. One can either maximize an utility function or minimize a cost function. I have chosen to do the latter and have set the cost equal to the unexplained variance.

The cost associated with different strategies could become very involved if there were a wide choice of rocket instrumentation available that gave about the same results for the same cost. However, a Loki rocket, complete with temperature and wind sensors and capable of sampling to 65 km, costs about \$850.00. A boosted or super Loki that will reach an altitude of 90 km costs \$1,100.00, while a comparable Arcas rocket costs \$3,000.00. There are no advantages in using the bigger rockets since the accuracies of the above three are about equal. It is clear which rocket system will give the most information for the least cost.

Computer Program

OPTML, a computer program written in Fortran IV, computes the optimal sampling times and the station locations to be used during a simulated sudden warming. This program is listed in Appendix C. OPTML contains the following subroutines or functions: INVERS, inverts a matrix; TIME, computes the minimum residual variance and the associated time; COV, computes the cross-covariance between the data at one point and the data at another point; TIMCK, computes the time used since the beginning of the program and when the subroutine is called; VAR, computes the unexplained variance; COST, computes the equivalent cost associated with a specific time.

A second program, EXPVAR, is listed after OPTMAL in Appendix C. EXPVAR computes the total expected variance utilizing the optimal times and station locations as computed in the OPTML program. The input parameters were the same for both programs, so they were not included in EXPVAR. The subroutine COV and function INVERS are common to both programs and were only listed in OPTML.

The following functions and subroutines are found in EXPVAR: REG, computes regression coefficients and outputs the objective analysis; EXPEC, computes the expected signal; CONTR, a plotting subroutine for the x - y plotter located at White Sands Missile Range, New Mexico; ACTUL, computes the actual signal; RED, adds red noise to the data by using the Function GAUSS and random number generator RANDOM.

Sensititivity Analysis

All the above parameters (see Chapter IV) were changed over a range of values to determine what effect each would have on the final analysis. $\bar{A}$ was assigned values of 7 to 13; σ_p^2 was assigned $7\pi/180$ to $10\pi/180$; ω_z ranged from 2 $\pi/15$ to 2 $\pi/24$; $\bar{\phi}$ from 15 $\pi/180$ to 25 $\pi/180$ and omega from 2 $\pi/16$ to 2 $\pi/24$. The analysis was done for t=10 hours and an altitude of 25 km. A comparison of the optimal station locations, times, and percentage explained average variance are given in Tables 4 to 13. The results with the standard values of the parameters ($\bar{A}$=10, $\bar{\phi}$ =20 $\pi/180$, σ_a^2 = .05, σ_p=10 $\pi/180$, ω_z=2$\pi/12$ and omega = 2$\pi/20$) are listed to the left of the enclosed parenthesis. The values inside the parenthesis are due to changing the one parameter.

Tables 4 and 5 list the changes in station location, time and explained variance when $\bar{A}$ was 7 or 13. The results indicate that when $\bar{A}$ had a value of 13 a better OVEA was obtained than when $\bar{A}$ was either 10 or 7. This was due to the maximum amplitude being fixed, and that the system covered a larger area of the grid when $\bar{A}$ was 13 as compared to the other two values. Note also that the times of station 5 in Tables 4 and 5 changed almost 5 hours from the standard. Both conditions chose the altitude of 3 for all five stations with only the x and y locations of stations 4 and 5 interchanging.

Omegaz (ω_z) was a vertical shape parameter and a term in the

TABLE 4

COMPARISON OF STATION LOCATIONS, TIME AND EXPLAINED VARIANCE WHEN $\bar{A}$ = 7 AND $\bar{A}$ = 10. VALUES IN PARENTHESIS ARE FROM $\bar{A}$ = 7.

STN	x	y	z	t	EXP. VAR.
1	4.0(4.0)	5.1(5.1)	3.0(3.0)	9.6(9.5)	34.12(29.20)
2	3.6(2.4)	1.3(3.4)	3.0(3.0)	10.0(10.1)	51.10(47.39)
3	2.4(3.6)	3.4(1.3)	3.0(3.0)	10.8(8.9)	61.56(61.19)
4	2.4(3.6)	3.4(1.3)	1.5(3.0)	13.9(5.3)	64.97(63.95)
5	2.4(2.4)	3.4(3.4)	3.0(3.0)	9.1(4.8)	65.38(66.49)

TABLE 5

COMPARISON OF STATION LOCATIONS, TIME AND EXPLAINED VARIANCE WHEN $\bar{A}$ = 13 AND $\bar{A}$ = 10. VALUES IN PARENTHESIS ARE FROM $\bar{A}$ = 13.

STN	x	y	z	t	EXP. VAR.
1	4.0(4.0)	5.1(5.1)	3.0(3.0)	9.6(9.9)	34.12(41.98)
2	3.6(2.4)	1.3(3.4)	3.0(3.0)	10.0(10.2)	51.10(58.21)
3	2.4(3.6)	3.4(1.3)	3.0(3.0)	10.8(10.0)	61.56(66.78)
4	2.4(2.4)	3.4(3.4)	1.5(3.0)	13.9(15.6)	64.97(68.57)
5	2.4(3.6)	3.4(1.3)	3.0(3.0)	9.1(15.3)	65.38(69.67)

expected altitude value function. ω_z usually had a value of $2\ \pi/12$. Little change occurred in the explained variance analysis when the two ranges were used (See Tables 6 and 7). The major difference is the altitude that was selected when ω_z was $2\ \pi/9$. Four out of the five altitudes given in Table 6 were 15 km, due to the signal being stronger there. The times chosen for both cases agree reasonably well with the standard case.

Phibar ($\bar{\phi}$) and Sigmap (σ_p^2) were vertical shape controlling parameters. Little change occurs in the analysis when these parameters are considered separately, as shown in Tables 8-11. Little change is expected in the vertical shape from sample to sample, except the downward propagation of the system with time.

Omega was a horizontal shape controlling parameter and changed very little from the standard example (Tables 12 and 13). This could be expected as the analysis was for the same time. More variation would have been noticed in the horizontal and vertical shape parameters if different analysis times had been compared.

The covariance function and the mean of the signal are parameters that could be hard to estimate. If the mean varies from season to season while the covariance function remains approximately the same, then it would be important to know what contribution the mean makes to the OVEA. Results from including and removing the expected average signal in the objective analysis are given in Table 14. The percentage average variance explained by regression term is shortened to explained variance. It can be seen that the mean contributers very little to the OVEA.

TABLE 6

COMPARISON OF STATION LOCATIONS, TIME AND EXPLAINED VARIANCE WHEN OMEGAZ = 2 π/9 AND 2π/12. VALUES IN PARENTHESIS ARE FROM OMEGAZ=2π/9

STN	x	y	z	t	EXP. VAR.
1	4.0(4.0)	5.1(5.1)	3.0(1.5)	9.6(9.7)	34.12(33.38)
2	3.6(3.6)	1.3(1.3)	3.0(1.5)	10.0(10.0)	51.10(52.74)
3	2.4(2.4)	3.4(3.4)	3.0(3.0)	10.8(10.6)	61.56(64.28)
4	2.4(2.4)	3.4(3.4)	1.5(1.5)	13.9(13.9)	64.97(68.78)
5	2.4(2.4)	3.4(3.4)	3.0(1.5)	9.1(8.0)	65.38(72.92)

TABLE 7

COMPARISON OF STATION LOCATIONS, TIME AND EXPLAINED VARIANCE WHEN OMEGAZ = 2 π/15 AND 2π/12. VALUES IN PARENTHESIS ARE FROM OMEGAZ=2π/15

STN	x	y	z	t	EXP. VAR.
1	4.0(4.0)	5.1(5.1)	3.0(3.0)	9.6(9.7)	34.12(34.40)
2	3.6(2.4)	1.3(3.4)	3.0(3.0)	10.0(9.7)	51.10(52.49)
3	2.4(3.6)	3.4(1.3)	3.0(3.0)	10.8(10.0)	61.56(60.16)
4	2.4(2.4)	3.4(3.4)	1.5(3.0)	13.9(12.9)	64.97(67.23)
5	2.4(3.6)	3.4(1.3)	3.0(3.0)	9.1(7.3)	65.38(69.63)

TABLE 8

COMPARISON OF STATION LOCATIONS, TIME AND EXPLAINED VARIANCE WHEN PHIBAR = 15 π/180 AND 20 π/180. VALUES IN PARENTHESIS ARE FROM PHIBAR = 15π/180

STN	x	y	z	t	EXP. VAR.
1	4.0(4.0)	5.1(5.1)	3.0(3.0)	9.6(9.7)	34.12(34.33)
2	3.6(3.6)	1.3(1.3)	3.0(3.0)	10.0(10.0)	51.10(51.74)
3	2.4(2.4)	3.4(3.4)	3.0(3.0)	10.8(10.6)	61.56(61.77)
4	2.4(2.4)	3.4(3.4)	1.5(3.0)	13.9(13.8)	64.97(65.64)
5	2.4(2.4)	3.4(3.4)	3.0(3.0)	9.1(7.6)	65.38(69.25)

TABLE 9

COMPARISON OF STATION LOCATIONS, TIME AND EXPLAINED VARIANCE WHEN PHIBAR = 25 π/180 AND 20 π/180. VALUES IN PARENTHESIS ARE FROM PHIBAR = 25π/180

STN	x	y	z	t	EXP. VAR.
1	4.0(4.0)	5.1(5.1)	3.0(3.0)	9.6(9.7)	34.12(34.10)
2	3.6(3.6)	1.3(1.3)	3.0(3.0)	10.0(10.1)	51.10(51.37)
3	2.4(2.4)	3.4(3.4)	3.0(3.0)	10.8(10.5)	61.56(61.72)
4	2.4(2.4)	3.4(3.4)	1.5(1.5)	13.9(13.8)	64.97(65.82)
5	2.4(2.4)	3.4(3.4)	3.0(3.0)	9.1(7.5)	65.38(69.28)

TABLE 10

COMPARISON OF STATION LOCATIONS, TIME AND EXPLAINED VARIANCE WHEN SIGMAP = 7 $\pi/180$ AND $10\pi/180$. VALUES IN PARENTHESIS ARE FROM SIGMAP = 7 $\pi/180$

STN	x	y	z	t	EXP. VAR.
1	4.0(4.0)	5.1(5.1)	3.0(3.0)	9.6(9.7)	34.12(35.12)
2	3.6(3.6)	1.3(1.3)	3.0(3.0)	10.0(10.0)	51.10(51.83)
3	2.4(2.4)	3.4(3.4)	3.0(3.0)	10.8(10.6)	61.56(61.92)
4	2.4(2.4)	3.4(3.4)	1.5(1.5)	13.9(13.8)	64.97(65.67)
5	2.4(2.4)	3.4(3.4)	3.0(1.5)	9.1(7.5)	65.38(69.30)

TABLE 11

COMPARISON OF STATION LOCATIONS, TIME AND EXPLAINED VARIANCE WHEN SIGMAP = 13 $\pi/180$ AND 10 $\pi/180$. VALUES IN PARENTHESIS ARE FROM SIGMAP = 13 $\pi/180$

STN	x	y	z	t	EXP. VAR.
1	4.0(4.0)	5.1(5.1)	3.0(3.0)	9.6(9.7)	34.12(39.89)
2	3.6(3.6)	1.3(1.3)	3.0(3.0)	10.0(10.1)	51.10(51.43)
3	2.4(2.4)	3.4(3.4)	3.0(3.0)	10.8(10.5)	61.56(61.73)
4	2.4(2.4)	3.4(3.4)	1.5(1.5)	13.9(13.9)	64.97(65.48)
5	2.4(2.4)	3.4(3.4)	3.0(1.5)	9.1(7.4)	65.38(69.14)

TABLE 12

COMPARISON OF STATION LOCATIONS, TIME AND EXPLAINED VARIANCE WHEN OMEGA = $2\pi/16$ AND $2\pi/20$. VALUES IN PARENTHESIS ARE FROM OMEGA=$2\pi/16$

STN	x	y	z	t	EXP. VAR.
1	4.0(4.0)	5.1(5.1)	3.0(3.0)	9.6(9.6)	34.12(34.28)
2	3.6(3.6)	1.3(1.3)	3.0(3.0)	10.0(10.0)	51.10(51.65)
3	2.4(2.4)	3.4(3.4)	3.0(3.0)	10.8(10.6)	61.56(60.44)
4	2.4(2.4)	3.4(3.4)	1.5(1.5)	13.9(14.3)	64.97(65.59)
5	2.4(2.4)	3.4(3.4)	3.0(3.0)	9.1(8.3)	65.38(69.73)

TABLE 13

COMPARISON OF STATION LOCATIONS, TIME AND EXPLAINED VARIANCE WHEN OMEGA = $2\pi/24$ AND $2\pi/20$. VALUES IN PARENTHESIS ARE FROM OMEGA=$2\pi/24$

STN	x	y	z	t	EXP. VAR.
1	4.0(4.0)	5.1(5.1)	3.0(3.0)	9.6(9.7)	34.12(34.19)
2	3.6(3.6)	1.3(1.3)	3.0(3.0)	10.0(10.1)	51.10(51.62)
3	2.4(2.4)	3.4(3.4)	3.0(3.0)	10.8(10.6)	61.56(60.47)
4	2.4(2.4)	3.4(3.4)	1.5(1.5)	13.9(13.8)	64.97(64.98)
5	2.4(2.4)	3.4(3.4)	3.0(3.0)	9.1(6.9)	65.38(66.73)

TABLE 14

COMPARISON OF STATION LOCATIONS, TIME, AND EXPLAINED VARIANCE COMPUTED FROM DATA WITH EXPECTED AVERAGE SIGNAL REMOVED AND WITH EXPECTED AVERAGE SIGNAL INCLUDED. VALUES INSIDE THE PARENTHESIS ARE FROM COMPUTATIONS WITH THE SIGNAL REMOVED

STN	x	y	z	t	EXP. VAR.
1	2.0(2.0)	3.5(3.5)	1.5(1.5)	11.5(10.2)	32.62(31.45)
2	2.8(0.3)	0.8(1.6)	1.5(1.5)	11.3(12.7)	43.02(47.87)
3	0.3(2.8)	1.6(0.8)	1.5(1.5)	11.7(11.2)	53.62(50.97)
4	2.0(2.0)	3.5(3.5)	1.5(3.0)	7.8(12.3)	60.71(55.66)
5	2.8(2.8)	0.8(0.8)	1.5(1.5)	7.9(7.7)	64.22(59.84)

The results used in Table 14 came from the case where a combination of altitude and time were used. A program was run from when z=10, t=8, z=25 and t=12. The point that gave the best explained variance was chosen. The pupose of performing the combination of time and altitude was to complicate the problem and make it difficult to predict the location of the optimal station. A 5 x 5 grid was used for the combination case to reduce computer time to approximately half of what it would take for 7 x 7 grid. The sample station locations were in the same place on the grid for each instance.

The station locations differ when the means are not included when station 2, 3, and 4 are considered. Even with these differences the time and explained variance underwent little change.

A plot of the unexplained variances for objective analyses performed at Station 1 and Station 5 is shown in Fig. 42. The plots of when the expected average signal was not included are indicated by an arrow with an N at the tail. The unexplained variances were normalized for comparison. The minimum variance occurred at the same time in almost every case with the most variation in station 5. The unexplained

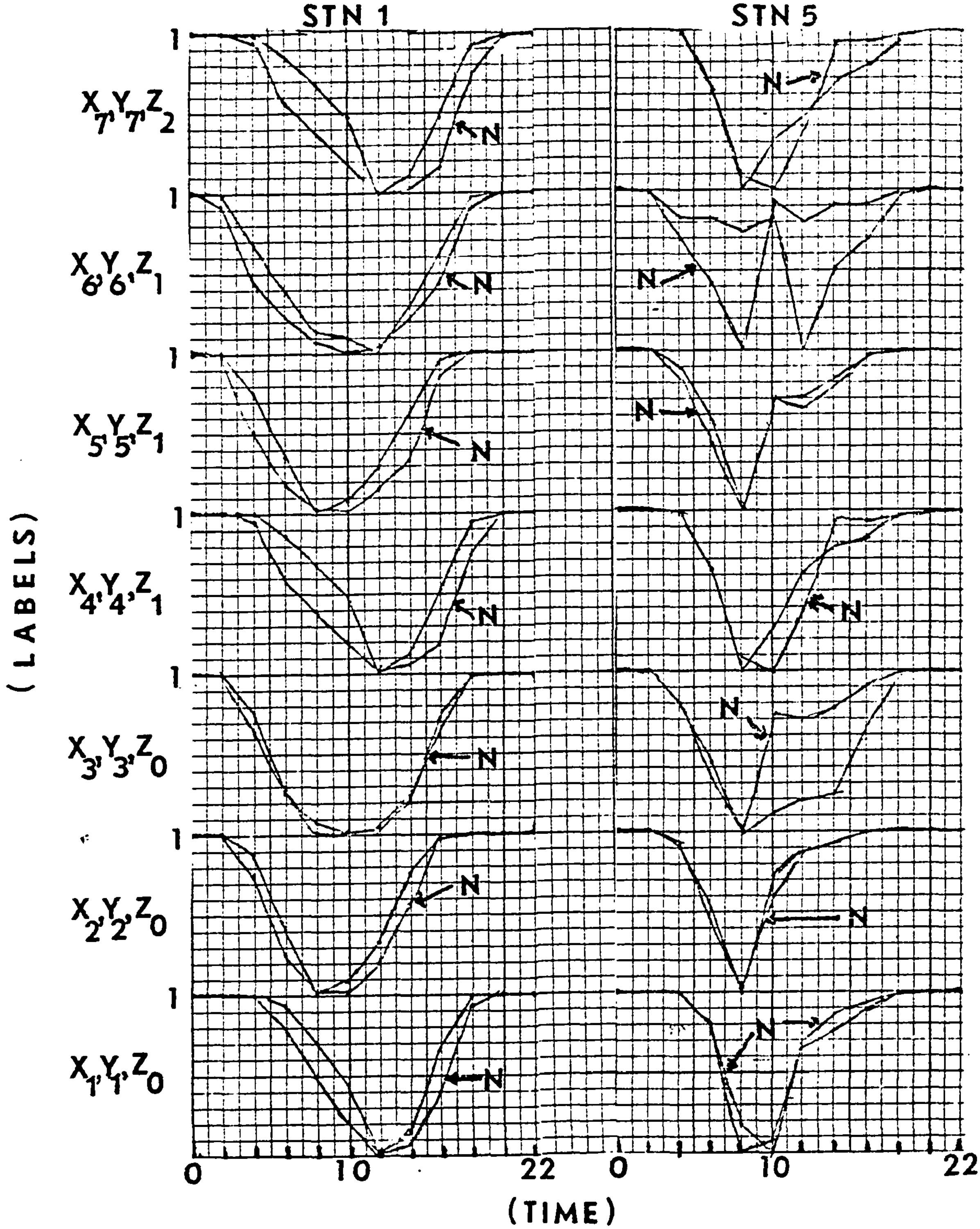

Fig. 42. Normalized variances computed for different stations when the mean was removed (N) and when the mean was included.

variance associated with station 5 (using five optimal "observations") shows sharper curves indicating a quicker minimum variance solution. The labels (X_1, Y_1, Z_1, etc) given in Fig. 42 are for seven of the nine available sensor locations. The correspondence between these labels and the actual station numbers was not part of the output; however, the order that the sensor locations were considered is the same for the two cases presented in Fig. 42.

Grid Point Analysis

The unexplained variance was computed for each grid point for three sub-optimal, first three optimal and first five optimal stations. A portion of these computations appear in Table 15. A smaller number of the unexplained variance indicates a better OVEA than a larger number. The values found in Table 15 are not percentage values, but are numbers resulting from computing the covariance when the various parameters and the expected signal are considered.

TABLE 15

UNEXPLAINED VARIANCE FOR DIFFERENT GRID POINTS AND OPTIMAL STATIONS

GRID POINT NUMBER	VARIANCE	3 SUB OPT.	FIRST OPT.	FIRST 3 OPT.	FIRST 5 OPT.
8	26.383	4.424	24.550	23.786	15.765
9	146.064	22.787	127.408	126.908	73.367
10	243.301	24.359	206.081	148.434	88.174
11	146.064	7.557	131.629	28.161	18.209
12	26.383	7.363	25.306	2.703	2.555
13	1.174	.704	1.159	.380	.380
14	.012	.010	.012	.007	.007
15	41.022	4.709	37.403	31.943	26.581
16	170.238	36.690	139.500	131.080	118.357
17	219.604	139.468	173.852	153.754	153.490
18	170.238	114.638	159.619	62.146	47.501

The smaller numbers do not maintain a consistency with grid points or optimal stations. For example, for grid point 8, the three sub-optimal staion solution is a better solution than the first optimal station, but just the opposite is true for grid point 18. A variation of the values in a column is quite apparent but this is due to the layout of the grid points. Grid point 7, 14, 21, etc., are the extreme right edge grid points and the maximum expected signal may be on the opposite side of the grid.

The first five optimal stations solution does not necessarily have to be the best solution for every grid point, but should have the least total when compared with the other staions.

Fig. 43 is the true signal of a simulated sudden warming of 60C amplitude when T=10 hours and at an altitude of 25 km. This will be the analysis which we are trying to achieve. The objective analysis (Fig. 44) for five optimal stations compares quite well with Fig. 43. The center of both analyses are at approximately the same location, however, the objective analysis is flatter as the 10 contour covers more area. There is a zero contour in Fig. 44 indicating below zero values in the upper and lower right corners.

The total signal variance is shown in Fig. 45. There is a ridge of maximum values extending from top to bottom located in the same position as the maximum signal values. This is not surprising as the maximum total signal variance is expected to be located near the maximum value of the signal.

The fraction unexplained variance accounted for by regression, or $1-R^2$, for five optimal stations are shown in Fig. 46. There is a line

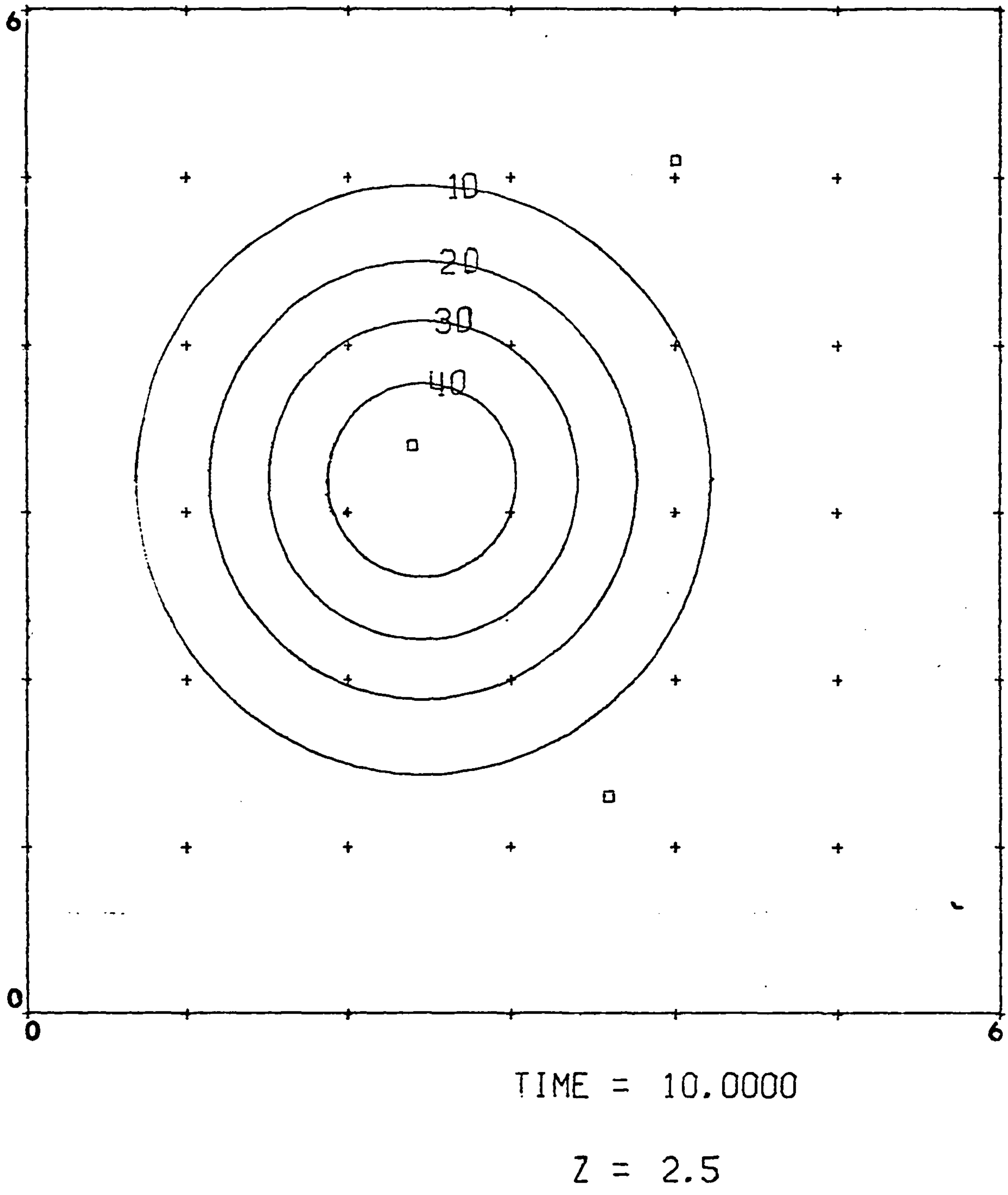

Fig. 43. The signal of a simulated sudden warming when T=10 hours and Z=25 km. A square represents possible sensor location and a plus represents a grid point location.

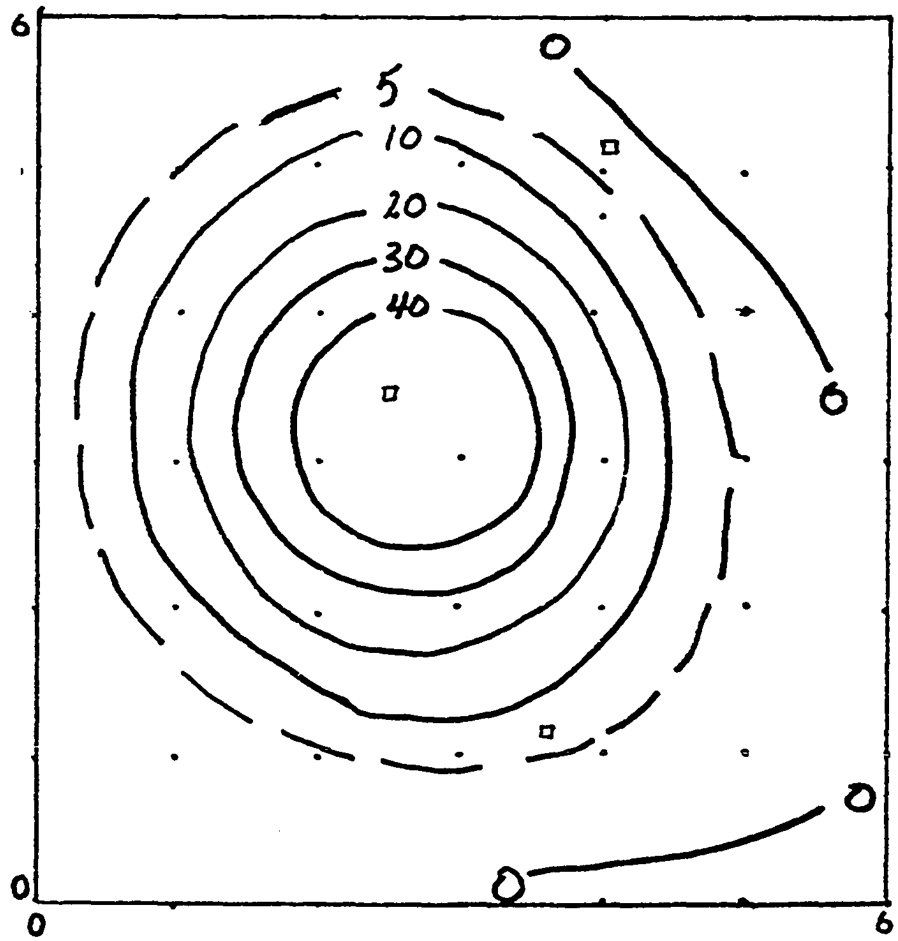

Fig. 44. The objective analysis of a simulated sudden warming when T=10 hours and H=25 km. A square represents possible sensor locations and a dot represents grid points.

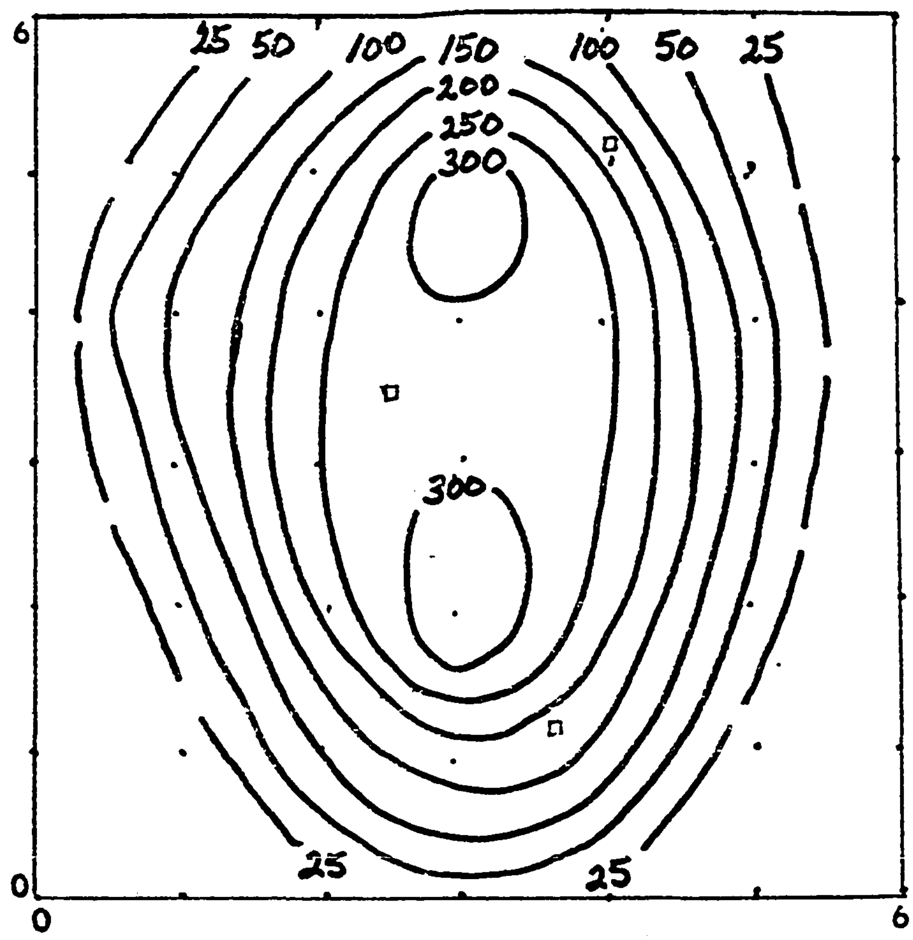

Fig. 45. The total signal variance of a simulated sudden warming when T=10 hours and H=25 km. A square represents possible sensor locations and a dot represents grid points.

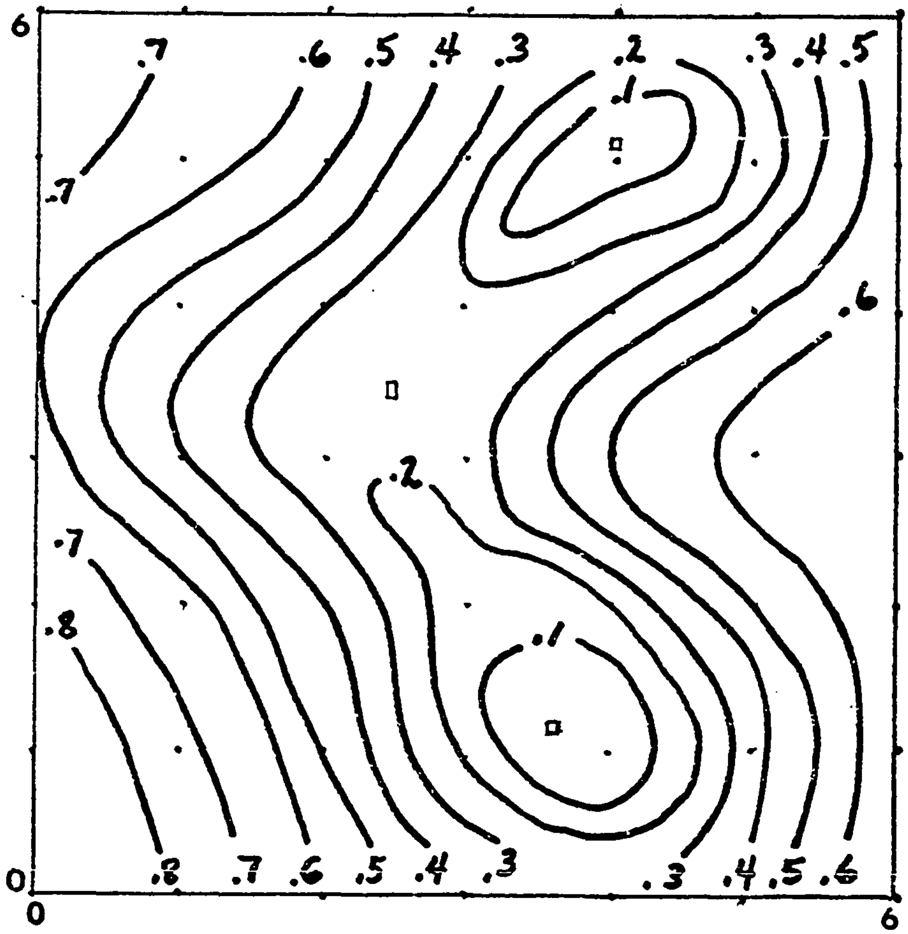

Fig. 46. The fraction unexplained variance accounted for by regression ($1-R^2$) of a simulated sudden warming when T=10 hours and H=25 km. R is the multiple correlation coefficient. A square represents possible sensor locations and a dot represents grid points.

of minimum values extending in a curved fashion from upper right to lower right. This minimum line coincides with the available sensor locations. It is expected that the points surrounding the sensor locations to account for most of the expected average variance.

Experiment

It was stated earlier that one of the objectives of this paper was to develope an optimal sampling technique and not to perform an actual experiment and present those results. This section will discuss how an actual experiment might be carried out.

The time of the occurrence of major stratospheric sudden warmings are from December to March. The NOAA personnel are constantly analyzing data for sudden warmings and issues a STRATWRM alert over the weather teletypes if a sudden warming is approaching North America. This gives some warning so rockets will not be fired just to see if a sudden warming is in the vicinity. However, most rocket installations collect data every Monday, Wednesday, and Friday.

An experimenter might want to set up some criteria to verify that a sudden warming is approaching. One method of determining if a sudden warming is approaching would be the linear discriminant function (LDF) as discussed by Morrison (1967). Morrison defines the LDF as

$$Y = (\bar{x}_1 - \bar{x}_2)^t \, S^{-1} \, (\bar{x}_1 - \bar{x}_2)$$

where $\bar{x}_1$ and $\bar{x}_2$ are the sample mean vectors of two categories and S is the pooled common covariance matrix.

The sample mean vectors come from data collected when a warming was and was not occurring. These data could be temperature at various levels, wind direction, or cloud type and amount derived from satellite photographs. The standard deviation of the pooled data is found, and by knowing the means of each sample, a critical point can be found. The critical point divides the future observations into two categories; a warming will occur or is occurring now, or one will not occur.

If it is decided that a warming is going to occur then rocket installations should be notified to take the necessary actions to insure timely firings. Stations located at Thule, Greenland, Fort Churchill, Canada and Wallops Island, Virginia would probably be the first to obtain samples. Other rocket stations would sample as the warming moved westward.

Each rocket station has problems to overcome to insure a successful firing. The bigger ranges require a mission request two weeks in advance. This can be handled by requesting firing times and cancelling the day before the firing. Other difficulties are the range work hours. Most will not work longer than 10 hours a day, making it impossible to collect data for 24 hours.

Full cooperation of many agencies would have to be had if a sudden warming is ever to be optimally sampled. The US Air Force, NASA, Army, and NOAA efforts would have to be extremely well coordinated by a few individuals. If such experiments such as GATE or GARP are successful, then a smaller experiment such as sampling a sudden warming should be extremely successful.

CHAPTER VII

SUMMARY AND CONCLUSIONS

A technique to sample optimally a stratospheric sudden warming has been presented. This technique uses the concept of time and space covariance relationships of the signal and noise, and a Bayesian approach for varying parameters. The objective analysis furnishes a relation between the sensor location and an estimated parameter through the modeled covariance.

An empirical model of a stratospheric sudden warming was constructed based upon observational studies. The empirical model was then transformed into a statistical-mathematical format that allowed simulation of the sudden warming. An exponential function with a quadratic exponent was used for simulation purposes. No claims are made that this particular function is the best, however, satisfactory results were obtained.

The simulation of the warming was performed using a 7 x 7 grid. The signal entered the grid from the upper right, proceeded to lower center, and departed from the upper left portion. The system changed from a circular form to an elliptic shape as it moved toward the lower center. As it moved up and to the left, the system regained the circular form. The simulated pattern was compared with the isotherm pattern that occurred during a warming, and the similarity was noted.

Various parameters were subjected to a sensitivity analysis and the time that the signal reached its maximum amplitude had more influence on the analysis than the horizontal or vertical shape parameters.

A combination of two altitudes and times for the analysis was interjected for the purpose of complication. The altitude selected for optimal sampling changed with the number of stations selected. The first five optimal station solution usually had a sample time just before the analysis time.

A comparison was made of the true signal and the objective analysis for the same time and altitude. The contours were very similar in shape and size indicating that a good estimate was made of the mean and covariance function.

A systems approach to an optimal experimental design has been developed by Martin C. Yerg (1973). His approach was different in many respects, and these differences will be briefly discussed.

Yerg used an operation research approach while a Bayesian approach was utilized in this paper. He minimized an objective function (minimum variance) that was subjected to constraints of aircraft operations and sampling time. Nonlinear programming (NLP) was used to minimize the objective function. The Bayesian approach allowed variation in the speed and curvature parameters. The combination of the varying parameters that gave the minimum variance solution was used.

Another difference in the two methods was the availability of data. Aircraft can collect volumes of data at many different altitudes and are not restricted in space or time, except by the range of the aircraft. Collection of rocket data is restricted to the immediate vicinity of the rocket installation, and only a vertical profile of the data may be obtained.

Yerg's method utilized simultaneous sampling instead of sequential. Simultaneous sampling may give a better solution due to all the stations being selected at the same time, while only a portion of the stations may sample using the sequential method; however, it was emphasized that sequential sampling has its advantages and is more applicable to rocket type experiments.

Both approaches are similar in that the signal was simulated by an exponential function of some form. Both approaches used an objective analysis technique developed by Eddy and his group at the University of Oklahoma.

The methodology developed in this paper was kept relatively simple, and yet seemed to yield reasonable results as to station locations and sampling times. Better optimal sampling requires for one thing, that work be done in developing a covariance model utilizing real data.

It is the hope of the author that this work will serve as an incentive to those individuals responsible in conducting experiments. The idea of the unplanned collecting of reams of data and hopefully reducing it to a useful form is becoming a thing of the past. Optimal design of experiments is a more logical answer to the conducting of a successful field experiment.

REFERENCES

Alaka, M.A., and R.C. Elvander, 1972: Matching of Observational Accuracy and Sampling Resolution of Meteorological Data Acquisition Experiments, J. Appl. Met., Vol II(4), 567-577.

Avara, E.P., 1973: Extensive Personal Communication

Belmont, A.D., G.W. Nicholas, and W.C. Shen, 1968: Comments on Midwinter Stratospheric Warming in the Southern Hemisphere; General Remarks and a case Study, J. Appl. Met., Vol 7(2), 300-302.

Belmont, A.D., G.W. Nicholas, and W.C. Shen, 1968a: Comparison of 15 Tiros VII Data with Radiosonde Temperatures, J. Appl. Met., Vol 7(2), 284-289.

Best, Larry, 1973: An Evaluation of Noise Characteristics, University of Oklahoma, Norman, Oklahoma, Masters Thesis.

Boville, B.W., 1960: The Aleutian Stratospheric Anticyclone, J. Met., Vol 17(3), 329-336.

Brewer, A.W., 1949: Evidence for a World Circulation Provided by the Measurements of Helium and Water Vapor Distribution in the Stratophere, Q. J. Roy. Met. Soc., Vol 75(326), 351-363.

Briggs, R.S., 1965: Meteorological Rocket Data, McMurdo Station, Antartica, 1962-63, J. Appl. Met., Vol 4(2), 238-245.

Craig, R.A., and W.S. Hering, 1959: The Stratospheric Warming of January-February 1957, J. Met., Vol 16(1), 91-107.

Craig, R.A., and M.A. Lateef, 1962: Vertical Motion During the 1957 Stratospheric Warming, J. Geo. Res., Vol 67(5), 1839-1854.

Dobson, G.M.B., 1956: Origin and Distributing of Polyatomic Molecules in the Atmosphere, Proc. Roy. Soc., Vol A236(1205), 187-193.

Eddy, Amos, 1973: Objective Analysis of Atmospheric Structure, J. Met. Soc. Japan, Vol 6.

Finger, F.G., and S. Teweles, 1964: The Midwinter 1963 Stratospheric Warming and Circulation Change, J. Appl. Met., Vol 3(1), 1-15.

Finger, F.G., and S. Teweles, and R.B. Mason, 1963: Synoptic Analysis Based on Meteorological Rocketsonde Data, J. Geo. Res., Vol 8(5) 1377-1399.

Finger, F.G., and H. Woolf, 1967: Southern Hemisphere Stratospheric Circulation as Indicated by Shipboard Meteorological Rocket Observations, J. Atmos. Sci., Vol 24(4), 387-395.

Fritz, Sigmund, 1970: Earth's Radiation to Space at 15 Microns: Stratospheric Temperature Variation. J. Appl. Met., Vol 9(5), 815-824.

Fritz, Sigmund and Raymond M. McInturff, 1972: Stratospheric Temperature in Autumn-Northern and Southern Hemispheres Compared. Mon. Wea. Rev., Vol 100, 1-7.

Fritz, S., and S.D. Soules, 1970: Large-Scale Temperature Changes in the Stratosphere Observed from Nimbus III. J. Atmos. Sci., Vol 27(7), 1091-1097.

Gandin, L.S., 1963: Objective Analysis of Meteorological Fields, Leningrad, USSR, Hydrometeor Publishing House, (English Version Israel Program for Scientific Translations, 1965). 242 pp.

Glasstone, Samuel, 1965: Sourcebook on the Space Sciences. D. Van Nostrand Co. Inc., Princeton, New Jersey.

Goldie, A.H.R., 1950: The Average Planetary Circulation in Vertical Meridian Planes, Cen. Proc. Roy. Met. Soc., Vol A236(1205), 175-180.

Hare, F.K., 1960: The Disturbed Circulation of the Arctic Stratosphere. J. Met., Vol 17(1), 36-51.

Hook, J.L., 1972: Wind Pattern at Meteor Altitudes (75-105 km) above College, Alaska, Associated with Midwinter Stratospheric Warmings, J. Geo. Res., Vol 77(21), 3865-3868.

Hunten, D.M., and W.L. Godson, 1967: Upper Atmospheric Sodium and Stratospheric Warmings at High Latitudes, J. Atmos. Sci., Vol 24(1), 80-87.

Johnson, K.W., 1969: A preliminary Study of the Stratospheric Warming of Dec. 1967- Jan. 1968, Mon. Wea. Rev., Vol 97(8), 553-564.

Jones, L.M., J.W. Peterson, E.J. Schaefer, and H.F. Schulte, 1959: Upper Air Density and Temperature: Some Variations and an Abrupt Warming of the Mesosphere, J. Geo. Res., Vol 64(12), 2331-2340.

Julian, Paul R., 1967: Midwinter Stratospheric Warmings in the Southern Hemisphere: General Remarks and a Case Study, J. Appl. Met., Vol 63(3), 557-563.

Julian, P.R. and K.B. Labitzke, 1965: A Study of Atmospheric Energetics During the January-February 1963 Stratospheric Warming, J. Atmos. Sci., Vol 22(6), 597-610.

Kasahara, Akira, 1972: GARP Topics, Simulation Experiments for Meteorological Observing Systems for GARP, Bull. Amer. Met. Soc., Vol 53(3), 252-264.

Keegan, T.J., 1962: Large Scale Disturbances of Atmospheric Circulation between 30 and 70 km in Winter, J. Geo. Res., Vol 67(5), 1831-1838.

Kellogg, W.W., 1969: The Dynamics of the Polar Mesosphere in Winter, Trans. Amer. Geo. Union, Vol 41, 620.

Kellogg, W.W., 1961: Chemical Heating above the Polar Mesopause in Winter, J. Met., Vol 18(3), 373-381.

Kellogg, W.W. and G.F. Schilling, 1951: A Proposed Model of the Circulation in the Upper Stratosphere, J. Met., Vol 8(4), 222-230.

Kennedy, James S. and William Nordbery, 1967: Circulation Features of the Stratosphere Derived from Radiometric Temperature Measured with the Tiros VII Satellite, J. Atmos. Sci., Vol 24(6), 711-719.

Kriester, B., K. Labitzke, Richard Scherhag, and R.S. Stuhrman, 1963-1965: Daily and Monthly Northern Hemisphere 10-millibar Synoptic Maps, Meteor. Abhandl., University of Free Berlin.

Kriester, B., K. Labitzke, K. Petzoldt, and K. Sieland, 1967-1968: Daily and Monthly Northern Hemisphere 5-millibar Synoptic Maps, Meteor, Abhandl. University of Free Berlin.

Labitzke, K., 1965: On the Mutual Relation Between Stratosphere and Troposphere during Periods of Stratospheric Warmings in Winter, J. Appl. Met., Vol 14(1), 91-99.

Labitzke, K., 1972: The Interaction Between Stratosphere and Mesophere in Winter, J. Atmos. Sci., Vol 29(7), 1395-1399.

Lacy, Claud, 1973: Objective Analysis Using Modeled Space-Time Covariances: An Evaluation. ECOM-5514, Atmospheric Sciences Laboratory, US Army Electronics Command, White Sands Missile Range, New Mexico.

Leovy, C., 1964: Radiative Equilibrium of the Mesosphere. J. Atmos. Sci., Vol 21(3), 238-248.

Lilly, W.F. and C.E. Palmer, 1960: Stratospheric Mixing for Radioactive Fallout, J. Geo. Res., Vol 65(10), 3307-3317.

Mahlman, J.D., 1969: Heat Balance and Mean Meridonal Circulation in the Polar Stratosphere During the Sudden Warming of January 1958, Mon. Wea. Rev., Vol 97(8), 534-540.

Miers, B.T., 1963: Zonal Wind Reversal Between 30 and 80 km Over the Southwestern States, J. Atmos. Sci., Vol 20(2), 87-93.

Miller, A.J. and K.W. Johnson, 1970: On the Interaction Between the Stratosphere and Troposphere During the Warming of December 1967-January 1968, J. Roy. Met. Soc., Vol 96(407), 24-31.

Morris, J.E. and B.T. Miers, 1964: Circulation Disturbances Between 25 and 70 km Associated with Sudden Warming of 1963, J. Geo. Res., Vol 69(2), 201-214.

Morrison, Donald F., 1967: Multivariate Statistical Methods, McGraw-Hill Inc., New York.

Mukherjee, B.K. and Bh.V. Ramana Murty, 1972: High-Level Warmings Over a Tropical Station, Mon. Wea. Rev., Vol 100(9), 674-681.

Nordberg, W., W.R. Bandeen, G. Warnecke, and V.G. Kunde, 1965: Stratospheric Temperature Patterns Based on Radio-Metric Measurements From Tiros VII Satellite, Space Research, Vol 5, Amsterdam, North Holland Publ. Co., 782-809.

Palmer, C.E., 1959: The Stratospheric Polar Vortex in Winter, J. Geo. Res., Vol 64(7), 749-764.

Powell, Tillman, 1974: Personal Communication

Quiroz, R.S., 1966: Midwinter Stratospheric Warming in the Antartic Revealed by Rocket Data, J. Appl. Met., Vol 5(10), 126-128.

Quiroz, R.S., 1969: The Warming of the Upper Stratosphere in February 1966 and the Associates Structure of the Mesosphere, Mon. Wea. Rev., Vol 97(8), 541-552.

Quiroz, R.S., 1971: The Determination of the Amplitude and Altitude of Stratospheric Warming from Satellite Measured Radiance Change, J. Appl. Met., Vol 10(3), 555-574.

Scherhag, Richard, 1952: Die Explosionsartigen Stratospharener-Warmungen des Spatwinters 1951/1952 (The Explosion-like Stratospheric Warmings of Late Winter 1951/1952), Berichie Deutscher Wetterdienst in der U.S. Zone, Vol 6(38), 51-63.

Scherhag, Richard, 1960: Stratospheric Temperature Changes and the Associated Changes in Pressure Distribution, J. Met., Vol 17(6), 575-582.

Scrase, F.J., 1953: Relatively High Stratosphere Temperature of February 1951, Met. Mag., Vol 82(967), 15-18.

Shapley, A.H. and J.G. Beynon, 1965: Winter Anomaly in Lionspheric Absorption and Stratospheric Warmings, Nature, Vol. 206, 1242-1243.

Shen, W.C., G.W. Nicholas, and A.D. Belmont, 1968: Antarctic Stratospheric Warmings During 1963 Revealed by 15 Tiros VII Data, J. Appl. Met., Vol 7(2), 268-283.

Shenk, W.E. and V.V. Salomonson, 1970: Visible and Infrared Imagery from Meteorological Satellites, Appl. Optics, Vol 9(8), 1747-1760.

Steinitz, G., 1970: Optimum Station Networks in the Tropics, Rept., ESSA Contract E-267-(68)N, Israel Met. Service, Bet Dagan, 71 pp.

Stroud, W.G., W. Nordberg, and W.R. Bandeen, 1960: Rocket-Grenade Measurements of Temperature and Winds in the Mesosphere over Fort Churchill, Canada, J. Geo. Res., Vol 69(3), 2307-2323.

Teweles, S., 1958: Anonalous Warming of the Stratosphere Over North America in Early 1957, Mon. Wea. Rev., Vol 86(4), 377-396.

Teweles, S., 1961: Time Section and Hodograph Analysis of Churchill Rocket and Radiosonde Winds and Temperatures, Mon. Wea. Rev., Vol 89(2), 125-136.

Teweles, S. and F.G. Finger, 1958: An Abrupt Change on Stratospheric Circulation Beginning in Mid-January 1958, Mon. Wea. Rev., Vol 68(1), 23-28.

Teweles, S., L. Rothenberg, and F.G. Finger, 1960: The Circulation at the 10-millibar Constant Pressure Surface Over North America and Adjacent Ocean Areas, July 1957 through June 1958, Mon. Wea. Rev., Vol 88(4), 137-150.

Warnecke, G. and W. Nordberg, 1965: Inferences of Stratospheric and Mesospheric Circulation Systems from Rocket Experiments, Space Research V, Amsterdam, North Holland Publ, Co., 1026-1038.

Webb, Willis L., W.E. Hurbert, R.L. Miller, and J.F. Spurling, 1961: The First Meteorological Rocket Network, Bull. of the Amer. Met. Soc., Vol 42(7), 482-494.

Webb, Willis L., 1966: Structure of the Stratosphere and Mesosphere, International Geophysics Series, Vol 9, Academic Press, New York.

Webb, Willis L., 1974: Personal Communication.

Williams, Ben H., 1968: Synoptic Analyses of the Upper Stratospheric Circulation During the Late Winter Storm Period of 1966, Mon. Wea. Rev., Vol 96(8), 549-558.

Williams, Ben H. and Bruce T. Miers, 1969: Synoptic Events of the Upper Stratospheric Warming of December 1967-January 1968, Progress in Astronautics and Aeronautics, Vol 22, Academic Press, New York.

Winkler, Robert L., 1972: An Introduction to Bayesian Inference and Decision, Holt, Rinehart and Winston, Inc., New York.

Yerg, Martin C., Jr., 1973: An Optimal Sampling and Analysis Methodology, Doctor's Dissertation, University of Oklahoma, Norman, Oklahoma.

Zak, J. Allen, and H.A. Panofsky, 1968: Estimates of Stratospheric Flow From Satellite 15 Radiation, J. Appl. Met., Vol 7(10), 136-140.

APPENDIX A

The expected values of the observation and height function are developed here and in Appendix B. Referring to Chapter IV,

$$S(x,y,h,t)=Z(x,y,h,t)+\varepsilon(x,y,h,t)$$

or the observation (S) at a point and time is equal to the signal (Z) and the noise (ε). The signal

$$Z(x,y,h,t)=A(t)[\exp[-\tfrac{1}{2}Q(x,y,t)]][f(h)]$$

where

A is an amplitude parameter, Q is a quadratic function and f(h) is an altitude function. The expected value of the signal can be expressed as

$$E\{s(x,y,h,t)\}=E\{A\}E\{\exp(-\tfrac{1}{2}Q)\}E\{f(h)\}+E\{\varepsilon\}$$

when it is assummed that $x_o(t)$ and $y_o(t)$ are stochastically independent of A(t).

From Morrison (1967), page 81, the expected value of the joint density function can be written for the general case

$$E\{f(X)\}=\frac{1}{(2\pi)^{p/2}|\Sigma|^{\frac{1}{2}}}\int_{-\infty}^{\infty} f(X)\ \exp[-\tfrac{1}{2}(X-u)^{t}\Sigma^{-1}(X-u)]\ dX$$

where u is the mean, Σ is the covariance matrix,

$$X=\begin{bmatrix} x_1 \\ x_2 \\ \vdots \\ x_p \end{bmatrix},\quad E\{X\}=u=\begin{bmatrix} u_1 \\ u_2 \\ \vdots \\ u_p \end{bmatrix}\qquad \text{and } VAR\{X\}=\Sigma.$$

For our case, let

$$Q=(X-X_o)^tB(X-X_o)=(X_o-X)^tB(X_o-X)$$

where

$$X=\begin{bmatrix} x \\ y \end{bmatrix}, \quad X_o=\begin{bmatrix} x_o(t) \\ y_o(t) \end{bmatrix}, \quad B=\begin{bmatrix} B_{xx}(t) & B_{xy}(t) \\ B_{xy}(t) & B_{yy}(t) \end{bmatrix} \text{ and } \hat{X}_o=\begin{bmatrix} \hat{x}_o(t) \\ \hat{y}_o(t) \end{bmatrix}$$

Since

$$X_o-X=(X_o-\hat{X}_o)+(\hat{X}_o-X)$$

$$Q=(X_o-\hat{X}_o)^tB(X_o-\hat{X}_o)+2(\hat{X}_o-X)^tB(X_o-\hat{X}_o)+(\hat{X}_o-X)^tB(\hat{X}_o-X).$$

For simplicity assume $x_o(t)$ and $y_o(t)$ are Gaussian with covariance matrix Σ. The expected value of $\exp(-\frac{1}{2}Q)$ can be written as

$$E\{\exp(-\tfrac{1}{2}Q)\}=\frac{1}{(2\pi)|\Sigma|^{\frac{1}{2}}}\int_{-\infty}^{\infty}\exp[-\tfrac{1}{2}\{Q+(X_o-\hat{X}_o)^t\Sigma^{-1}(X_o-\hat{X}_o)\}]\,dX_o$$

$$=\frac{1}{(2\pi)|\Sigma|^{\frac{1}{2}}}\int_{-\infty}^{\infty}\exp[-\tfrac{1}{2}\{(X_o-\hat{X}_o)^t(B+\Sigma^{-1})(X_o-\hat{X}_o)+$$

$$2(\hat{X}_o-X)^tB(X_o-\hat{X}_o)+(\hat{X}_o-X)^tB(\hat{X}_o-X)\}]\,dX_o \quad \ldots\ldots\ldots\ldots\ldots(A1)$$

It would be convenient to have part of Eqn A1 in the form

$$(1/2\pi|H|^{\frac{1}{2}})\int_{-\infty}^{\infty}\exp(-\tfrac{1}{2}U^tH^{-1}U)\,dU$$

as this equals unity. Let

$$H=(B+\Sigma^{-1})^{-1}$$

$$U=(X_o-\hat{X}_o)+G(\hat{X}_o-X)$$

with G being an unknown variable to be determined.

$$U^tH^{-1}U=(X_o-\hat{X}_o)^t(B+\Sigma^{-1})(X_o-\hat{X}_o)+2(X_o-\hat{X}_o)^t(B+\Sigma^{-1})G(\hat{X}_o-X)+$$

$$(\hat{X}_o-X)^tG^t(B+\Sigma^{-1})G(\hat{X}_o-X) \quad \ldots\ldots\ldots\ldots\ldots(A2)$$

Let $(B+\Sigma^{-1})G=B$, then $G=(B+\Sigma^{-1})^{-1}B$,

then $U=(X_o-\hat{X}_o)+(B+\Sigma^{-1})^{-1}B(\hat{X}_o-X)$.

Consider only the last term in Eqn A1. Substituting $(B+\Sigma^{-1})G$ for B gives

$$(\hat{X}_o-X)^t(B+\Sigma^{-1})G(\hat{X}_o-X). \qquad \text{............(A3)}$$

Now the portion $G^t(B+\Sigma^{-1})G$ in Eqn A2 can be written

$$G^t(B+\Sigma^{-1})G=B(B+\Sigma^{-1})^{-1}(B+\Sigma^{-1})(B+\Sigma^{-1})^{-1}B$$
$$=B(B+\Sigma^{-1})^{-1}B.$$

Eqn A2 becomes

$$(\hat{X}_o-X)^tB(B+\Sigma^{-1})^{-1}B(\hat{X}_o-X). \qquad \text{............(A4)}$$

Adding and subtracting Eqn A3 to the last term in Eqn A1 gives

$$(\hat{X}_o-X)^tB(\hat{X}_o-X)-(\hat{X}_o-X)^tB(B+\Sigma^{-1})^{-1}B(\hat{X}_o-X)+$$
$$(\hat{X}_o-X)^tB(B+\Sigma^{-1})^{-1}B(\hat{X}_o-X). \qquad \text{............(A5)}$$

The last term in Eqn A5 is what is needed to add to Eqn A1 to almost obtain the desired equation. Now

$$E\{\exp(-\tfrac{1}{2}Q)\}=\frac{1}{(2\pi)|\Sigma|^{\frac{1}{2}}}\exp\{-\tfrac{1}{2}(\hat{X}_o-X)^t[B-B(B+\Sigma^{-1})^{-1}B](\hat{X}_o-X)\}$$
$$\int_{\infty}^{-\infty}\exp[-\tfrac{1}{2}U^t(B+\Sigma^{-1})U]\,dU. \qquad \text{............(A6)}$$

The coefficient of Eqn A6 is $\frac{1}{(2\pi)|\Sigma|^{\frac{1}{2}}}$ and the desired form is

$\frac{1}{(2\pi)|B+\Sigma^{-1}|^{\frac{1}{2}}}$ for the last term to be unity.

$$\frac{1}{(2\pi)|\Sigma|^{\frac{1}{2}}}=\left(\frac{1}{|\Sigma|^{\frac{1}{2}}|B+\Sigma^{-1}|^{\frac{1}{2}}}\right)\left(\frac{1}{(2\pi)|B+\Sigma^{-1}|^{-\frac{1}{2}}}\right).$$

Eqn A5 becomes

$$E\{\exp(-\tfrac{1}{2}Q)\}=\frac{1}{(2\pi)\,|B+\Sigma^{-1}|^{\frac{1}{2}}}\exp\{-\tfrac{1}{2}(\hat{X}_o-X)^t[B-B(B+\Sigma^{-1})^{-1}B]\;(\hat{X}_o-X)\}$$

$$\frac{1}{(2\pi)\,|B+\Sigma^{-1}|^{-\frac{1}{2}}}\int_{-\infty}^{\infty}\exp[-\tfrac{1}{2}U^t(B+\Sigma^{-1})U\quad dU]\;\ldots\ldots\ldots\ldots(A7)$$

The last part of Eqn A7 is equal to unity, however, more modification is needed on the first part. The term $B-B(B+\Sigma^{-1})^{-1}B$ can be written as $B^{\frac{1}{2}}(I+B^{\frac{1}{2}}\Sigma B^{\frac{1}{2}})^{-1}B^{\frac{1}{2}}$. This can be proven from the identity

$$(F+GHG^t)^{-1}=F^{-1}-F^{-1}G(H^{-1}+G^tF^{-1}G)^{-1}G^tF^{-1}.$$

This can be obtained by writing

$$\begin{aligned}(F+GHG^t)&=F+GH(H^{-1}+G^tF^{-1}G)(H^{-1}+G^tF^{-1}G)^{-1}G\\&=F+(G+GHG^tF^{-1}G)(H^{-1}+G^tF^{-1}G)^{-1}G^t\\&=F+(F+GHG^t)F^{-1}G(H^{-1}+G^tF^{-1}G)^{-1}G^t\\F&=(F+GHG^t)[I-F^{-1}G(H^{-1}+G^tF^{-1}G)^{-1}G^t]\\I&=(F+GHG^t)\;[F^{-1}-F^{-1}G(H^{-1}+G^tF^{-1}G)^{-1}G^tF^{-1}]\\(F+GHG^t)^{-1}&=F^{-1}-F^{-1}G(H^{-1}+G^tF^{-1}G)^{-1}G^tF^{-1}\end{aligned}$$

Let $B^{-1}=F$, $I=G$, $\Sigma=H$, then

$$\begin{aligned}B-B(B+\Sigma^{-1})^{-1}B&=(B^{-1}+\Sigma)^{-1}\\&=[B^{-\frac{1}{2}}(I+B^{\frac{1}{2}}\Sigma B^{\frac{1}{2}})B^{\frac{1}{2}}]^{-1}\\&=B^{\frac{1}{2}}(I+B^{\frac{1}{2}}\Sigma B^{\frac{1}{2}})^{-1}B^{\frac{1}{2}}.\end{aligned}$$

$|\Sigma|^{\frac{1}{2}}|B+\Sigma^{-1}|^{\frac{1}{2}}$ can be written as $|\Sigma B+I|^{\frac{1}{2}}$.

Eqn A7 now becomes

$$E\{\exp(-\tfrac{1}{2}Q)\}=\frac{1}{|I+\Sigma B|^{\frac{1}{2}}}\exp[-\tfrac{1}{2}(\hat{X}_o-X)^tB^{\frac{1}{2}}(I+B^{\frac{1}{2}}\Sigma B^{\frac{1}{2}})^{-1}B^{\frac{1}{2}}(\hat{X}_o-X)].$$

Let the quadratic form $Q(x,y,t)$ be an ellipse with one axis in the direction of propagation of the system and the other axis perpendicular to the first. Let $\theta(t)$ be the angle between the velocity vector of the system and the x-axis of the grid. Now we can write

$$B=R^t B_o R$$

where R is a rotation vector and written as

$$R=\begin{bmatrix} \text{Cos}\theta\ (t) & \text{Sin}\theta\ (t) \\ -\text{Sin}\theta\ (t) & \text{Cos}\theta\ (t) \end{bmatrix} \quad \text{and } B_o=\begin{bmatrix} b_x(t) & 0 \\ 0 & b_y(t) \end{bmatrix}.$$

An additional requirement will be that the variations in the point $[x_o(t), y_o(t)]$ about $[\hat{x}_o(t), \hat{y}_o(t)]$ have a component along the direction of propagation of the system which is independent of the component perpendicular to the direction of the system. Therefore,

$$\Sigma=R^t \Sigma_o R$$

where

$$\Sigma_o=\begin{bmatrix} \sigma_x^2(t) & 0 \\ 0 & \sigma_y^2(t) \end{bmatrix}$$

Let $M=B^{\frac{1}{2}}(I+B^{\frac{1}{2}}\Sigma B^{\frac{1}{2}})^{-1}B^{\frac{1}{2}}$.

Substituting for B, Σ, and remembering that $I=R^tR$

$$M=(R^tB_o^{\frac{1}{2}}R)\ \ [I+(R^tB_o^{\frac{1}{2}}R)(R^t\Sigma_oR)(R^tB_o^{\frac{1}{2}}R)]^{-1}\ \ (R^tB_o^{\frac{1}{2}}R)$$

$$=(R^tB_o^{\frac{1}{2}}R)\ \ [I+R^t(B_o^{\frac{1}{2}}\Sigma_oB_o^{\frac{1}{2}})R]^{-1}(R^tB_o^{\frac{1}{2}}R)$$

$$=(R^tB_o^{\frac{1}{2}}B)[R^tR+R^t(B_o^{\frac{1}{2}}\Sigma_oB_o^{\frac{1}{2}})R]^{-1}R^tB_o^{\frac{1}{2}}R)$$

$$=(R^tB_o^{\frac{1}{2}}R)R^t(I+B_o^{\frac{1}{2}}\ \Sigma B_o^{\frac{1}{2}})^{-1}R(R^tB_o^{\frac{1}{2}}R)$$

$$=R^t[B_o^{\frac{1}{2}}(I+B_o^{\frac{1}{2}}\Sigma_oB_o^{\frac{1}{2}})^{-1}B_o^{\frac{1}{2}}]R.$$

If $D=B_o^{\frac{1}{2}}(I+B_o^{\frac{1}{2}}\Sigma_o B_o^{\frac{1}{2}})^{-1}B_o^{\frac{1}{2}}$, then

$$M=R^t DR.$$

Evaluating $(I+B_o^{\frac{1}{2}}\Sigma_o B_o^{\frac{1}{2}})$ by substituting the appropriate values for B_o and Σ_o yields

$$\underset{I}{\begin{bmatrix} 1 & 0 \\ 0 & 1 \end{bmatrix}} + \underset{B_o^{\frac{1}{2}}}{\begin{bmatrix} b_x^{\frac{1}{2}}(t) & 0 \\ 0 & b_y^{\frac{1}{2}}(t) \end{bmatrix}} \underset{\Sigma_o}{\begin{bmatrix} \sigma_x^2(t) & 0 \\ 0 & \sigma_y^2(t) \end{bmatrix}} \underset{B_o^{\frac{1}{2}}}{\begin{bmatrix} b_x^{\frac{1}{2}}(t) & 0 \\ 0 & b_y^{\frac{1}{2}}(t) \end{bmatrix}}$$

$$= \begin{bmatrix} 1+b_x(t)\sigma_x^2(t) & 0 \\ 0 & 1+b_y(t)\sigma_y^2(t) \end{bmatrix}.$$

Taking the inverse, pre and post multiplying by $B_o^{\frac{1}{2}}$

$$D= \begin{bmatrix} \dfrac{b_x(t)}{1+b_x(t)\sigma_x^2(t)} & 0 \\ 0 & \dfrac{b_y(t)}{1+b_y(t)\sigma_y^2(t)} \end{bmatrix} = \begin{bmatrix} dx(t) & 0 \\ 0 & dy(t) \end{bmatrix}$$

Therefore

$$M= \begin{bmatrix} dx\ \mathrm{Cos}^2\theta + dy\ \mathrm{Sin}^2\theta & (dx-dy)\ \mathrm{Sin}\theta\ \mathrm{Cos}\theta \\ (dx-dy)\ \mathrm{Sin}\theta\ \mathrm{Cos}\theta & dx\ \mathrm{Sin}^2\theta + dy\ \mathrm{Cos}^2\theta \end{bmatrix}$$

$$= \begin{bmatrix} M_{xx}(t) & M_{xy}(t) \\ M_{xy}(t) & M_{yy}(t) \end{bmatrix}$$

$$\boxed{E\{S(x,y,h,t)\}=(A_o/\{[(1+b_x\sigma_x^2)(1+b_y\sigma_y^2)]^{\frac{1}{2}}\})\exp\{-\tfrac{1}{2}[M_{xx}(x-\hat{x}_o)^2+ 2M_{xy}(x-\hat{x}_o)(y-\hat{y}_o)+M_{yy}(y-\hat{y}_o)^2]\}E\{f(h)\}} \quad \ldots\ldots\ldots(A8)$$

The expected value between two observations will now be found.

$$E\{S(x_1,y_1,t_1)S(x_2,y_2,t_2)\}=E\{Z(x_1,y_1,t_1)Z(x_2,y_2,t_2)\}+$$

$$E\{\varepsilon(x_1,y_1,t_1)\varepsilon(x_2,y_2,t_2)\}$$

$$=E\{A(t_1)A(t_2)\}E\{\exp\{-\tfrac{1}{2}[Q(x_1,y_1,t_1)+Q(x_2,y_2,t_2)]\}\}E\{f(h_1)f(h_2)\}$$

$$+\rho_n^{|t_2-t_1|}\sigma_n(x_1,y_1,t_1)\sigma_n(x_2,y_2,t_2)\ .$$

Using Matrices let

$$\tilde{Q}=Q(x_1,y_1,t_1)+Q(x_2,y_2,t_2) = (\tilde{X}-\tilde{X}_o)^t\tilde{B}(\tilde{X}-\tilde{X}_o)$$

where

$$\tilde{X} = \begin{bmatrix} X_1 \\ X_2 \end{bmatrix} = \begin{bmatrix} x_1 \\ y_1 \\ x_2 \\ y_2 \end{bmatrix}, \quad \tilde{X}_o = \begin{bmatrix} X_o(t_1) \\ X_o(t_2) \end{bmatrix} = \begin{bmatrix} x_o(t_1) \\ y_o(t_1) \\ x_o(t_2) \\ y_o(t_2) \end{bmatrix}$$

$$\hat{\tilde{X}} = \begin{bmatrix} \hat{X}_o(t_1) \\ \hat{X}_o(t_2) \end{bmatrix} = \begin{bmatrix} \hat{X}_o(t_1) \\ \hat{y}_o(t_1) \\ \hat{x}_o(t_2) \\ \hat{y}_o(t_2) \end{bmatrix} \quad \text{and}$$

$$\tilde{B} = \begin{bmatrix} B(t_1) & 0 \\ 0 & B(t_2) \end{bmatrix} = \begin{bmatrix} B_{xx}(t_1) & B_{xy}(t_1) & 0 & 0 \\ B_{xy}(t_1) & B_{yy}(t_1) & 0 & 0 \\ 0 & 0 & B_{xx}(t_2) & B_{xy}(t_2) \\ 0 & 0 & B_{xy}(t_2) & B_{yy}(t_2) \end{bmatrix}.$$

Assume $X_o(t_1)$ and $X_o(t_2)$ are multivariate normal variates with covariance matrix

$$\tilde{\Sigma} = \begin{bmatrix} \Sigma(t_1) & \$(t_1,t_2) \\ \$(t_1,t_2) & \Sigma(t_2) \end{bmatrix} .$$

From the previous development

$$E\{\exp(-\tfrac{1}{2}Q)\} = (1/(|I+\tilde{\Sigma}\tilde{B}|^{\frac{1}{2}}))\exp\{-\tfrac{1}{2}(\tilde{\tilde{x}}_o-\tilde{x})^t\tilde{B}^{\frac{1}{2}}(I+\tilde{B}^{\frac{1}{2}}\tilde{\Sigma}\tilde{B}^{\frac{1}{2}})^{-1}\tilde{B}^{\frac{1}{2}}(\tilde{\tilde{X}}_o-\tilde{X})\}.$$

Also

$$\tilde{B}=\tilde{R}^t\tilde{B}_o\tilde{R}$$

where

$$\tilde{R}=\begin{bmatrix} \mathrm{Cos}\theta_1 & \mathrm{Sin}\theta_1 & 0 & 0 \\ -\mathrm{Sin}\theta_1 & \mathrm{Cos}\theta_1 & 0 & 0 \\ 0 & 0 & \mathrm{Cos}\theta_2 & \mathrm{Sin}\theta_2 \\ 0 & 0 & -\mathrm{Sin}\theta_2 & \mathrm{Cos}\theta_2 \end{bmatrix} = \begin{bmatrix} R(t_1) & 0 \\ 0 & R(t_2) \end{bmatrix}$$

and

$$\tilde{B}_o= \begin{bmatrix} B_o(t_1) & 0 \\ 0 & B_o(t_2) \end{bmatrix} = \begin{bmatrix} b_x(t_1) & 0 & 0 & 0 \\ 0 & b_y(t_1) & 0 & 0 \\ 0 & 0 & b_x(t_2) & 0 \\ 0 & 0 & 0 & b_y(t_2) \end{bmatrix}.$$

Assume $\tilde{\Sigma}=\tilde{R}^t\tilde{\Sigma}_o\tilde{R}$

where

$$\tilde{\Sigma}_o=\begin{bmatrix} \sigma_x^2(t_1) & 0 & \rho_x^\tau\sigma_x(t_1)\sigma_x(t_2) & 0 \\ 0 & \sigma_y^2(t_1) & 0 & \rho_y^\tau\sigma_y(t_1)\sigma_y(t_2) \\ \rho_x^\tau\sigma_x(t_1)\sigma_x(t_2) & 0 & \sigma_x^2(t_2) & 0 \\ 0 & \rho_y^\tau\sigma_y(t_1)\sigma_y(t_2) & 0 & \sigma_y^2(t_2) \end{bmatrix}$$

and $\tau = |t_2 - t_1|$.

This means that the components of the variation of $[x_o(t), y_o(t)]$ about $[\hat{x}_o(t), \hat{y}_o(t)]$ along and perpendicular to the direction of motion of the system are stochastically independent linear first order Markov processes with lag $-\tau$ correlation coefficients ρ_x^τ and ρ_y^τ.

Let $\tilde{M}=\tilde{B}^{-\frac{1}{2}}(I+\tilde{B}^{-\frac{1}{2}}\tilde{\Sigma}\tilde{B}^{-\frac{1}{2}})^{-1}\tilde{B}^{-\frac{1}{2}}$ ....(A9)

$=\tilde{R}^t\tilde{D}\tilde{R}$

where

$$\tilde{D}=\tilde{B}_o^{-\frac{1}{2}}(I+\tilde{B}_o^{-\frac{1}{2}}\tilde{\Sigma}_o\tilde{B}_o^{-\frac{1}{2}})^{-1}\tilde{B}_o^{-\frac{1}{2}} = \begin{bmatrix} dx_{11} & 0 & dx_{12} & 0 \\ 0 & dy_{11} & 0 & dy_{12} \\ dx_{21} & 0 & dx_{22} & 0 \\ 0 & dy_{21} & 0 & dy_{22} \end{bmatrix} \text{........(A10)}$$

A 4X4 matrix is obtained when $(I+\tilde{B}_o^{-\frac{1}{2}}\tilde{\Sigma}_o\tilde{B}_o^{-\frac{1}{2}})$ is evaluated. The inverse can become involved and is best computed by letting the partitioned matrix

$$\left[\begin{array}{c|c} \alpha_{11} & \alpha_{12} \\ \hline \alpha_{21} & \alpha_{22} \end{array}\right]$$

be the inverse of the non-singular matrix, $B_o^{\frac{1}{2}}\,(I+\tilde{B}_o^{-\frac{1}{2}}\,\tilde{\Sigma}_o\tilde{B}_o^{-\frac{1}{2}})B_o^{\frac{1}{2}}$

represented by

$$\left[\begin{array}{c|c} A_{11} & A_{12} \\ \hline A_{21} & A_{22} \end{array}\right] = (I+\tilde{B}_o^{-\frac{1}{2}}\tilde{\Sigma}_o\tilde{B}_o^{-\frac{1}{2}})^{-1}.$$

It is well known that

$$\alpha_{11}=A_{11}^{-1}+A_{11}^{-1}A_{12}(A_{22}-A_{21}A_{11}^{-1}A_{12})^{-1}A_{21}A_{11}^{-1}$$

$$\alpha_{12}=-A_{11}^{-1}A_{12}(A_{22}-A_{21}A_{11}^{-1}A_{12})^{-1}$$

$$\alpha_{21}=-(A_{22}-A_{21}A_{11}^{-1}A_{12})^{-1}A_{21}A_{11}^{-1}$$

$$\alpha_{22}=(A_{22}-A_{21}A_{11}^{-1}A_{12})^{-1}.$$

Computing $(I+\tilde{B}_o^{\frac{1}{2}}\Sigma_o\tilde{B}_o^{\frac{1}{2}})$ gives

$$A_{11}=\begin{bmatrix} 1+b_x(t_1)\sigma_x^2(t_1) & 0 \\ 0 & 1+b_y(t_1)\sigma_y^2(t_1) \end{bmatrix}$$

$$A_{12}=A_{21}=\begin{bmatrix} b_x^{\frac{1}{2}}(t_1)b_x^{\frac{1}{2}}(t_2)\rho_x^{\tau}\sigma_x(t_1)\sigma_x(t_2) & 0 \\ 0 & b_y^{\frac{1}{2}}(t_1)b_y^{\frac{1}{2}}(t_2)\rho_y^{\tau}\sigma_y(t_1)\sigma_y(t_2) \end{bmatrix}$$

$$A_{22}=\begin{bmatrix} 1+b_x(t_2)\sigma_x^2(t_2) & 0 \\ 0 & 1+b_y(t_2)\sigma_y^2(t_2) \end{bmatrix}.$$

Several terms will now be evaluated.

$$A_{11}^{-1}=\begin{bmatrix} \dfrac{1}{1+b_x(t_1)\sigma_x^2(t_1)} & 0 \\ 0 & \dfrac{1}{1+b_y(t_1)\sigma_y^2(t_1)} \end{bmatrix}$$

$$A_{21}A_{11}^{-1}A_{12}=\begin{bmatrix} \dfrac{b_x(t_1)b_x(t_2)\rho_x^{2\tau}\sigma_x^2(t_1)\sigma_x^2(t_2)}{1+b_x(t_1)\sigma_x^2(t_1)} & 0 \\ 0 & \dfrac{b_y(t_1)b_y(t_2)\rho_y^{2\tau}\sigma_y^2(t_1)\sigma_y^2(t_2)}{1+b_y(t_1)\sigma_y^2(t_1)} \end{bmatrix}$$

$$A_{22}-A_{21}A_{11}^{-1}A_{12}=\begin{bmatrix} \dfrac{g_x(t_1,t_2)}{1+b_x(t_1)\sigma_x^2(t_1)} & 0 \\ 0 & \dfrac{g_y(t_1,t_2)}{1+b_y(t_1)\sigma_y^2(t_1)} \end{bmatrix}$$

where

$$g_x(t_1,t_2)=1+b_x(t_1)\sigma_x^2(t_1)+b_x(t_2)\sigma_x^2(t_2)+(1-\rho_x^{2\tau})b_x(t_1)b_x(t_2)\sigma_x^2(t_1)\sigma_x^2(t_2)$$

and a similar expression containing y's instead of x's for $g_y(t_1,t_2)$.

$$\alpha_{22}=(A_{22}-A_{21}A_{11}^{-1}A_{12})^{-1}=\begin{bmatrix} \dfrac{1+b_x(t_1)\sigma_x^2(t_1)}{g_x(t_1,t_2)} & 0 \\ 0 & \dfrac{1+b_y(t_1)\sigma_y^2(t_1)}{g_y(t_1,t_2)} \end{bmatrix} .$$

This term is common in all the elements of the inverse matrix and is the α_{22} term. The upper left and lower right terms are identical and will be evaluated next.

$$-A_{11}^{-1}A_{12}=\begin{bmatrix} \dfrac{-b_x^{\frac{1}{2}}(t_1)b_x^{\frac{1}{2}}(t_2)\rho_x^{\tau}\sigma_x(t_1)\sigma_x(t_2)}{1+b_x(t_1)\sigma_x^2(t_1)} & 0 \\ 0 & \dfrac{-b_y^{\frac{1}{2}}(t_1)b_y^{\frac{1}{2}}(t_2)\rho_y^{\tau}\sigma_y(t_1)\sigma_y(t_2)}{1+b_y(t_1)\sigma_y^2(t_1)} \end{bmatrix}.$$

$$\alpha_{22}=\alpha_{21}=-A_{11}^{-1}A_{12}(A_{22}-A_{21}A_{11}^{-1}A_{12})^{-1}=$$

$$\begin{bmatrix} \dfrac{-\rho_x^{\tau}b_x^{\frac{1}{2}}(t_1)b_x^{\frac{1}{2}}(t_2)\sigma_x(t_1)\sigma_x(t_2)}{g_x(t_1,t_2)} & 0 \\ 0 & \dfrac{-\rho_y^{\tau}b_y^{\frac{1}{2}}(t_1)b_y^{\frac{1}{2}}(t_2)\sigma_y(t_1)\sigma_y(t_2)}{g_y(t_1,t_2)} \end{bmatrix}.$$

Post multiplying the above by $A_{22}A_{11}^{-1}$ and adding A_{11}^{-1} will yield α_{11}.

$$\alpha_{11}=\begin{bmatrix} \dfrac{g_x(t_1,t_2)+\rho_x^{2\tau}b_x(t_1)b_x(t_2)\sigma_x^2(t_1)\sigma_x^2(t_2)}{g_x(t_1,t_2)[1+b_x(t_1)\sigma_x^2(t_1)]} & 0 \\ & \dfrac{g_y(t_1,t_2)+\rho_y^{2\tau}b_y(t_1)b_y(t_2)\sigma_y^2(t_1)\sigma_y^2(t_2)}{g_y(t_1,t_2)[1+b_y(t_1)\sigma_y^2(t_1)]} \end{bmatrix}.$$

Pre and post multiplying $(I+\tilde{B}_o^{\frac{1}{2}}\tilde{\Sigma}^{-\frac{1}{2}}\tilde{B}_o^{\frac{1}{2}})^{-1}$ by $\tilde{B}_o^{\frac{1}{2}}$ and letting the partitioned matrix

$$\begin{bmatrix} \beta_{11} & \beta_{12} \\ \beta_{21} & \beta_{22} \end{bmatrix} = \tilde{B}_o^{\frac{1}{2}}(I+\tilde{B}_o^{\frac{1}{2}}\tilde{\Sigma}\tilde{B}_o^{\frac{1}{2}})^{-1}\tilde{B}_o^{\frac{1}{2}} \qquad \text{will result in}$$

$$\beta_{11}=\begin{bmatrix} \dfrac{b_x(t_1)[g_x(t_1,t_2)+\rho_x^{2\tau}b_x(t_1)b_x(t_2)\sigma_x^2(t_1)\sigma_x^2(t_2)]}{g_x(t_1,t_2)[1+b_x(t_1)\sigma_x^2(t_1)]} & 0 \\ 0 & \dfrac{b_y(t_1)[g_y(t_1,t_2)+\rho_y^{2\tau}b_y(t_1)b_y(t_2)\sigma_y^2(t_1)\sigma_y^2(t_2)]}{g\;(t_1,t_2)[1+b_y(t_1)\sigma_y^2(t_1)]} \end{bmatrix}$$

$$\beta_{12}=\beta_{21}=\begin{bmatrix} \dfrac{b_x^{\frac{1}{2}}(t_1)b_x^{\frac{1}{2}}(t_2)[-\rho_x^{\tau}b_x^{\frac{1}{2}}(t_1)b_x^{\frac{1}{2}}(t_2)\sigma_x(t_1)\sigma_x(t_2)]}{g_x(t_1,t_2)} & 0 \\ 0 & \dfrac{b_y^{\frac{1}{2}}(t_1)b_y^{\frac{1}{2}}(t_2)[-\rho_y^{\tau}b_y^{\frac{1}{2}}(t_1)b_y^{\frac{1}{2}}(t_2)\sigma_y(t_1)\sigma_y(t_2)]}{g_y(t_1,t_2)} \end{bmatrix}$$

$$\beta_{22}=\begin{bmatrix} \dfrac{b_x(t_2)[1+b_x(t_1)\sigma_x^2(t_1)]}{g_x(t_1,t_2)} & 0 \\ 0 & \dfrac{b_y(t_2)[1+b_y(t_1)\sigma_y^2(t_1)]}{g_y(t_1,t_2)} \end{bmatrix}.$$

These terms can be simplified. Using β_{11} as an example, substituting for $g_x(t_1,t_2)$ in the numerator eliminates the $\rho_x^{2\tau}\, b_x(t_1)b_x(t_2)\sigma_x^2(t_1)\sigma_x^2(t_2)$ term leaving

$$\frac{b_x(t_1)[1+b_x(t_1)\sigma_x^2(t_1)+b_x(t_2)\sigma_x^2(t_2)+b_x(t_1)b_x(t_2)\sigma_x^2(t_1)\sigma_x^2(t_2)]}{g_x(t_1,t_2)\;[1+b_x(t_1)\sigma_x^2(t_1)]}\;.$$

The quantity inside the brackets of the numerator factors and becomes

$$b_x(t_1)[1+b_x(t_1)\sigma_x^2(t_1)][1+b_x(t_2)\sigma_x^2(t_2)].$$

and $1+b_x(t_1)\sigma_x^2(t_1)$ is common in the numerator and denominator. Referring to Eqn A10,

$$dx_{11}=\frac{[1+b_x(t_2)\sigma_x^2(t_2)]b_x(t_1)}{g_x(t_1,t_2)}\quad .$$

Using the same substitution results in

$$dx_{12}=dx_{21}=\frac{-\rho_x^\tau b_x(t_1)b_x(t_2)\sigma_x(t_1)\sigma_x(t_2)}{g_x(t_1,t_2)}$$

and

$$dx_{22}=\frac{[1+b_x(t_1)\sigma_y^2(t_1)]b_x(t_2)}{g_x(t_1,t_2)}\quad .$$

Eqn A9 becomes

$$\tilde{M}=\begin{bmatrix} M_{xx11} & M_{xy11} & M_{xx12} & M_{xy21} \\ M_{xy11} & M_{yy11} & M_{xy12} & M_{yy12} \\ M_{xx21} & M_{xy12} & M_{xx22} & M_{xy22} \\ M_{xy21} & M_{yy21} & M_{xy22} & M_{yy22} \end{bmatrix}\quad .$$

where

$$M_{xxij}=dx_{ij}\text{Cos}\theta_i\text{Cos}\theta_j+dy_{ij}\text{Sin}\theta_i\text{Sin}\theta_j$$

$$M_{xyij}=dx_{ij}\text{Sin}\theta_i\text{Cos}\theta_j-dy_{ij}\text{Cos}\theta_i\text{Sin}\theta_j$$

$$M_{yyij}=dx_{ij}\text{Sin}\theta_i\text{Sin}\theta_j+dy_{ij}\text{Cos}\theta_i\text{Cos}\theta_j$$

for i and j-1,2.

$$|I+\tilde{\Sigma}\tilde{B}|^{\frac{1}{2}}=[g_x(t_1,t_2)g_y(t_1,t_2)]^{\frac{1}{2}}$$

and

$$E\{A(t_1)A(t_2)\}=\rho_a^{\tau}\sigma_a(t_1)\sigma_a(t_2)+A_o(t_1)A_o(t_2)$$

therefore

$$\boxed{E\{S(x_1,y_1,t_1)S(x_2,y_2,t_2)\}=\frac{\rho_a^{\tau}\sigma_a(t_1)\sigma_a(t_2)+A_o(t_1)A_o(t_2)}{[g_x(t_1,t_2)g_y(t_1,t_2)]^{\frac{1}{2}}}(\exp[-\tfrac{1}{2}(\tilde{X}-\tilde{\tilde{X}}_o)^t M(\tilde{X}-\tilde{\tilde{X}}_o)])E\{f(h_1)f(h_2)\}+\rho_n^{\tau}\sigma_n(x_1,y_1,t_1)\sigma_n(x_2,y_2,t_2)}.$$

APPENDIX B

The altitude function adds another dimension to the model. The expected value of the altitude function $\mathrm{Sin}(\omega h+\theta)$ will be evaluated where $\omega=2\pi/T$, θ is the phase angle, T is the period, and h is the altitude variable.

Assume $(f(\theta)=[1/(2\pi)^{\frac{1}{2}}\sigma_\theta]\ \exp[-\frac{1}{2}(\theta-u_\theta/\sigma_\theta)^2]$.

$$E\ \mathrm{Sin}(\omega h+\theta) = \frac{1}{(2\pi)^{\frac{1}{2}}\sigma_\theta}\int_{-\infty}^{\infty} \mathrm{Sin}(\omega h+\theta)[\exp -\tfrac{1}{2}((\theta-u_\theta)/\sigma_\theta)^2]\ d\theta.$$

Let $W=(\theta-u_\theta)/\sigma_\theta$, $dW=d\theta/\sigma_\theta$, $\theta=W\sigma_\theta+u_\theta$.

Substituting for θ and $d\theta$

$$E\{\mathrm{Sin}(\omega h+\theta)\}= \frac{1}{(2\pi)^{\frac{1}{2}}}\int_{-\infty}^{\infty} \mathrm{Sin}(\omega h+W\sigma_\theta+u_\theta)\exp(-\tfrac{1}{2}W^2)\ dW.$$

Consider the sine term, let $A=\omega h+u_\theta$, $W\sigma_\theta=B$, and remembering that

$$\mathrm{Sin}(A+B)=\mathrm{Sin}A\mathrm{Cos}B+\mathrm{Cos}A\mathrm{Sin}B$$

results in

$$\mathrm{Sin}(\omega h+u_\theta+W\sigma_\theta)=\mathrm{Sin}(\omega h+u_\theta)\mathrm{Cos}(W\sigma_\theta)+\mathrm{Cos}(\omega h+u_\theta)\mathrm{Sin}(W\sigma_\theta).$$

Now let $C=\mathrm{Cos}(\omega h+u_\theta)$ and $D=\mathrm{Sin}(\omega h+u_\theta)$ so that

$$E\{\mathrm{Sin}(\omega h+\theta)\}= \frac{1}{(2\pi)^{\frac{1}{2}}}\int_{-\infty}^{\infty} [D\ \mathrm{Cos}(W\sigma_\theta)+C\ \mathrm{Sin}(W\sigma_\theta)]\exp(-\tfrac{1}{2}W^2)\ dW.$$

The $C\ \mathrm{Sin}\ (W\sigma_\theta)$ is zero when integrated because it is an odd function. From the table of integrals

$$\int_{-\infty}^{\infty} [\exp(-a^2x^2)]\mathrm{Cos}\ b_x dx=[(\pi)^{\frac{1}{2}}/a]\ \exp(-b^2/4a^2).$$

If $a^2=\frac{1}{2}$, $x^2=W^2$, and $b=\sigma_\theta$, then

$$E\{\mathrm{Sin}(\omega h+\theta)\}=D\ \frac{\pi}{(2\pi)^{\frac{1}{2}}(\frac{1}{2})^{\frac{1}{2}}}\ \exp\ [-\sigma^2/4(\tfrac{1}{2})]$$

$$=[\exp(-\tfrac{1}{2}\sigma_\theta^2)]\ \mathrm{Sin}(\omega h+u_\theta).$$

Now Eqn A8 of Appendix A can be written as

$$\boxed{\begin{gathered}E\{S(x,y,h,t)\}=A_o\exp\{-\tfrac{1}{2}[M_{xx}(x-\hat{x}_o)^2+2M_{xy}(x-\hat{x}_o)(y-\hat{y}_o)+M_{yy}(y-\hat{y}_o)^2][-\tfrac{1}{2}\sigma_\theta^2]\}\\ [\sin(\omega h+u_\theta)]/[(1+b_x\sigma_x^2)(1+b_y\sigma_y^2)]^{\frac{1}{2}}.\end{gathered}}$$

Consider the cross-product where the covariance can be expressed as

$$\mathrm{Cov}(S_1,S_2)=E\{Z_1,Z_2\}f_{12}-E\{Z_1\}E\{Z_2\}f_1f_2+E\{\varepsilon_1\varepsilon_2\}$$

where

$$E\{f(h_1)f(h_2)\}=\frac{1}{(2\pi)^{\frac{1}{2}}}\int_{-\infty}^{\infty} \mathrm{Sin}(\omega h_1+\theta)\mathrm{Sin}(\omega h_2+\theta)\exp[-\tfrac{1}{2}((\theta-u_\theta)/\sigma_\theta)^2]d\theta.$$

Let $W=(\theta-u_\theta)/\sigma_\theta$, $dW+d\theta/\sigma_\theta$ or $d\theta=dW\sigma_\theta$ and $\theta=W\sigma_\theta+u_\theta$.

$$E\{f(h_1)f(h_2)\}=\frac{1}{(2\pi)^{\frac{1}{2}}}\int_{-\infty}^{\infty} [\mathrm{Sin}(\omega h_1+W\sigma_\theta+u_\theta)][\mathrm{Sin}(\omega h_2+W\sigma_\theta+u_\theta)]\exp(-\tfrac{1}{2}W^2)dW.$$

Using the identity $\mathrm{SinASinB}=\frac{1}{2}[\mathrm{Cos}(A-B)-\mathrm{Cos}(A+B)]$ gives

$$E\{f(h_1)f(h_2)\}= \frac{1}{(2\pi)^{\frac{1}{2}}}\int_{-\infty}^{\infty} \tfrac{1}{2}\{\mathrm{Cos}[\omega h_1+W\sigma_\theta+u_\theta)-(Wh_2+W\sigma_\theta+u_\theta)]-$$

$$\mathrm{Cos}[(\omega h_1+W\sigma_\theta+u_\theta)-(\omega h_2+W\sigma_\theta+u_\theta)]\}\exp(-\tfrac{1}{2}W^2)\ dW$$

$$= \frac{1}{2(2\pi)^{\frac{1}{2}}}\int_{-\infty}^{\infty}\mathrm{Cos}[\omega(h_1-h_2)]-\mathrm{Cos}[\omega(h_1+h_2)+2W\sigma_\theta+2u_\theta]\ \exp(-\tfrac{1}{2}W^2)\ dW$$

$$= \frac{-\mathrm{Cos}\ \omega(h_1-h_2)}{2(2\pi)^{\frac{1}{2}}}\int_{-\infty}^{\infty}\{\mathrm{Cos}[\omega(h+h)+2u_\theta+2W\sigma_\theta]\}\exp(-\tfrac{1}{2}W^2)\ dW.$$

The cosine term can be thought of as Cos(C+D) where $C=\omega(h_1+h_2)+2u_\theta$ and $D=2W\sigma_\theta$, then

$$\mathrm{Cos}(C+D)=\mathrm{Cos}C\ \mathrm{Cos}D-\mathrm{Sin}C\ \mathrm{Sin}D$$

$$E\{f(h_1)f(h_2)\}= \frac{-\mathrm{Cos}[\omega(h_1-h_2)]}{2(2\pi)^{\frac{1}{2}}}\int_{-\infty}^{\infty}\{\mathrm{Cos}[\omega(h_1+h_2)+2u_\theta][\mathrm{Cos}(2W\sigma_\theta)]-$$

$$\mathrm{Sin}[\omega(h_1+h_2)+2u_\theta]\mathrm{Sin}(2W\sigma_\theta)\}\ \exp(-\tfrac{1}{2}W^2)\ dw.$$

The sine terms are equal to zero. Rearranging terms

$$E\{f(h_1)f(h_2)\}= \frac{-\mathrm{Cos}[\omega(h_1-h_2)]\{\mathrm{Cos}[\omega(h_1+h_2+2u_\theta)]\}}{2(2\pi)^{\frac{1}{2}}}\int_{-\infty}^{\infty}[\exp(-\tfrac{1}{2}W\ )][\mathrm{Cos}(2W\sigma_\theta)dW].$$

Utilizing the same integral as before results in

$$\int_{-\infty}^{\infty}[\exp(-\tfrac{1}{2}W^2)][\mathrm{Cos}(2W\sigma_\theta)dW]= \frac{(\pi)^{\frac{1}{2}}}{(\frac{1}{2})^{\frac{1}{2}}}\exp\left[\frac{-4\sigma_\theta^{\ 2}}{4(\frac{1}{2})}\right].$$

$$\boxed{E\{f(h_1)f(h_2)\}=\tfrac{1}{2}\{\mathrm{Cos}[\omega(h_1-h_2)]-[\exp(-2\sigma_\theta^2)]\mathrm{Cos}[\omega(h_1+h_2)+2u_\theta]\}}.$$

APPENDIX C

```
?• IS           •OPTML

      PROGRAM OPTML
      OPTML DETERMINES THE OPTIMAL SAMPLING TIME AND WHICH OF
        THE NSTN POSSIBLE LOCATIONS SHOULD BE USED. A TOTAL
        OF NTOTAL SAMPLING TIMES AND THE CORRESPONDING LOCAT-
        IONS WILL BE FOUND GIVEN THAT THERE ARE NFIX SAMPLING
        TIMES WHICH CANNOT BE ALTERED (THIS COULD INCLUDE ROU-
        TINE SAMPLING OR PAST SAMPLES WHICH CAN INFLUENCE THE
        ANALYSIS). THE ANALYST WILL HAVE A TOTAL OF NTOTAL +
        NFIX SAMPLES TO USE IN THE ANALYSIS. THE ANALYSIS IT-
        SELF IS COMPOSED OF USING ALL AVAILABLE SAMPLES IN A
        LINEAR REGRESSION PROCEDURE TO PREDICT THE OBSERVATION
        AL (BUT NOISE FREE) VALUES AT GRID POINTS IN SPACE AT
        PARTICULAR TIMES.

        OPTML FINDS THE OPTIMAL SAMPLING TIMES SEQUENTIALLY NOT
        ALL OF THEM SIMULTANEOUSLY.

      THE FUNCTION TO BE SAMPLED IS
            S(X,Y,Z,T) = R(X,Y,Z,T) + E(X,Y,Z,T)

                WHERE
R(X,Y,Z,T) IS THE TRUE SIGNAL AND E(X,Y,Z,T) IS THE NOISE.

 R(X,Y,Z,T) = A(T)*EXP(-0.5*Q(X,Y,T))*SIN(OMEGAZ*Z+PHIZ)

      A IS A MARKOV PROCESS WITH EXPECTED VALUE
            AZERO(T) = APEAK*EXP(-SIGMAA*(T-ABAR)**2)

        STANDARD DEVIATION EQUAL TO SIGA*AZERO(T) AND LAG-ONE
       CORRELATION COEFFICIENT RHOA.

       Q(X,Y,T) = BXX(T)*DX(T)**2 + 2.0*BXY(T)*DX(T)*DY(T)
                                   + BYY(T)*DY(T)**2
      BXX,BXY AND BYY CHANGE WITH T TO FORM AN ELLIPSE IN THE
       X-Y PLANE WITH ONE AXIS ALONG THE DIRECTION OF MOTION
      AND THE OTHER PERPENDICULAR TO THE DIRECTION OF MOTION
      FOR ALL VALUES OF T.
```

```
C         DX(T) = X - XZERO(T)
C         DY(T) = Y - YZERO(T)
C
C      XZERO(T) AND YZERO(T) ARE INDEPENDENT MARKOV PROCESSES
C        WITH EXPECTED VALUES XO(T) AND YO(T), STANDARD DEVIA-
C        TIONS SIGX(T) AND SIGY(T), AND LAG ONE CORRELATION
C        COEFFICIENTS RHOX AND RHOY.
C
C      PHIZ IS A NORMALLY DISTRIBUTED RANDOM VARIABLE WITH
C        MEAN PHIBAR AND STANDARD DEVIATION SIGMAP.
C
C      THE EXPECTED VALUE OF S AND THE COVARIANCE BETWEEN S AT
C        ONE POINT IN SPACE AND TIME AND S AT A DIFFERENT POINT
C        IS FOUND BY TAKING THE EXPECTED VALUES OVER A(T),
C        XZERO(T),YZERO(T) AND PHIZ.
C
      DIMENSION X(100),Y(100),T(100),XX(100),YY(10),RES(10),
     2R(200),TT(200),PORY(10,10,5),PROB(20,20),DGMA(10),
     3DUMC(10),ZZ(10),Z(100),
      COMMON /DATA/APEAK,SIGMAA,ABAR,SIGXX,SIGYY,OMEGA,SIGX
     2,SIGY,RHOX,RHOY,SGGA,XXZERO,YYZERO,TMIN,TMAX,DELT,
     3OMEGAZ,PHIBAR,SIGMAP
      COMMON /TIMEC/TZERO
C
C........................START INPUT PARAMETERS .............
C
C          1 - STATISTICAL PARAMETERS
C
C              A - AMPLITUDE
C
      APEAK=60.0
      SIGMAA=0.05
      ABAR=10.0
      RHOA=0.95
      SIGA=0.1
C
C              B - HORIZONTAL SHAPE
C
      OMEGA=6.2831853/20.0
      SIGXX=0.5
      SIGYY=0.5
C
C              C - HORIZONTAL POSITION OF STORM CENTER
C
      XXZERO=3.0
      YYZERO=3.5
      SIGX=0.5
      RHOX=0.95
      SIGY=1.0
      RHOY=0.95
```

```
C
C          D - VERTICAL SHAPE
C
      OMEGAZ=6.2831853/12.0
      PHIBAR=20.0
      SIGMAP=10.0
C
C          2 - SAMPLING-TIME SEARCH INFORMATION
C
      TMIN=0.0
      TMAX=22.0
      DELT=2.0
      NTOTAL=8
C
C          3 - SPEED PARAMETERS
C
      NUMC=3
      CMEAN=-0.3
      DELC=0.1
C
C          4 - CURVATURE PARAMETERS
C
      NUMA=3
      AMEAN=0.166666667
      DELA=0.111111111
C




C          5 - GRID POINT INFORMATION
C
      NGRIDX=5
      NGRIDY=5
C
      N=0
      DO 1 J=1,NGRIDY
      JJ=J-1
      DO 1 K=1,NGRIDX
      KK=K-1
      N=N+1
      Z(N)=2.5
      Y(N)=JJ
      X(N)=KK
    1 T(N)=12.0
C
```

```
C          6 - POINTS FOR FIXED SAMPLING
C
      NFIX=0
      NMIN=NGRIDX*NGRIDY
      NMAX=NMIN+NFIX
      X(NMIN+1)=1.3
      Y(NMIN+1)=2.6
      Z(NMIN+1)=0.0
      T(NMIN+1)=2.0
      X(NMIN+2)=3.8
      Y(NMIN+2)=1.8
      Z(NMIN+2)=0.0
      T(NMIN+2)=2.0
      X(NMIN+3)=3.0
      Y(NMIN+3)=5.5
      Z(NMIN+3)=0.0
      T(NMIN+3)=2.0
C
C          7 - STATION LOCATIONS FOR OPTIMAL SAMPLING
C
      NSTN=9
      XX(1)=0.3
      YY(1)=1.6
      ZZ(1)=0.0
      XX(2)=2.8
      YY(2)=0.8
      ZZ(2)=0.0
      XX(3)=2.0
      YY(3)=3.5
      ZZ(3)=0.0
      XX(4)=0.3
      YY(4)=1.6
      ZZ(4)=1.5
      XX(5)=2.8
      YY(5)=0.8
      ZZ(5)=1.5
      XX(6)=2.0
      YY(6)=3.5
      ZZ(6)=1.5
      XX(7)=0.3
      YY(7)=1.6
      ZZ(7)=3.0
      XX(8)=2.8
      YY(8)=0.8
      ZZ(8)=3.0
      XX(9)=2.0
      YY(9)=3.5
      ZZ(9)=3.0
```

```
C          8 - BAYES PARAMETERS FOR SPEED (C) AND CURVATURE (A)
C
      NPROBC=3
      NPROBA=3
      CSTAR=-0.3
      ASTAR=0.166666667
      DELCC=0.1
      DELAA=0.111111111
C
      NPROBY=NPROBC+1
      NPROBX=NPROBA+1
      NC=NPROBY/2
      NA=NPROBX/2
      S=0.
      SS=0.0
      DO 26 J=1,NPROBA
      D=J-NA
      R(J)=EXP(-0.125*D*D)
      PROB(J,NPROBY)=0.0
   26 S=S+R(J)
      DO 27 J=1,NPROBC
      D=J-NC
      TT(J)=EXP(-0.125*D*D)
      PROB(NPROBX,J)=0.0
   27 SS=SS+TT(J)
      S=S*SS
      PROB(NPROBX,NPROBY)=0.0
      DO 28 J=1,NPROBA
      DO 28 K=1,NPROBC
      PROB(J,K)=R(J)*TT(K)/S
      PROB(NPROBX,NPROBY)=PROB(NPROBX,NPROBY)+PROB(J,K)
      PROB(J,NPROBY)=PROB(J,NPROBY)+PROB(J,K)
   28 PROB(NPROBX,K)=PROB(NPROBX,K)+PROB(J,K)
C
C          9 - MAXIMUM REAL TIME (IN SECONDS) ALLOWED TO RUN OPTM
      RTMAX=10800.0
C
C...............................END INPUT PARAMETERS .................
C
      TZERO=0.0
      CALL TIMCK(TOTAL)
      TZERO=TOTAL
C
C                         BEGIN MINIMUM VARIANCE SOLUTION
C
      SIGMAP=3.1415926*SIGMAP/180.0
      PHIBAR=3.1415926*PHIBAR/180.0
C
      NCOUNT=0
   29 MC=(NUMC+1)/2
      MA=(NUMA+1)/2
      CA=CMEAN-FLOAT(MC-1)*DELC
```

```
      AA=AMEAN-FLOAT(MA-1)*DELA
C
      NCOUNT=NCOUNT+1
      CS=CSTAR-FLOAT(NC-1)*DELCC
      AS=ASTAR-FLOAT(NA-1)*DELAA
C
      A=AA-DELA
      DO 3 KA=1,NUMA
      KKA=KA
      A=A+DELA
      DUMA(KA)=A
C
      C=CA-DELC
      DO 3 KC=1,NUMC
      C=C+DELC
      DUMC(KC)=C
C
      VARMIN=1.0E+10
      LL=1
      DO 2 L=1,NSTN
      CALL TIME(X,Y,Z,T,NMIN,NMAX,XX(L),YY(L),ZZ(L)
     1,C,A,TX,VAR,1)
      IF(VAR.GE.VARMIN) GO TO 2
      LL=L
      VARMIN=VAR
      TX=TIM
    2 CONTINUE
C
      POPT(KA,KC,1)=XX(LL)
      POPT(KA,KC,2)=YY(LL)
      POPT(KA,KC,3)=ZZ(LL)
      POPT(KA,KC,4)=TX
    3 POPT(KA,KC,5)=VARMIN
      IF(NCOUNT.EQ.1) WRITE(6,4)
    4 FORMAT(1H1,20X,22HOPTIMAL SAMPLING TIMES//)
C
      WRITE(6,5) NCOUNT
    5 FORMAT(22H1ADDING STATION NUMBER,I5//3X,9HCURVATURE,3X,
     15HSPEED,7X,1HX,9X,1HY,9X,1HZ,9X,1HT,5X,8HVARIANCE/)
      DO 6 KA=1,NUMA
      WRITE(6,7)
      DO 6 KC=1,NUMC
    6 WRITE(6,8) DUMA(KA),DUMC(KC),(POPT(KA,KC,J),J=1,5)
    7 FORMAT(1H0)
    8 FORMAT(2F10.2,4F10.4,F10.6)
C
      WRITE(6,5) NCOUNT
      DO 9 KC=1,NUMC
      WRITE(6,7)
      DO 9 KA=1,NUMA
```

```
C       X,Y,Z,T ARE SPACE-TIME COORDINATES OF THE GRID POINTS
C       AND THE FIXED SAMPLING STATIONS
C
C       NMIN IS THE NUMBER OF GRID POINTS
C       NMAX IS THE TOTAL OF GRID
      9 WRITE(6,8) DUMA(KA),DUMC(KC),(POPT(KA,KC,J),J=1,5)
C
        CALL TIMCK(TOTAL)




C
C                    END MINIMUM VARIANCE SOLUTION
C
C                    BEGIN BAYES SOLUTION
C
        VARMIN=1.0E+10
        LL=1
        DO 14 L=1,NSTN
C
        N=0
        TX=TMIN-DELT
     10 N=N+1
        TX=TX+DELT
C
        TT(N)=TX
        R(N)=0.0
C
        A=AS-DELAA
        DO 11 KA=1,NPROBA
        A=A+DELAA
        DUMA(KA)=A
C
        C=CS-DELCC
        DO 11 KC=1,NPROBC
        C=C+DELCC
        DUMC(KC)=C
C
        CALL TIME(X,Y,Z,T,NMIN,NMAX,XX(L),YY(L),ZZ(L),C,A,
       2TX,VAR,I)
     11 R(N)=R(N)+VAR*PROB(KA,KC)
C
        IF(TX.LT.TMAX) GO TO 10
C
C
```

```
C
      WRITE(6,200) L,(J,TT(J),R(J),J=1,N)
  200 FORMAT(1H0,I5/(I6,2F12.6))
      J=1
      D=1.0E+10
      DO 12 K=1,N
      RXXX=COST(L,R(K),TT(K))
      IF(RXXX.GE.D) GO TO 12
      J=K
      D=RXXX
   12 CONTINUE
C
      RXXX=D
      RX=R(J)
      TX=TT(J)
      IF(J.EQ.1.OR.J.EQ.N) GO TO 13
      RXY=COST(L,R(J-1),TT(J-1))
      RYX=COST(L,R(J+1),TT(J+1))
      DEL=0.5*(RYX-RXY)/(RXY+RYX-2.0*D)
      RXXX=D-0.25*(RYX-RXY)*DEL
      TX=TX-DELT*DEL
      RX=((R(J+1)+R(J-1)-2.0*R(J))*DEL*DEL-(R(J+1)-R(J-1))*
     1DEL+2.0*R(J))
C
      IF(RXXX.GE.VARMIN) GO TO 14




      VARMIN=RXXX
      RXX=RX
      TXX=TX
      LL=L
   14 CONTINUE
C
      NMAX=NMAX+1
      X(NMAX)=XX(LL)
      Y(NMAX)=YY(LL)
      Z(NMAX)=ZZ(LL)
      T(NMAX)=TXX
      RES(NCOUNT)=RXX
      IF(NCOUNT.EQ.1) GO TO 41
      NCOU=NCOUNT-1
      DO 40 JUM=1,NCOU
      JUMP=NMAX-JUM
      SUB=ABS(X(NMAX)-X(JUMP))+ABS(Y(NMAX)-Y(JUMP))
     1+ABS(T(NMAX)-T(JUMP))
      IF(SUB.LE.0.001) NTOTAL=NCOUNT
   40 CONTINUE
   41 CONTINUE
```

```
C
      CALL TIMCK(TOTAL)
      TOT=TOTAL*FLOAT(NCOUNT+1)/FLOAT(NCOUNT)
      IF(TOT.GE.RTMAX) NTOTAL=NCOUNT
      TMIN=T(NMAX)
      TMIN=0.
      DELT=(TMAX-TMIN)/20.0
      DELT=2.0
      IF(ABS(TMAX-TMIN).LE.0.1) NTOTAL=NCOUNT
      IF(NCOUNT.LT.NTOTAL) GO TO 29
C
      WRITE(6,15) (DUMC(K),K=1,NPROBC)
   15 FORMAT(1H1,40X,25HBAYES OPTIMUM INFORMATION///43X,
     120HPROBABILITY FUNCTION//50X,5HSPEED//10X,10F6.2)
      WRITE(6,33)
   33 FORMAT(9X,122(1H*))
      DO 16 J=1,NPROBA
      JJ=NPROBX-J
   16 WRITE(6,17) DUMA(JJ),(PROB(JJ,K),K=1,NPROBY)
   17 FORMAT(1H ,F8.2,1H*,20F6.3)
      WRITE(6,30) (PROB(NPROBX,K),K=1,NPROBY)
   30 FORMAT(9X,1H*,20F6.3/9X,122(1H*))
C
      WRITE(6,18) (K,XX(K),YY(K),ZZ(K),K=1,NSTN)
   18 FORMAT(1HO//60= STATION LOCATIONS FOR USE IN FINDING
     1OPTIMAL SAMPLING TIMES//7H NUMBER,5X,1HX,9X,1HY,9X,1HZ/
     2(I7,3F10.4))
C
      WRITE(6,19) (K,X(K),Y(K),Z(K),T(K),K=1,NMIN)
   19 FORMAT(1H1,20X,15HGRID POINT DATA//7H NUMBER,5X,1HX,9X,
     11HY,9X,1HZ,19X,1HT//(I7,4F10.4))
C
      WRITE(6,20)
   20 FORMAT(19H1FIXED STATION DATA//7H NUMBER,5X,1HX,9X,1HY,
     11HZ,9X,1HT/)
      IF(NFIX.EQ.0) GO TO 31
      DO 21 K=1,NFIX
      KK=NMIN+K

   21 WRITE(6,22) K,X(KK),Y(KK),Z(KK),T(KK)
   22 FORMAT(I7,5F10.4)
      GO TO 23
   31 WRITE(6,32)
   32 FORMAT(1H0,9X,16H***** NONE *****////)
```

```
C
   23 WRITE(6,24)
   24 FORMAT(47H0OPTIMAL SAMPLING TIMES FOR ALLOWABLE LOCAT-
     1IONS//7HNUMBER,5X,1HX,9X,1HY,9X,1HZ,9X,1HT,4X,20HUNEX-
     2PLAINED VARIANCE)
C
      NN=NMIN+NFIX
      DO 25 K=1,NTOTAL
      KK=NN+K
   25 WRITE(6,22) K,X(KK),Y(KK),Z(KK),T(KK),RES(K)
C
      CALL TIMCK(TOTAL)
C
C                 END BAYES SOLUTION
C
      STOP
      END
,FOR,IS          ,INVER
C
C     INVERSE WILL INVERT THE SUBMATRIX BETWEEN THE ROWS NRA
C        AND NRB AND THE COLMS NCA AND NCB. THE INVERSE OF A
C         IS RETURNED IN A.
      SUBROUTINE INVERS(A,NRA,NRB,NCA,NCB,NCODE,XMIN,XMAX,
     2PVTMIN,PVTMAX,IZ)
C
      DIMENSION M(20),MC(20),A(IZ,IZ),E(20,20)
C
      DO 20 J=NRA,NRB
      MC(J)=J
      DO 20 K=NCA,NCB
   20 E(J,K)=A(J,K)
C
      NM=NCB-1
      NCODE=0
      PVTMIN=1.0E+16
      PVTMAX=0.0
      DO 1 K=NCA,NCB
    1 M(K)=K
C
      DO 7 J=NRA,NRB
      H=ABS(A(J,NCA))
      MMJJ=NCA+J-NRA
      I=MMJJ
      MMKK=J
      KK=NCB+NRA-J
C
      DO 2 L=J,NRB
      DO 2 K=NCA,KK
      IF(ABS(A(L,K)).LE.H) GO TO 2
C
      KX=K+J-NRA
      MMJJ=M(KX)
      KJ=L
```

```
      MMKK=MC(L)
      H=ABS(A(L,K))
C
    2 CONTINUE
C
      IF(MMJJ.EQ.I.AND.MMKK.EQ.J) GO TO 4
C
      IF(MMJJ.EQ.I) GO TO 13
C
      M(KX)=M(I)
      M(I)=MMJJ
      MM=KX-J+NRA
C
      DO 3 K=NRA,NRB
      B=A(K,NCA)
      A(K,NCA)=A(K,MM)
    3 A(K,MM)=B
C
      IF(MMKK.EQ.J) GO TO 4
C
   13 MC(KJ)=MC(J)
      MC(J)=MMKK
C
      DO 14 K=NCA,NCB
      B=A(KJ,K)
      A(KJ,K)=A(J,K)
   14 A(J,K)=B
C
    4 H=1.0/A(J,NCA)
      BB=ABS(A(J,NCA))
      IF(PVTMIN.GT.BB) PVTMIN=BB
      IF(PVTMAX.LT.BB) PVTMAX=BB
C
   18 DO 5 K=NCA,NM
    5 A(J,K)=A(J,K+1)*H
      A(J,NCB)=H
C
      DO 7 K=NRA,NRB
      H=A(K,NCA)
      IF(K.EQ.J) GO TO 7
C
      DO 6 L=NCA,NM
    6 A(K,L)=A(K,L+1)-A(J,L)*H
      A(K,NCB)=-A(J,NCB)*H
C
    7 CONTINUE
C
      DO 12 J=NCA,NCB
      IF(M(J).EQ.J) GO TO 12
C
```

```
      DO 8 K=J,NCB
      IF(M(K).EQ.J) MM=K
    8 CONTINUE
      DO 9 K=NRA,NRB
      B=A(K,J)
      A(K,J)=A(K,MM)
    9 A(K,MM)=B
      M(MM)=M(J)
C
   12 M(J)=J
C
      DO 17 J=NRA,NRB
      IF(MC(J).EQ.J) GO TO 17
C
      DO 15 K=J,NRB
      IF(MC(K).EQ.J) MM=K
   15 CONTINUE
      DO 16 K=NCA,NCB
      B=A(J,K)
      A(J,K)=A(MM,K)
   16 A(MM,K)=B
      MC(MM)=MC(J)
C
   17 MC(J)=J
C
      XMIN=1.0E+16
      XMAX=0.0
      NRAA=NRA-NCA
      DO 22 J=NRA,NRB
      DO 22 K=NCA,NCB
      BB=0.0
      DO 21 L=NCA,NCB
      LL=NRAA+L
   21 BB=BB+F(J,L)*A(LL,K)
      IF((K+NRAA).EQ.J) BB=BB-1.0
      BB=ABS(BB)
      IF(XMIN.GT.BB) XMIN=BB
      IF(XMAX.LT.BB) XMAX=BB
   22 CONTINUE
C
      IF(XMAX.LT.1.0) RETURN
C
   10 WRITE(6,11)
   11 FORMAT(29H0THIS MATRIX IS SINGULAR.....//)
      NCODE=1
```

```
C
      RETURN
      END
@FOR,IS         .TIMEX
C
C     WHEN NCOD = 0 .....
C     TIME COMPUTES THE MINIMUM RESIDUAL VARIANCE AT A LOCA-
C       TION XX,YY,ZZ
C
C     WHEN NCOD = 1 .....
C     THE RESIDUAL VARIANCE AT TIME TX IS COMPUTED AND
C       RETURNED IN VAR
C        POINTS AND FIXED STATIONS
C
C     C IS THE SPEED OF THE SYSTEM
C     A IS THE CURVATURE OF THE SYSTEM
C
      SUBROUTINE TIME(X,Y,Z,T,NMIN,NMAX,XX,YY,ZZ,C,A,TX,VAR,
     2NCOD)
      DIMENSION X(100),Y(100),Z(100),T(100),R(200),B(10,10),
     2W(20,20)
      COMMON /DATA/APEAK,SIGMAA,ABAR,SIGXX,SIGYY,OMEGA,SIGX
     2,SIGY,RHOX,RHOY,SGGA,XXZERO,YYZERO,TMIN,TMAX,DELT,
     3OMEGAZ,PHIBAR,SIGMAP
C
      M=0
      MM=0
C
      IF(NMAX.EQ.NMIN) GO TO 2
C
      N=NMIN+1
      DO 1 J=N,NMAX
      M=M+1
      MM=M-1
      DO 1 K=J,NMAX
      MM=MM+1
      B(M,MM)=COV(X(J),Y(J),Z(J),T(J),X(K),Y(K),Z(K),T(K),A,C)
      IF(M.EQ.MM) B(M,M)=B(M,M)+1.0
    1 B(MM,M)=B(M,MM)
C
    2 NN=0
      TTX=TMIN-DELT
    3 TTX=TTX+DELT
C
      IF(NCOD.EQ.1) TTX=TX
```

```
C
      NN=NN+1
C
      IF(M.EQ.0) GO TO 6
C
      DO 4 J=1,M
      DO 4 K=1,M
    4 W(J,K)=B(J,K)
      MM=0
      DO 5 J=N,NMAX
      MM=MM+1
      W(M+1,MM)=COV(X(J),Y(J),Z(J),T(J),XX,YY,ZZ,TTX,A,C)
      B(M+1,MM)=W(M+1,MM)
      B(MM,M+1)=W(M+1,MM)
    5 W(MM,M+1)=W(M+1,MM)
C
    6 W(M+1,M+1)=COV(XX,YY,ZZ,TTX,XX,YY,ZZ,TTX,A,C)+1.
      B(M+1,M+1)=W(M+1,M+1)
      MM=M+1
C
      IF(M.EQ.0) W(1,1)=1.0/W(1,1)
      IF(M.GT.0) CALL INVERS(W,1,MM,1,MM,NCODE,XM,XN,PM,PN,20)
C
      IF(NCODE) 51,51,50
   50 WRITE(6,55) M,MM,N,NMIN,NMAX
   55 FORMAT(//,32HTHESE ARE M, MM, N, NMIN, NMAX   ,5I10,/)
      DO 52 I=1,MM
      WRITE(6,56) (B(I,J),J=1,10)
   56 FORMAT(1H ,10F10.4,/)
   52 CONTINUE
      WRITE(6,66)
   66 FORMAT(//,19H    PT COORDINATES   ,//)
      DO 60 J=N,NMAX
      WRITE(6,65) J,X(J),Y(J),Z(J),T(J)
   65 FORMAT(I10,4F10.4)
   60 CONTINUE
      WRITE(6,67)



   67 FORMAT(//,15H SPECIAL POINT ,//)
      WRITE(6,65) MM,XX,YY,ZZ,TTX
   51 CONTINUE
      SUM=0.0
      DO 10 K=1,NMIN
C
      IF(M.EQ.0) GO TO 8
C
```

```
      MM=0
      DO 7 J=N,NMAX
      MM=MM+1
      W(M+2,MM)=COV(X(J),Y(J),Z(J),T(J),X(K),Y(K),Z(K)
     2,T(K),A,C)
    7 W(MM,M+2)=W(M+2,MM)
C
    8 W(M+1,M+2)=COV(XX,YY,ZZ,TTX,X(K),Y(K),Z(K),T(K),A,C)
      W(M+2,M+1)=W(M+1,M+2)
C
      W(M+2,M+2)=COV(X(K),Y(K),Z(K),T(K),X(K),Y(K),Z(K),T
     2(K),A,C)
C
      MM=M+1
      SUM=W(M+2,M+2)+SUM
      DO 10 L=1,MM
      S=0.
      DO 9 LL=1,MM
    9 S=S+W(L,LL)*W(LL,M+2)
   10 SUM=SUM-W(M+2,L)*S
C
   11 R(NN)=SUM/FLOAT(NMIN)
C
      VAR=R(NN)
      IF(NCOD.EQ.1) RETURN
C
      IF(TTX.LT.TMAX) GO TO 3
C
      VAR=1.0E+10
      MM=1
      DO 12 J=1,NN
      IF(R(J).GE.VAR) GO TO 12
      MM=J
      VAR=R(J)
   12 CONTINUE
C
      VAR=R(MM)
      TX=TMIN+DELT*FLOAT(MM-1)
      IF(MM.EQ.1.OR.MM.EQ.NN) RETURN
      VAR=R(MM)-(R(MM+1)-R(MM-1))**2/(8.0*(R(MM+1)+R(MM-1)-
     22.0*R(MM)))
      TX=TX-(R(MM+1)-R(MM-1))*DELT/(2.0*(R(MM+1)+R(MM-1)
     22.0*R(MM)))
C
      RETURN
      END
 FOR,IS          ,COVAR
C
C     COV COMPUTES THE CROSSCOVARIANCE BETWEEN THE DATA AT
C        ONE POINT AND THE DATA AT ANOTHER POINT
C
```

```
C        COORDINATES ARE GIVEN AS (X,Y,Z,TIME)
C     XA,YA,ZA,TA ARE THE COORDINATES OF THE FIRST POINT
C     XB,YB,ZB,TB ARE THE COORDINATES OF THE SECOND POINT
C
C     THETA IS THE CURVATURE OF THE SYSTEM
C     C IS THE SPEED OF THE SYSTEM
C
      FUNCTION COV(XA,YA,ZA,TA,XB,YB,ZB,TB,THETA,C)
      DIMENSION DT(2),X(2),Y(2),AMP(2),DIR(2),AZERO(2),
     2BX(2),BY(2),TR(4),COEFF(1  ),DXX(3),DYY(3),Z(2)
      COMMON /DATA/APEAK,SIGMAA,ABAR,SIGXX,SIGYY,OMEGA,SIGX
     2,SIGY,RHOX,RHOY,SGGA,XXZERO,YYZERO,TMIN,TMAX,DELT,
     3OMEGAZ,PHIBAR,SIGMAP
C
      DT(1)=TA-ABAR
      DT(2)=TB-ABAR
C
      X(1)=XA
      Y(1)=YA
      Z(1)=ZA
      X(2)=XB
      Y(2)=YB
      Z(2)=ZB
C
      VARX=SIGX*SIGX
      VARY=SIGY*SIGY
      VARPHI=SIGMAP*SIGMAP
      DO 1 J=1,2
      AZERO(J)=APEAK*EXP(-SIGMAA*DT(J)*DT(J))
C
      DUM=ABS(COS(OMEGA*DT(J)))
      BX(J)=SIGXX*(1.0+DUM)
      BY(J)=SIGYY*(3.0-DUM)
      AMP(J)=AZERO(J)/SQRT((1.   BX(J)*VARX)*(1.0+BY(J)*VARY))
      DX=BX(J)/(1.0+BX(J)*VARX)
      DY=BY(J)/(1.0+BY(J)*VARY)
C
      DUM=C*DT(J)
      DM=THETA*DUM
      X(J)=X(J)-DUM-XXZERO
      Y(J)=Y(J)-DM*DUM-YYZERO
C
      DIR(J)=ATAN(2.0*DM)
      TR(J)=COS(DIR(J))
      TR(J+2)=SIN(DIR(J))
      CC=TR(J)*TR(J)
      SS=TR(J+2)*TR(J+2)
      SC=TR(J)*TR(J+2)
C
      COEFF(1)=DX*CC+DY*SS
      COEFF(2)=(DX-DY)*SC
      COEFF(3)=DX*SS+DY*CC
```

```
C
      DUM=COEF(1)*X(J)+2.0*COEF(2)*X(J)*Y(J)+COEF(3)*
     2Y(J)*Y(J)
    1 AMP(J)=AMP(J)*EXP(-0.5*(DUM+VARPHI))*SIN(OMEGAZ
     2*Z(J)+PHIBAR)
C
      DTT=ABS(TB-TA)



      RHOXX=RHOX**DTT
      RHOYY=RHOY**DTT
      RHOAA=RHOA**DTT
C
      GX=BX(1)+BX(2)+(1.0-RHOXX*RHOXX)*BX(1)*BX(2)*VARX
      GX=1.0+GX*VARX
C
      GY=BY(1)+BY(2)+(1.0-RHOYY*RHOYY)*BY(1)*BY(2)*VARY
      GY=1.0+GY*VARY
C
      DXX(1)=(1.0+BX(2)*VARX)*BX(1)/GX
      DXX(3)=(1.0+BX(1)*VARX)*BX(2)/GX
C
      DXX(2)=-RHOXX*BX(1)*BX(2)*VARX/GX
      DYY(1)=(1.0+BY(2)*VARY)*BY(1)/GY
      DYY(2)=-RHOYY*BY(1)*BY(2)*VARY/GY
      DYY(3)=(1.0+BY(1)*VARY)*BY(2)/GY
C
      CC=TR(1)*TR(1)
      SS=TR(3)*TR(3)
      SC=TR(1)*TR(3)
C
      COEF(1)=DXX(1)*CC+DYY(1)*SS
      COEF(2)=(DXX(1)-DYY(1))*SC
      COEF(3)=DXX(1)*SS+DYY(1)*CC
C
      CC=TR(2)*TR(2)
      SS=TR(4)*TR(4)
      SC=TR(2)*TR(4)
C
      COEF(4)=DXX(3)*CC+DYY(3)*SS
      COEF(5)=(DXX(3)-DYY(3))*SC
      COEF(6)=DXX(3)*SS+DYY(3)*CC
C
      CC=TR(1)*TR(2)
      SS=TR(3)*TR(4)
      SC=TR(1)*TR(4)
      CS=TR(2)*TR(3)
```

```
      COEF(7)=DXX(2)*CC+DYY(2)*SS
      COEF(8)=DXX(2)*SC-DYY(2)*CS
      COEF(9)=DXX(2)*CS-DYY(2)*SC
      COEF(10)=DXX(2)*SS+DYY(2)*CC
C
      DUM=COEF(1)*X(1)*X(1)+2.  *COEF(2)*X(1)*Y(1)+COEF(3)
     2*Y(1)+COEF(4)*X(2)*X(2)+2.0*COEF(5)*X(2)*Y(2)+COEF(6)
     3*Y(2)+2.0*COEF(7)*X(1)*X(2)+COEF(8)*X(1)*Y(2)+COEF(9)
     4*Y(1)*X(2)+COEF(10)*Y(1)*Y(2))
C
      COV=AZERO(1)*AZERO(2)*(1.0+SIGA*SIGA*RHOAA)/SQRT(GX*GY)
      COV=0.5*COV*(COS(OMEGAZ*(ZA-ZB))-COS(OMEGAZ*(ZA+ZB)+
     12.0*PHIBAR)*EXP(-2.0*VARPHI))
      COV=COV*EXP(-0.5*DUM)-AMP(1)*AMP(2)
C
      RETURN
      END
 FOR,IS         .COSTX
C
C     COST COMPUTES THE EQUIVALENT COST ASSOCIATED WITH A
C        SPECIFIC TIME T AND AN UNEXPLAINED VARIANCE VAR
C     THE COST MAY BE ASSOCIATED WITH THE LOCATION OF THE
C        SAMPLING STATION GIVEN BY THE STATION NUMBER N
C
C     A UTILITY FUNCTION MAY BE USED TO COMPUTE THE COST
C        (NOTE THAT POOR TIMES FOR SAMPLING MAY BE ASSOCIATED
C        WITH A VERY LARGE COST VALUE
C
      FUNCTION COST(N,VAR,T)
      COST=VAR
      RETURN
      END
 FOR,IS         .TIMC
C
C     TIMCK RETURNS THE TIME SINCE THE BEGINNING OF THE
C        PROGRAM IN SECONDS IN THE VARIABLE TIME
C
      SUBROUTINE TIMCK(TIME)
      COMMON /TIMEC/TZERO
C
      K=0
      TIME=MILTIM(K)
      TIME=0.001*TIME-TZERO
      TIME=ABS(TIME)
C
      DELT=TIME-TLAST
      TLAST=TIME
C
      IF(TIME.GT.10000.0) RETURN
      WRITE(6,1) TIME,DELT
    1 FORMAT(18H0TOTAL TIME USED =,F10.3,10X,12HTIME CHANGE
     2 =,F10.3)
```

c BEGIN PROGRAM EXPVAR

```
C
C.........................END INPUT PARAMETERS ...............
C
      CALL INITAL(1,200,11,0,0,0)
      CALL RED(1,0,0,ANOI)
      PSI=ANOI(1)*SIGMAP+PHIBAR
      CALL RED(50,RHOA,ANOI)
      CALL RED(50,RHOX,XNOI)
      CALL RED(50,RHOY,YNOI)
      DO 21 J=1,50
      XNOI(J)=SIGX*XNOI(J)
   21 YNOI(J)=SIGY*YNOI(J)
      MEN=
      TW=TMIN-DELT
   20 TW=TW+DELT
      MEN=MEN+1
      IF(TW.GT.(TMAX+0.001)) GO TO 3
      DO 2 J=1,3
      JJ=3*J-2
    2 CALL CONTR(ZZ(JJ),TW,CONTOR,XX,YY,NST,X,Y,NMIN,CMEAN,
     1AMEAN,ANOI,XNOI,YNOI,MEN,PSI)
      GO TO 20
    3 CALL CONTR(Z(1),T(1),CONTOR,XX,YY,NST,X,Y,NMIN,CMEAN,
     1AMEAN,XNOI,YNOI,MEN,PSI)
      CALL PSTR(3)
      N=0
      TW=TMIN-1.0
    4 TW=TW+1.0
      IF(TW.GT.(TMAX+0.001)) GO TO 5
      N=N+1
      TP(N)=TW
      GO TO 4
    5 DO 7 J=1,NSTN
      DO 6 K=1,N
      VARE(K)=EXPEC(XX(J),YY(J),ZZ(J),TP(K),CMEAN,AMEAN)
    6 VARM(K)=COV(XX(J),YY(J),ZZ(J),TP(K),XX(J),YY(J),ZZ(J),
     2TP(K),AMEAN,CMEAN)
    7 WRITE(6,8) J,(TP(K),VARM(K),VARE(K),K=1,N)
    8 FORMAT(17H1STATION NUMBER =I2/21H TIME      VAR     MEAN/
     2(F5.1,2F9.4))
      DO 9 J=1,NMIN
    9 VARU(1,J)=COV(X(J),Y(J),Z(J),T(J),X(J),Y(J),Z(J),T(J),
     1AMEAN,CMEAN)
      M=2
      XM=1.0E+10
      K=1
      DO 10 J=1,NSTN
```

```
      IF(ABS(ZZ(J)-Z(1)).GE.XM) GO TO 10
      K=J
      XM=ABS(ZZ(J)-Z(1))
   10 CONTINUE
      DO 11 J=1,NST
      XXX(J)=XX(J)
      YYY(J)=YY(J)
      ZZZ(J)=ZZ(K)
   11 TTT(J)=T(1)
      NQ=NST
     2VARU,ANOI,XNOI,YNOI,MEN,PSI)



      CALL REG(XXX,YYY,ZZZ,TTT,X,Y,Z,T,NQ,M,NMIN,AMEAN,CMEAN,
      DO 13 LL=1,3
      M=M+1
      NQ=2*LL-1
      DO 12 J=1,NQ
      KX=NMIN+J
      XXX(J)=X(KX)
      YYY(J)=Y(KX)
      ZZZ(J)=Z(KX)
   12 TTT(J)=T(KX)
      CALL REG(XXX,YYY,ZZZ,TTT,X,Y,Z,T,NQ,M,NMIN,AMEAN,CMEAN,
     2VARU,ANOI,XNOI,YNOI,MEN,PSI)
   13 CONTINUE
      DO 14 J=2,5
      DO 14 K=1,NMIN
   14 VARU(J,K)=VARU(1,K)-VARU(J,K)
      DO 15 J=1,NMIN
      VARU(6,J)=VARU(2,J)-VARU(3,J)
      VARU(7,J)=VARU(2,J)-VARU(4,J)
      VARU(8,J)=VARU(2,J)-VARU(5,J)
      VARU(9,J)=VARU(3,J)-VARU(4,J)
      VARU(10,J)=VARU(3,J)-VARU(5,J)
C
   15 VARU(11,J)=VARU(4,J)-VARU(5,J)
      WRITE(6,16) (J,(VARU(K,J),K=1,11),J=1,NMIN)
   16 FORMAT(21H1 UNEXPLAINED VARIANCE//(I5,11F11.6))
      MEX=NMIN+1
      DO 24 J=1,11
      VARU(J,MEX)=0.0
      DO 24 K=1,NMIN
   24 VARU(J,MEX)=VARU(J,MEX)+VARU(J,K)
      WRITE(6,26) (VARU(J,MEX),J=1,11)
      DO 17 J=2,11
      DO 17 K=1,NMIN
```

```
   17 VARU(J,K)=VARU(J,K)/VARU(1,K)
      WRITE(6,18) (J,(VARU(K,J),K=1,11),J=1,NMIN)
   18 FORMAT(26H1RATIO OF COLUMNS 2 - 11 TO COLUMN 1//(I5,11F11
      DO 25 J=1,11
      VARU(J,MEX)=0.0
      DO 25 K=1,NMIN
   25 VARU(J,MEX)=VARU(J,MEX)+VARU(J,K)
      WRITE(6,26) (VARU(J,MEX),J=1,11)
   26 FORMAT(1H0/,5H TOT ,11F11.6)
      STOP
      END
,FOR,IS         ,REGX
      SUBROUTINE REG(XXX,YYY,ZZZ,TTT,X,Y,Z,T,NQ,M,NMIN,AMEAN,
     2CMEAN,VARU,ANOI,XNOI,YNOI,MEN,PSI)
      DIMENSION XXX(5),YYY(5),ZZZ(5),X(100),Y(100),Z(1   ),
     2T(100),TP(50),P(5,5),Q(5,50),VARU(11,50),BETA(5,50),
     3OBJ(50),TTT(5),ANOI(50),XNOI(50),YNOI(50)
      DO 11 J=1,NQ
      DO 10 K=J,NQ
      P(J,K)=COV(XXX(J),YYY(J),ZZZ(J),TTT(J),XXX(K),YYY(K),
     2ZZZ(K),TTT(K),AMEAN,CMEAN)
      IF(J.EQ.K) P(J,J)=P(J,J) 1.0
   10 P(K,J)=P(J,K)
      DO 11 K=1,NMIN
   11 Q(J,K)=COV(XXX(J),YYY(J),ZZZ(J),TTT(J),X(K),Y(K),Z(K),



     2T(K),AMEAN,CMEAN)
      WRITE(6,1)  (K,(Q(J,K),J=1,5),K=1,NMIN)
    1 FORMAT (1H1/(I5,5E20.8))
      IF(NQ.EQ.1) P(1,1)=1.0/P(1,1)
      IF(NQ.GT.1) CALL INVERS(P,1,NQ,1,NQ,NCOD,XMA,XMB,PMA,PMB,}
      DO 12 L=1,NMIN
      DO 12 J=1,NQ
      BETA(J,L)=0.0
      DO 12 K=1,NQ
   12 BETA(J,L)=BETA(J,L)+P(J,K)*Q(K,L)
      DO 13 J=1,NQ
   13 TP(J)=ACTUL(XXX(J),YYY(J),ZZZ(J),TTT(J),CMEAN,AMEAN,
     2ANOI,XNOI,YNOI,MEN,PSI)-EXPEC(XXX(J),YYY(J),ZZZ(J),TTT
     3(J),CMEAN,AMEAN)
      WRITE(6,1) NQ,(TP(J),J=1,5),(L,(BETA(J,L),J=1,5),L=1,NMIN
      DO 14 L=1,NMIN
      OBJ(L)=EXPEC(X(L),Y(L),Z(L),T(L),CMEAN,AMEAN)
      VARU(M,L)=0.0
      DO 14 J=1,NQ
```

```
      OBJ(L)=OBJ(   L)+BETA(J,L)*TP(J)
   14 VARU(M,L)=VARU(M,L)+BETA(J,L)*Q(J,L)
      MM=M-1
      WRITE(6,15) MM,(J,OBJ(J),J=1,NMIN)
   15 FORMAT(19H1OBJECTIVE ANALYSIS,I3//(I5,F20.8))
      RETURN
      END
*FOR,IS      .EXPECX
      FUNCTION EXPEC(XA,YA,ZA,TA,S,THETA)
      DIMENSION COEF(3)
      COMMON /DATA/APEAK,SIGMAA,ABAR,SIGXX,SIGYY,OMEGA,SIGX,
     1SIGY,RHOX,RHOY,RHOA,SIGA,XXZERO,YYZERO,TMIN,TMAX,DELT,
     2OMEGAZ,PHIBAR,SIGMAP
      DT=TA-ABAR
      VARX=SIGX*SIGX
      VARY=SIGY*SIGY
      VARPHI=SIGMAP*SIGMAP
      AZERO=APEAK*EXP(-SIGMAA*DT*DT)
      DUM=ABS(COS(OMEGA*DT))
      BX=SIGXX*(1.0+DUM)
      BY=SIGYY*(3.0-DUM)
      AMP=AZERO/SQRT((1.0+BX*VARX)*(1.0+BY*VARY))
      DX=BX/(1.0+BX*VARX)
      DY=BY/(1.0+BY*VARY)
      DUM=S*DT
      DM=THETA*DUM
      XB=XA-DUM-XXZERO
      YB=YA-DM*DUM-YYZERO
      DIR=ATAN(2.0*DM)
      TC=COS(DIR)
      TS=SIN(DIR)
      CC=TC*TC
      SS=TS*TS
      SC=TC*TS
      COEF(1)=DX*CC+DY*SS
      COEF(2)=(DX-DY)*SC
      COEF(3)=DX*SS+DY*CC
      DUX=AMP*EXP(-0.5*VARPHI)*SIN(OMEGAZ*ZA+PHIBAR)
      DUM=COEF(1)*XB*XB+2.0*COEF(2)*XB*YB+COEF(3)*YB*YB
      EXPEC=DUX*EXP(-0.5*DUM)

      RETURN
      END
```

```
*FOR,IS        .CONTRX
      SUBROUTINE CONTR(ZA,TA,C,XX,YY,NST,XG,YG,NMIN,S,THETA,
     1ANOI,XNOI,YNOI,MEN,PSI)
      DIMENSION C(5),X(100),Y(100),V(5),F(5),XX(10),YY(10),
     1XG(100),YG(100),ANOI(50),XNOI(50),YNOI(50)
      COMMON /DATA/APEAK,SIGMAA,ABAR,SIGXX,SIGYY,OMEGA,SIGX,
     1SIGY,RHOX,RHOY,RHOA,SIGA,XXZERO,YYZERO,TMIN,TMAX,DELT,
     2OMEGAZ,PHIBAR,SIGMAP
      NUMX=40
      CALL PLOT(1.0,1.0,-3)
      DT=TA-ABAR
      AMP=APEAK*EXP(-SIGMAA*DT*DT)*(1.0+SIGA*ANOI(MEN))
      DUM=ABS(COS(OMEGA*DT))
      DX=SIGXX*(1.0+DUM)
      DX=1.0/SQRT(ABS(DX))
      DY=SIGYY*(3.0-DUM)
      DY=1.0/SQRT(ABS(DY))
      DUM=S*DT
      DM=THETA*DUM
      DIR=ATAN(2.0*DM)
      TC=COS(DIR)
      TS=SIN(DIR)
      CORX=DUM+XXZERO+TC*XNOI(MEN)-TS*YNOI(MEN)
      CORY=DM*DUM+YYZERO+TS*XNOI(MEN)+TC*YNOI(MEN)
      DUX=AMP*SIN(OMEGAZ*ZA+PSI)
      DO 1 J=1,5
      DMM=C(J)/DUX
      F(J)=1.0
      IF(DMM.LE.0.0)  F(J)=-1.
      DMM=ABS(DMM)
    1 V(J)=-2.0*ALOG(DMM)
      NX=2*NUMX+1
      NXM=NX-1
      DANGLE=3.14159265/FLOAT(NUMX)
      DO 2 J=1,5
      IF(V(J).LT.0.0) GO TO 2
      RAD=SQRT(V(J))
      ANGLE=-DANGLE
      DO 5 K=1,NXM
      ANGLE=ANGLE+DANGLE
      X(K)=RAD*DX*COS(ANGLE)
      Y(K)=RAD*DY*SIN(ANGLE)
      DMM=TC*X(K)-TS*Y(K)
      Y(K)=TS*X(K)+TC*Y(K)+CORY
      X(K)=DMM+CORX
      IF(X(K).LT.0.0) X(K)=0.0
      IF(Y(K).LT.0.0) Y(K)=0.0
      IF(X(K).GT.6.0) X(K)=6.0
    5 IF(Y(K).GT.6.0) Y(K)=6.0
      X(NX)=X(1)
      Y(NX)=Y(1)
      CALL LINE(X,Y,NX,0,1)
```

```
      NXX=(NUMX+1)/2
      XJ=J
      XJ=XJ*[illegible]
      XLOC=X(NXX)
      YLOC=Y(NXX)-0.07

      CALL NUMBER(XLOC,YLOC,0.14,XJ,0.0,-1)
    2 CONTINUE
      DO 6 J=1,NST
      CALL PLOT(XX(J),YY(J),3)
    6 CALL MARKER(4)
      DO 7 J=1,NMIN
      CALL PLOT(XG(J),YG(J),3)
    7 CALL MARKER(1)
      X(1)=0.0
      X(2)=6.0
      X(3)=X(2)
      X(4)=X(1)
      X(5)=X(1)
      Y(1)=0.0
      Y(2)=Y(1)
      Y(3)=6.0
      Y(4)=Y(3)
      Y(5)=Y(1)
      CALL LINE(X,Y,5,0,1)
      CALL SYMBOL(3.0,-0.5,0.14,'TIME =',0.0,6)
      CALL NUMBER(3.9,-0.5,0.14,TA,0.0,4)
      CALL SYMBOL(3.0,-1.0,0.14,'   Z =',0.0,6)
      CALL NUMBER(3.9,-1.0,0.14,ZA,0.0,1)
      CALL RSTR(2)
      RETURN
      END
*FOR,IS      .COVAR
C
C     COV COMPUTES THE CROSSCOVARIANCE BETWEEN THE DATA AT
C        ONE POINT AND THE DATA AT ANOTHER POINT
C
C          COORDINATES ARE GIVEN AS (X,Y,Z,TIME)
C     XA,YA,ZA,TA ARE THE COORDINATES OF THE FIRST POINT
C     XB,YB,ZB,TB ARE THE COORDINATES OF THE SECOND POINT
C
C     THETA IS THE CURVATURE OF THE SYSTEM
C     C IS THE SPEED OF THE SYSTEM
C
```

```
!FOR,IS          .INVER
C
C     INVERSE WILL INVERT THE SUBMATRIX BETWEEN THE ROWS NRA
C       AND NRB AND THE COLMS NCA AND NCB. THE INVERSE OF A
C       IS RETURNED IN A.
      SUBROUTINE INVERS(A,NRA,NRB,NCA,NCB,NCODE,XMIN,XMAX,
     2PVTMIN,PVTMAX,IZ)
C
```

```
FOR,IS           .ACTULX
      FUNCTION ACTUL(XA,YA,ZA,TA,S,THETA,ANOI,XNOI,YNOI,MEN,PSI
      COMMON /DATA/APEAK,SIGMAA,ABAR,SIGXY,SIGYY,OMEGA,SIGX,
     1SIGY,RHOX,RHOY,RHOA,SIGA,XXZERO,YYZERO,TMIN,TMAX,DELT,
     2OMEGAZ,PHIBAR,SIGMAB
      DIMENSION COEF(3),ANOI(5 ),XNOI(50),YNOI(50)
      DT=TA-ABAR
      AMP=APEAK*EXP(-SIGMAA*DT*DT)*(1.0+SIGA*ANOI(MEN))
      DUM=ABS(COS(OMEGA*DT))
      DX=SIGXX*(1.0+DUM)
      DY=SIGYY*(3.0-DUM)
      DUM=S*DT
      DM=THETA*DUM
      XB=XA-DUM-XXZERO
      YB=YA-DM*DUM-YYZERO
      DIR=ATAN(2.0*DM)
      TC=COS(DIR)
      TS=SIN(DIR)
      CC=TC*TC
      SS=TS*TS
      SC=TC*TS
      XB=XB-TC*XNOI(MEN)+TS*YNOI(MEN)
      YB=YB-TS*XNOI(MEN)-TC*YNOI(MEN)
      COEF(1)=DX*CC+DY*SS
      COEF(2)=(DX-DY)*SC
      COEF(3)=DX*SS+DY*CC
      DUX=AMP*SIN(OMEGAZ*ZA+PSI)
      DUM=COEF(1)*XB*XB+2.0*COEF(2)*XB*YB+COEF(3)*YB*YB
      ACTUL=DUX*EXP(-0.5*DUM)
      RETURN
      END
```

```
IFOR,IS        .REDX
      SUBROUTINE RED(N,P,X)
      DIMENSION X(50)
      XBAR=0.0
      SIGMA=SQRT(1.0-P*P)
      X(1)=GAUSS(12,XBAR,SIGMA)
      NN=1
      PP=ABS(P)
      IF(P.NE.0.)NN=ALOG(0.001)/ALOG(PP)
      DO 2 J=1,NN
      X(1)=P*X(1)+GAUSS(12,XBAR,SIGMA)
    2 CONTINUE
      DO 1 J=2,N
    1 X(J)=P*X(J-1)+GAUSS(12,XBAR,SIGMA)
      RETURN
      END
FOR,IS        .GAUSSX
      FUNCTION GAUSS(N,XBAR,SIGMA)
      X=0.
      IF(C.EQ.0.0) C=-1.0
      DO 1 J=1,N
      CALL RANDOM(C)
    1 X=X+C
      XN=N
      X=SQRT(12.0/XN)*(X-0.5*XN)
      GAUSS=SIGMA*X+XBAR
      RETURN
      END
FOR,IS        .RANDOM
      SUBROUTINE RANDOM(C)
C.....    START WITH C = -1.0  AS INPUT.
      DATA ONE/1/
      IF(C.NE.-1.0) GOTO 1
      I=1234567
    1 I=262147*I
      IF(I.LT.0) I=I+34359738367+ONE
      C=I
      C=C*.291038304E-10
      RETURN
      END
```